

UCSF

UC San Francisco Electronic Theses and Dissertations

Title

PREDICTING INTESTINAL TRANSPORTER EFFECTS IN FOOD-DRUG INTERACTIONS AND THE
ROLE OF FOOD ON DRUG ABSORPTION

Permalink

<https://escholarship.org/uc/item/59d3d1dr>

Author

Custodio, Joseph M

Publication Date

2008-09-09

Peer reviewed|Thesis/dissertation

PREDICTING INTESTINAL TRANSPORTER EFFECTS IN FOOD-DRUG INTERACTIONS
AND THE ROLE OF FOOD ON DRUG ABSORPTION

by

JOSEPH M. CUSTODIO

DISSERTATION

Submitted in partial satisfaction of the requirements for the degree of

DOCTOR OF PHILOSOPHY

in

PHARMACEUTICAL SCIENCES AND PHARMACOGENOMICS

in the

GRADUATE DIVISION

of the

UNIVERSITY OF CALIFORNIA, SAN FRANCISCO

MOM AND DAD
I THANK YOU
I LOVE YOU
I COULD NOT HAVE DONE THIS WITHOUT YOU

I am honored to enter the next stage of my life
as the 45th student of Dr. Leslie Z. Benet.

Thank you Les

I proceed with deep gratitude for the former,
current and future members of the Benet Group.

ABSTRACT

The ability to predict transporter effects on drug absorption and disposition involves concurrent consideration of many chemical and physiological variables and the effect of food on the rate and extent of availability adds further complexity due to postprandial changes in the gastrointestinal (GI) tract. A system that allows for the assessment of the multivariate intestinal interplay occurring following administration of an oral dose, in the presence or absence of a meal, would greatly benefit the early stages of drug development. In this thesis research, we focus on how the Biopharmaceutics Classification System (BCS) and our laboratory's Biopharmaceutics Drug Disposition Classification System (BDDCS) in combination with *in vitro* and *in vivo* model systems are useful in predicting when intestinal transporter function may be clinically relevant. We investigate the role of transporters in food-drug interactions specifically asking the question: Could high fat meals be inhibiting transporters? We find that simulated physiological intestinal media, designed

for dissolution testing, does not allow for transporter effects to be isolated from viscosity and solubility effects. However, a less complex media supplemented with monoglycerides to mimic the postprandial intestine is applicable to bidirectional transport studies resulting in inhibition of efflux but not uptake. We find that the Caco-2 cell system is representative of the human intestine and is an adequate model for studies with Class 1 and 2 compounds but an inadequate model for Class 3 and 4 compounds. Our data suggest that intestinal transporters belong on the list of variables that must be considered in food-drug interactions. Overall, the results from this thesis research reinforce the importance of intestinal transporters in drug absorption and demonstrate how *in vitro* model systems, when properly applied, can be a powerful and valuable predictive tool in determining clinical relevance.

TABLE OF CONTENTS

ABSTRACT	v
LIST OF TABLES	xvii
LIST OF FIGURES	xix

CHAPTER 1

INTRODUCTION: DRUGS AND THE INTESTINAL INTERPLAY

1.1	Introduction	1
1.2	The intestinal environment	5
1.2.1	The gastrointestinal (GI) tract	5
1.2.2	Known food effects and the FDA	7
1.2.3	The postprandial intestine	12
1.3	Drug classification systems	16
1.3.1	The Biopharmaceutics Classification Systems (BCS)	16
1.3.2	The Biopharmaceutics Drug Disposition Classification System (BDDCS)	23
1.4	Significance of intestinal transporters	25
1.4.1	The tools to study transporters	25

1.4.2	Transporter effects with Class 1 compounds	32
1.4.3	Transporter effects with Class 2 compounds	33
1.4.4	Transporter effects with Class 3 and 4 compounds	34
1.4.5	Transporter effects in food-drug interactions	36
1.4.5.1	Class 1 compounds	37
1.4.5.2	Class 2 compounds	38
1.4.5.3	Class 3 and Class 4 compounds	39
1.5	Hypothesis and rationale	41
1.6	Specific aims	41
1.7	Summary	42
1.8	References	44

CHAPTER 2

EVALUATION OF THE EFFECTS OF SIMULATED PHYSIOLOGICAL INTESTINAL MEDIA ON CELLULAR STUDIES TO EXAMINE ITS POTENTIAL INFLUENCE ON TRANSPORTER FUNCTION *IN VITRO*

2.1	Introduction	60
2.2	Materials and methods	67
2.2.1	Materials	67

2.2.2	Cell culture	68
2.2.3	Bidirectional transport experiments	69
2.2.4	Analysis of samples	70
2.2.4.1	Sample preparation	70
2.2.4.2	Sample analysis	72
2.3	Results	72
2.3.1	Effect of FeSSIF on the bidirectional transport of vinblastine across MDR1-MDCK cell monolayers	72
2.3.2	Effect of GG918 on the bidirectional transport of vinblastine across MDR1-MDCK cell monolayers	73
2.3.3	Effect of biorelevant media on the bidirectional transport of vinblastine across MDR1-MDCK cell monolayers	73
2.3.4	Effect of monoolein supplemented media on the bidirectional transport of vinblastine across MDR1-MDCK cell monolayers	75
2.4	Discussion	78
2.5	References	84

CHAPTER 3

INVESTIGATING THE INHIBITORY INFLUENCE OF LIPIDIC CONDITIONS IN THE INTESTINE: *IN VITRO* STUDIES

3.1	Introduction	91
3.2	Materials and methods	102
3.2.1	Materials	102
3.2.2	Cell culture	103
3.2.2.1	MDR1-MDCK and MDCK cell lines	103
3.2.2.2	Caco-2 cell line	104
3.2.3	Intracellular accumulation Experiments	105
3.2.4	Bidirectional transport experiments	106
3.2.5	Analysis of samples	107
3.2.5.1	Sample preparation	108
3.2.5.2	Analysis of samples	108
3.3	Results	108
3.3.1	Evaluation of various lipidic conditions on the intracellular accumulation of vinblastine in Caco-2 cells	108
3.3.2	Evaluation of monoolein supplemented media on the intracellular accumulation	

	of cyclosporine in Caco-2 and MDR1-MDCK cells.	109
3.3.3	Effect of monoolein supplemented media on the bidirectional transport of cyclosporine across MDR1-MDCK and MDCK cell monolayers	111
3.3.4	Effect of GG918 on the bidirectional transport of saquinavir across MDR1-MDCK cell monolayers	113
3.3.5	Effect of monoolein supplemented media on the bidirectional transport of saquinavir across MDR1-MDCK and MDCK cell monolayers	113
3.3.6	Effect of GG918 on the bidirectional transport of saquinavir across Caco-2 cell monolayers	116
3.3.7	Effect of monoolein supplemented media on the bidirectional transport of saquinavir across Caco-2 cell monolayers	116
3.3.8	Net flux and apparently permeability changes in MDR1-MDCK, MDCK and Caco-2 cell monolayers	118
3.4	Discussion	119
3.5	References	127

CHAPTER 4

APPLICATION OF VARIOUS MODEL SYSTEMS IN DETERMINING THE ROLE OF TRANSPORTERS IN THE ABSORPTION OF SELECT MODEL CLASS 3 COMPOUNDS

4.1	Introduction	135
4.1.1	Rationale	135
4.1.2	Selecting Class 3 model compounds	138
4.2	Materials and methods	148
4.2.1	Materials	148
4.2.2	Cell culture	149
4.2.2.1	Caco-2 cell line	149
4.2.2.2	PMAT-MDCK and MDCK cell lines	150
4.2.3	Intracellular accumulation experiments	150
4.2.4	Bidirectional transport experiments	151
4.2.5	<i>In situ</i> rat intestinal studies	153
4.2.5.1	Animals	153
4.2.5.2	Single-pass intestinal perfusion procedure	154
4.2.5.3	Single-pass intestinal perfusion data analysis	155

4.2.6	Analysis of samples	157
4.2.6.1	Non-radiolabeled samples	157
4.2.6.1.1	Sample preparation	157
4.2.6.1.2	Sample analysis	158
4.2.6.2	Radiolabeled samples	159
4.2.6.2.1	Sample preparation	159
4.2.6.2.2	Sample analysis	159
4.3	Results	159
4.3.1	Studies with captopril in Caco-2 cells	159
4.3.2	Studies with metformin in Caco-2 cells	161
4.3.3	Bidirectional transport assays and intracellular accumulation studies of metformin in PMAT-MDCK and VECTOR-MDCK cells	162
4.3.4	The multiple transporter effect of metformin in PMAT-MDCK and VECTOR-MDCK cells	171
4.3.5	Exploring the multiple transporter effect of metformin in Caco-2 cells	175
4.3.6	Single pass intestinal perfusion experiments in the rat model	176
4.4	Discussion	178
4.5	References	188

CHAPTER 5

DIFFERENTIAL TRANSPORT OF CLASS 1 AND 2 COMPOUNDS IN TWO WELL-CHARACTERIZED CELL SYSTEMS: THE CACO-2 AND MDCK CELL LINES

5.1	Introduction	198
5.2	Materials and methods	201
5.2.1	Materials	201
5.2.2	Cell culture	203
5.2.2.1	Caco-2 cell line	203
5.2.2.2	MDR1-MDCK (MM) and MDCK cell lines	204
5.2.3	Bidirectional transport experiments	204
5.2.4	Analysis of samples	206
5.2.4.1	Sample preparation	206
5.2.4.2	Sample analysis	206
5.3	Results	206
5.3.1	Bidirectional transport studies with verapamil in MDR1-MDCK (MM) and MDCK cells	206
5.3.2	Bidirectional transport studies with verapamil in Caco-2 cells	209
5.3.3	Bidirectional transport studies with saquinavir in MDR1-MDCK (MM) cells	209

5.3.4	Bidirectional transport studies with saquinavir in Caco-2 cells	212
5.3.5	Net flux and apparent permeability changes in Caco-2 and MDR1-MDCK cells	213
5.4	Discussion	216
5.5	References	222

CHAPTER 6

CONCLUSIONS AND PERSPECTIVES

6.1	The intestinal interplay: the past, the present and the future	226
6.2	References	233

LIST OF TABLES

Table 1.1	Lipinski's "Rule of 5"	19
Table 1.2	130 compounds by BCS Class	21
Table 1.3a	168 compounds categorized by BDDCS Class; (a) Class 1 and Class 2	26
Table 1.3b	168 compounds categorized by BDDCS Class; (b) Class 3 and Class 4	27
Table 2.1	The composition of two physiological media commonly utilized to simulate fasted (FaSSIF) and fed (FeSSIF) intestinal conditions	61
Table 2.2	Examples of typical protocols employed in dissolution testing experiments	62
Table 2.3	Fed State Simulated Intestinal Fluid (FeSSIF) affects MDR1-MDCK monolayer integrity	72
Table 2.4	Apparent permeability values (P_{app}) for vinblastine in MDR1-MDCK cells	78
Table 3.1	Net flux ratios (B to A / A to B) for saquinavir (20 μ M) in MDR1-MDCK and Caco-2 cells in the presence or absence of potential inhibitors	119

Table 3.2	Apparent permeability values (P_{app}) for saquinavir (20 μ M) in MDR1-MDCK, MDCK, and Caco-2 cells	120
Table 5.1	Net flux ratios (B to A / A to B) for verapamil (10 μ M) in Caco-2 and MDR1-MDCK cells in the presence or absence of the known P-gp inhibitor, GG918 (0.5 μ M)	214
Table 5.2	Net flux ratios (B to A / A to B) for saquinavir (20 μ M) in Caco-2 and MDR1-MDCK cells in the presence or absence of the known P-gp inhibitor, GG918 (0.5 μ M)	215
Table 5.3	Apparent permeability values (P_{app}) for verapamil (10 μ M) in Caco-2 and MDR1-MDCK cells	215
Table 5.4	Apparent permeability values (P_{app}) for saquinavir (20 μ M) in Caco-2 and MDR1-MDCK cells	215

LIST OF FIGURES

Figure 1.1	Mechanisms of intestinal transport	3
Figure 1.2	Schematic representing the fate and transit of a drug through the gastrointestinal (GI) tract following oral dosing	4
Figure 1.3	An illustration of the human small intestine	7
Figure 1.4	A diagram of the structural features of the human small intestine	8
Figure 1.5	Various intestinal transporters	9
Figure 1.6	The Biopharmaceutics Classification System (BCS)	17
Figure 1.7	Predominant routes of elimination by BCS class	22
Figure 1.8	The Biopharmaceutics Drug Disposition Classification System (BDDCS)	24
Figure 1.9	Transporter effects, following oral dosing, by BDDCS class	32
Figure 1.10	Predicted high fat meal effects by BDDCS class	37
Figure 2.1a	Simulated physiological media has	63

	no effect on the dissolution for three different tablets of metoprolol, a BCS Class 1 compound	
Figure 2.1b	The dissolution of capsules of danazol is dependent upon the types of simulated physiological media applied	64
Figure 2.2	Bidirectional transport of vinblastine in MDR1-MDCK cells in the presence or absence of the known P-gp inhibitor, GG918	74
Figure 2.3	Bidirectional transport of vinblastine in MDR1-MDCK cells with or without the simulated physiological oil formulation media	74
Figure 2.4	Bidirectional transport of vinblastine in MDR1-MDCK cells in the absence or presence of half-strength (0.5X) or full strength (1.0X) Ensure Plus	76
Figure 2.5	Bidirectional transport of vinblastine in MDR1-MDCK cells with or without monoolein supplemented media	77
Figure 3.1a	mRNA expression profile of mdr-1 (478bp) and GAPDH (230bp) with or without Peceol [®] (0.25% and 1% v/v) following 1 week incubation with	96

	Peceol [®]	
Figure 3.1b	Bar graph of the digital quantification of the mRNA bands from Figure 3.1a	96
Figure 3.2	Western blot of P-gp (170kD) in Caco-2 cells with or without a 1 week incubation with Peceol [®]	97
Figure 3.3	Effect of various monoglycerides on the intracellular accumulation of daunomycin in Caco-2 cells	99
Figure 3.4	The concentration dependent effect of 1-monopalmitin on the intracellular accumulation of daunomycin in Caco-2 cells	100
Figure 3.5	Cytotoxicity assay of various concentrations of 1-monopalmitin on Caco-2 cells examined by lactate dehydrogenase (LDH) release	101
Figure 3.6	Intracellular accumulation of vinblastine in Caco-2 cells in the presence or absence of monoglycerides	109
Figure 3.7	Intracellular accumulation of cyclosporine in Caco-2 cells in the presence or absence of 1-monoolein	110
Figure 3.8	Accumulation of cyclosporine in the	111

	apical to intracellular (A to C) direction and the basolateral to intracellular (B to C) direction in MDR1-MDCK cells in the presence or absence of 1-monoolein	
Figure 3.9	Bidirectional transport of cyclosporine in MDR1-MDCK cells with or without 1-monoolein supplemented media	112
Figure 3.10	Bidirectional transport of cyclosporine in MDCK cells with or without 1-monoolein supplemented media	112
Figure 3.11	Bidirectional transport of saquinavir in MDR1-MDCK cells in the presence or absence of known P-gp inhibitor, GG918	114
Figure 3.12	Bidirectional transport of saquinavir in MDR1-MDCK cells with or without 1- monoolein supplemented media	115
Figure 3.13	Bidirectional transport of saquinavir in MDCK cells with or without 1- monoolein supplemented media	115
Figure 3.14	Bidirectional transport of saquinavir in Caco-2 cells in the presence or absence of known P-gp inhibitor, GG918	117
Figure 3.15	Bidirectional transport of saquinavir	118

	in Caco-2 cells with or without 1- monoolein supplemented media	
Figure 4.1a	The Biopharmaceutics Classification System	136
Figure 4.1b	The Biopharmaceutics Drug Disposition Classification System	136
Figure 4.2	Ranitidine plasma concentrations in 24 healthy volunteers after administration of 150 mg ranitidine solution with or without sorbitol	141
Figure 4.3a	PMAT expression in human small intestine by (a) RT-PCR	143
Figure 4.3b	PMAT expression in human small intestine by (b) Western blotting	143
Figure 4.4	PMAT expression in human small intestine by immunohistochemistry	144
Figure 4.5a	Localization of (a) PMAT in polarized PMAT-MDCK cellular monolayers grown on semiporous filter inserts	144
Figure 4.5b	Localization of (b) YFP-PMAT in polarized PMAT-MDCK cellular monolayers	144
Figure 4.5c	Localization of (c) YFP in polarized PMAT-MDCK cellular monolayers grown on semiporous filter inserts	144

Figure 4.6	The varying levels of uptake of MPP ⁺ into PMAT-MDCK cells in the presence of a range of compounds as compared to control MDCK cells	146
Figure 4.7	The uptake of metformin in PMAT-MDCK cells in comparison to MDCK cell transfected with the empty vector only. Also, the influence of pH on metformin uptake	147
Figure 4.8	LC/MS chromatograms of captopril (MW 216.3) and the internal standard, enalapril (MW 376.4)	161
Figure 4.9a	Uptake of varying concentrations of metformin in Caco-2 cells at 37°C and 4°C	163
Figure 4.9b	The inhibitory profile of metformin in Caco-2 cells in the presence of various compounds	163
Figure 4.9c	The concentration dependent inhibition of metformin uptake in Caco-2 cells by L-carnitine	164
Figure 4.9d	The inhibition of metformin uptake in Caco-2 cells by monoolein	164
Figure 4.10a	Bidirectional transport of metformin (10•M) in PMAT-MDCK cells at pH 6; pH	165

	7; pH 8	
Figure 4.10b	Bidirectional transport of metformin (10•M) in VECTOR-MDCK cells at pH 6; pH 7; pH 8	166
Figure 4.11a	Bidirectional transport of metformin (10•M) PMAT-MDCK cells in the presence or absence of the known PMAT inhibitor, MPP ⁺	167
Figure 4.11b	Bidirectional transport of metformin (10•M) VECTOR-MDCK cells in the presence or absence of the known PMAT inhibitor, MPP ⁺	168
Figure 4.12a	Intracellular accumulation of metformin (10•M) in PMAT-MDCK cells in the presence or absence of MPP ⁺	169
Figure 4.12b	Intracellular accumulation of metformin (10•M) in VECTOR-MDCK cells in the presence or absence of MPP ⁺	170
Figure 4.13a	Bidirectional transport of metformin (10•M) in PMAT-MDCK cells in control media; MPP ⁺ ; and TEA	172
Figure 4.13b	Bidirectional transport of metformin (10•M) in VECTOR-MDCK cells in control media; MPP ⁺ ; and TEA	173
Figure 4.14a	Intracellular accumulation of	174

	metformin (10•M) in PMAT-MDCK cells in control media, MPP ⁺ , or TEA	
Figure 4.14b	Intracellular accumulation of metformin (10•M) in VECTOR-MDCK cells in control media, MPP ⁺ , or TEA	175
Figure 4.15	Bidirectional transport of metformin (10•M) in Caco-2 cells in control media; MPP ⁺ ; and TEA	176
Figure 4.16	The effective permeability (P_{eff}) of metformin in the rat intestinal perfusion model when dosed alone, with MPP ⁺ , or with TEA	177
Figure 5.1	The transwell plate system utilized for bidirectional transport studies	200
Figure 5.2	Bidirectional transport of verapamil (10 nM) in MDR1-MDCK cells (MM) and parental MDCK cells in the presence or absence of the known P-gp inhibitor, GG918 (0.5 •M)	207
Figure 5.3	Bidirectional transport of verapamil (10 •M) in MDR1-MDCK cells (MM) and parental MDCK cells in the presence or absence of the known P-gp inhibitor, GG918 (0.5 •M)	208
Figure 5.4	Bidirectional transport of verapamil	210

	(10 nM) in Caco-2 cells in the presence or absence of the known P-gp inhibitor, GG918 (0.5 μ M)	
Figure 5.5	Bidirectional transport of verapamil (10 μ M) in Caco-2 cells in the presence or absence of the known P-gp inhibitor, GG918 (0.5 μ M)	211
Figure 5.6	Bidirectional transport of saquinavir in MDR1-MDCK cells in the presence or absence of the known P-gp inhibitor, GG918 (0.5 μ M)	212
Figure 5.7	Bidirectional transport of saquinavir in Caco-2 cells in the presence or absence of the known P-gp inhibitor, GG918 (0.5 μ M)	213

CHAPTER 1*

- INTRODUCTION: DRUGS AND THE INTESTINAL INTERPLAY

1.1 Introduction

Human physiology is as astounding as it is complex. Proper bodily function involves multifarious and congruent physiological mechanisms, an essential one being the ability to intake nutrients while eliminating nonnutrients. The body is continuously exposed to compounds or organisms foreign to our body that possess no physiological function. These toxins are presented to us through a vast range of everyday variables such as the air we breath, the objects we touch, the liquids we drink, and the foods we eat. Through this constant barrage of xenobiotics, humans have evolutionarily developed certain defense mechanisms that aid in detoxifying the body. One inherent drawback of this evolution, however, is that the human body recognizes medicine in much the same manner. In order for medicine to achieve it's desired effect, it must first get

* This chapter contains material modified from a published manuscript by Custodio *et al.* entitled "Predicting drug disposition, absorption/elimination/transporter interplay and the role of food on drug absorption," *Adv. Drug Deliv. Rev.* 60 (2008) 717-733.

"inside" the body. The fact that, from the viewpoint of drug absorption, the human intestines are considered "outside" the body presents a physical barrier that must be overcome. This is an unremitting challenge to the drug development industry because a majority of medicines marketed worldwide are administered orally. The efficacy of these drugs is dependent on the oral bioavailability, which in turn, is dependent on extent of absorption. Oral absorption, in basic terms, is dependent on intestinal drug solubilization and intestinal drug permeability. The amount of drug that goes into solution is affected by factors such as gastrointestinal fluid volume, pH, temperature and the compound's octanol / water partition coefficient, $\log P_{o/w}$. Thermodynamically, the solubility of a drug is determined by the intermolecular forces in the solid state versus the intermolecular forces of the solute-solvent state.¹ Mechanistically, the permeability of a drug is additively determined by a number of parallel processes such as a passive component and one or more active components (Figure 1.1).²⁻⁶

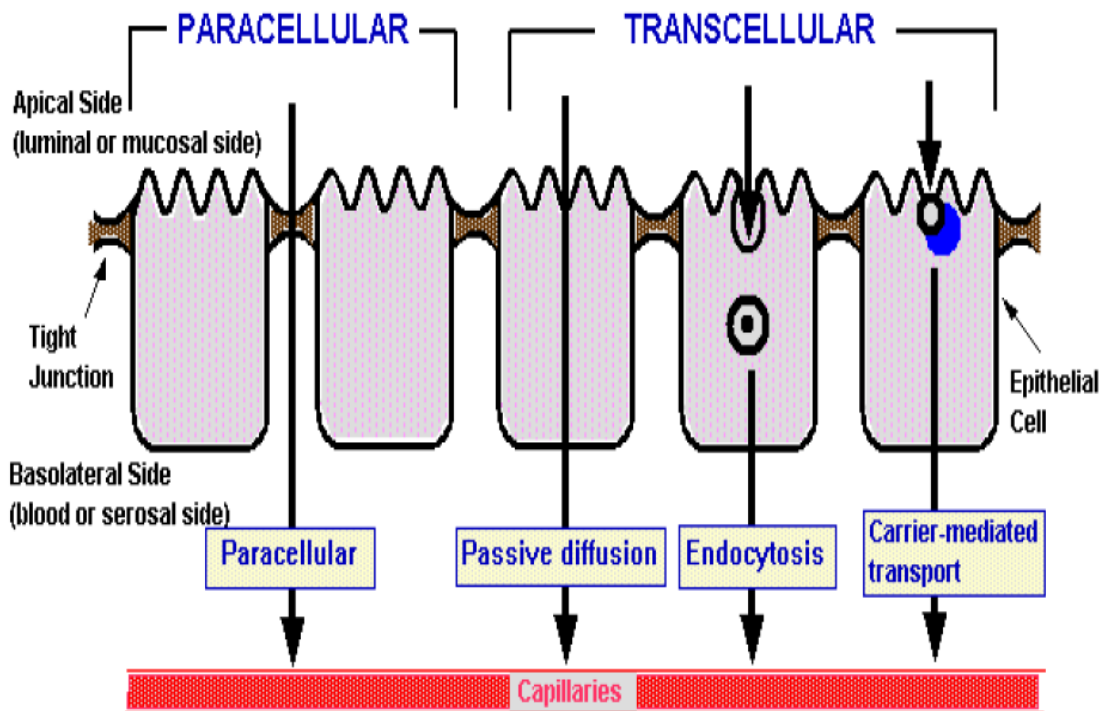


Figure 1.1 Various mechanisms of intestinal transport across the cell membrane from the apical (luminal or mucosal) side to the basolateral (blood or serosal) side.⁷

The amount of drug that crosses the membrane is affected by factors such as concentration, temperature, time, surface area, viscosity, and affinity for intestinal uptake and efflux carriers. Interest within the scientific community in intestinal transporters has been building and is now undoubtedly a rapidly emerging field in the pharmaceutical sciences. Such absorptive and secretory transporters and their role in drug disposition have been an ongoing focus of our laboratory for many years.⁸ These transporters are a central component of this thesis research.

As an oral dose transits through the gastrointestinal (GI) tract (Figure 1.2), it is exposed to a myriad of varying factors that influence its absorption.

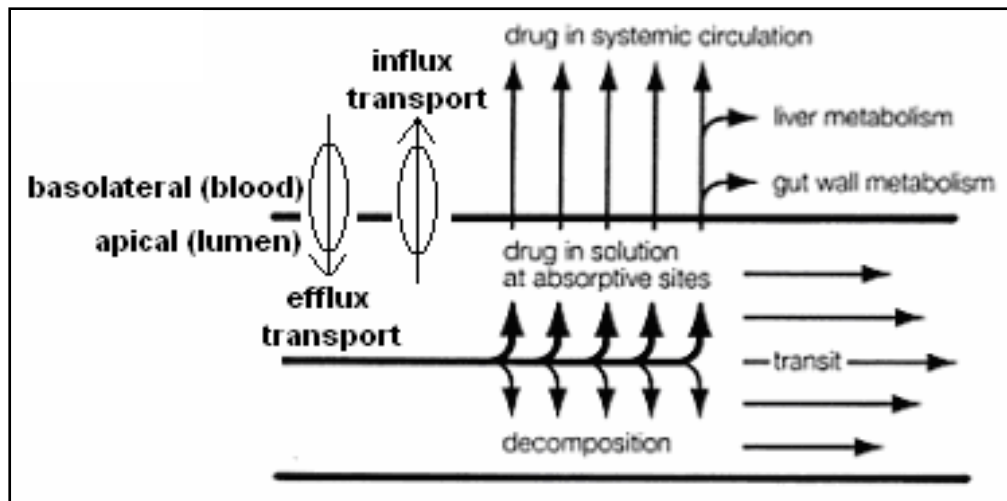


Figure 1.2 Schematic representing the fate and transit of a drug through the gastrointestinal (GI) tract following oral dosing.

Subsequent to gastric emptying from the stomach, an oral dose transits first through the small intestine and then into the large intestine. As digestion and nutrient absorption principally occur in the small intestine, it follows that drug absorption primarily occurs in the small intestine as well. Moreover, it is no surprise that the environment of the GI tract varies markedly following meal ingestion.^{9,10} Accordingly, the role of food, and its ensuing digestion, may affect the extent of

availability of a concomitant dose and is therefore, a significant concern during drug development. This thesis examines the role of intestinal transporters in drug disposition with an emphasis on food effects with the goal of establishing a comprehensive system to predict when transporters may play a significant role in food-drug interactions.

1.2 The intestinal environment

1.2.1 The gastrointestinal (GI) tract

For an orally administered drug to achieve its desired effect it must first overcome the structurally complex and highly efficient physiological barrier that is the gastrointestinal (GI) tract. Briefly touched on above, an oral dose passes from the mouth through the esophagus to the stomach. Following stomach emptying, it then enters the small intestine before passing into the large intestine. It is in the small intestinal region of the GI tract where drug absorption primarily occurs.

There are three main segments of the small intestine. The first segment is the duodenum, the second is the jejunum, and the third is the ileum. On average, the small intestine is about three meters in length. The duodenum accounts for roughly 30 cm, the jejunum accounts for about 110 cm, while the ileum accounts for the remaining 160 cm (Figure 1.3).

The intestine is of cylindrical form with an average diameter of 2-3 cm for the small intestine and 7-8 cm for the large intestine. The gastrointestinal environment is composed of specific cell types organized to create a cellular structure of remarkable surface area. The epithelial surface of the small intestinal cylinder consists of folds holding the villi, which contain goblet cells and absorptive cells. It is the microvilli in the absorptive cells, with their striated border, that predominantly amplifies the surface area of the small intestine (Figure 1.4).

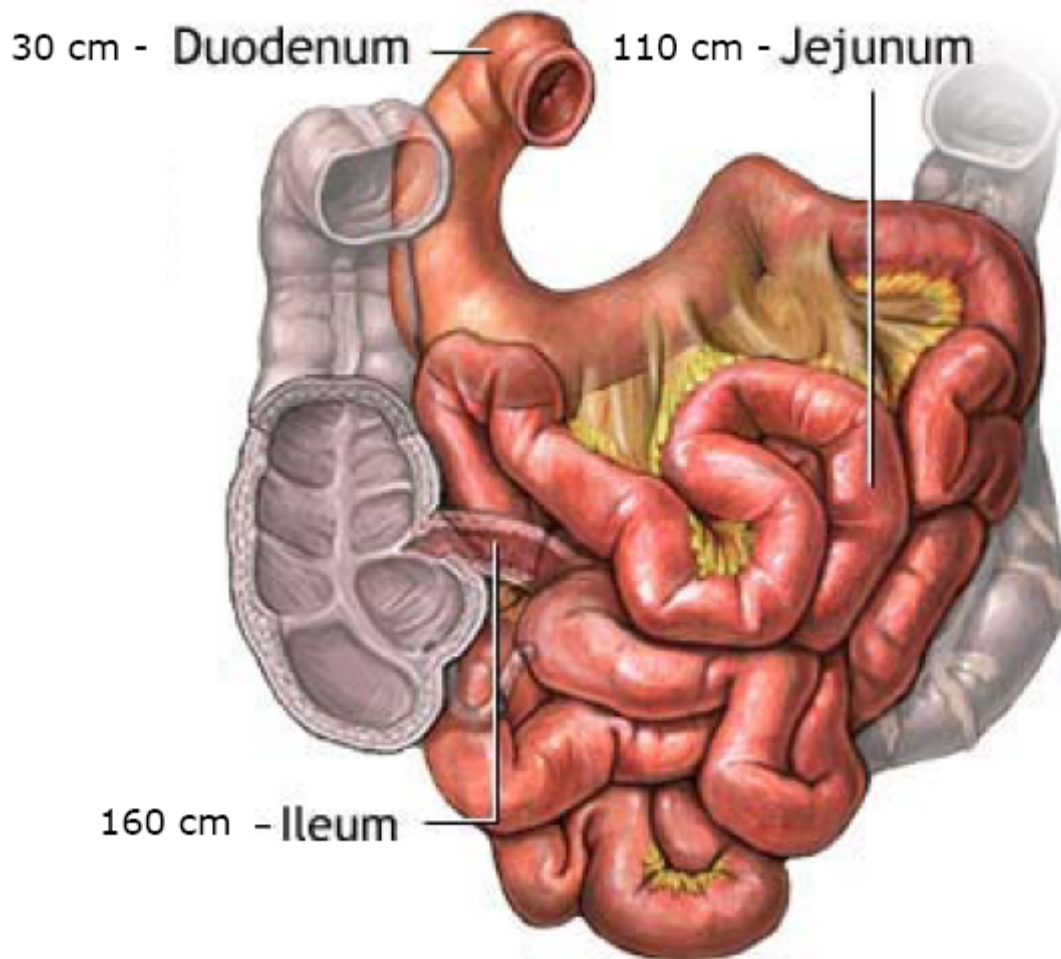


Figure 1.3 An illustration of the human small intestine denoting the region and average length of the duodenum, jejunum, and ileum.¹¹

1.2.2 Known food effects and the FDA

As the drug passes through the GI tract, not only can it decompose but it may also undergo gut wall metabolism.^{12,13} Moreover, the drug is exposed to

intestinal transporters, both efflux and absorptive (Figure 1.5).¹⁴⁻¹⁷

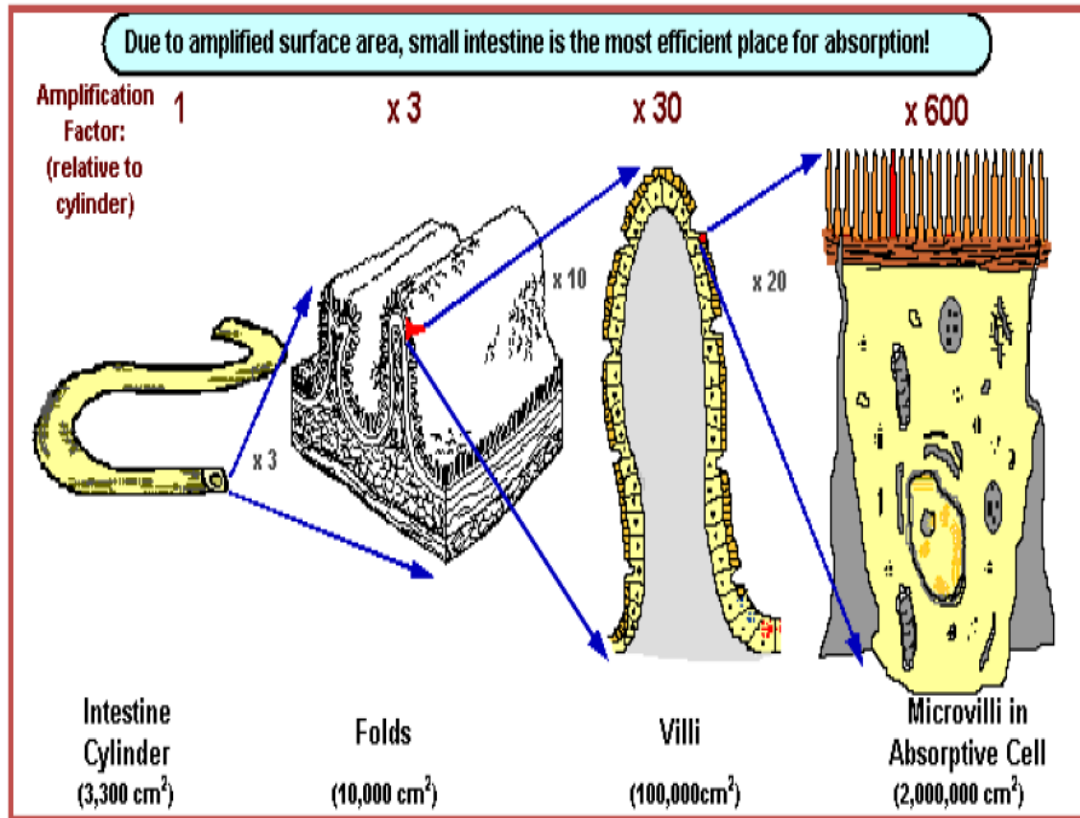


Figure 1.4 A diagram of the structural features of the human small intestine that allow for substantial amplification of surface area, which facilitates absorption.⁷

As stated above, the environment of the GI tract varies markedly following meal ingestion.^{9,10} It is well known that food can influence drug bioavailability, both increasing and decreasing the extent of availability and the rate of availability. Food-drug interactions have been widely associated with alterations of

pharmacokinetic and pharmacodynamic parameters and proven to have significant clinical implications.^{18,19}

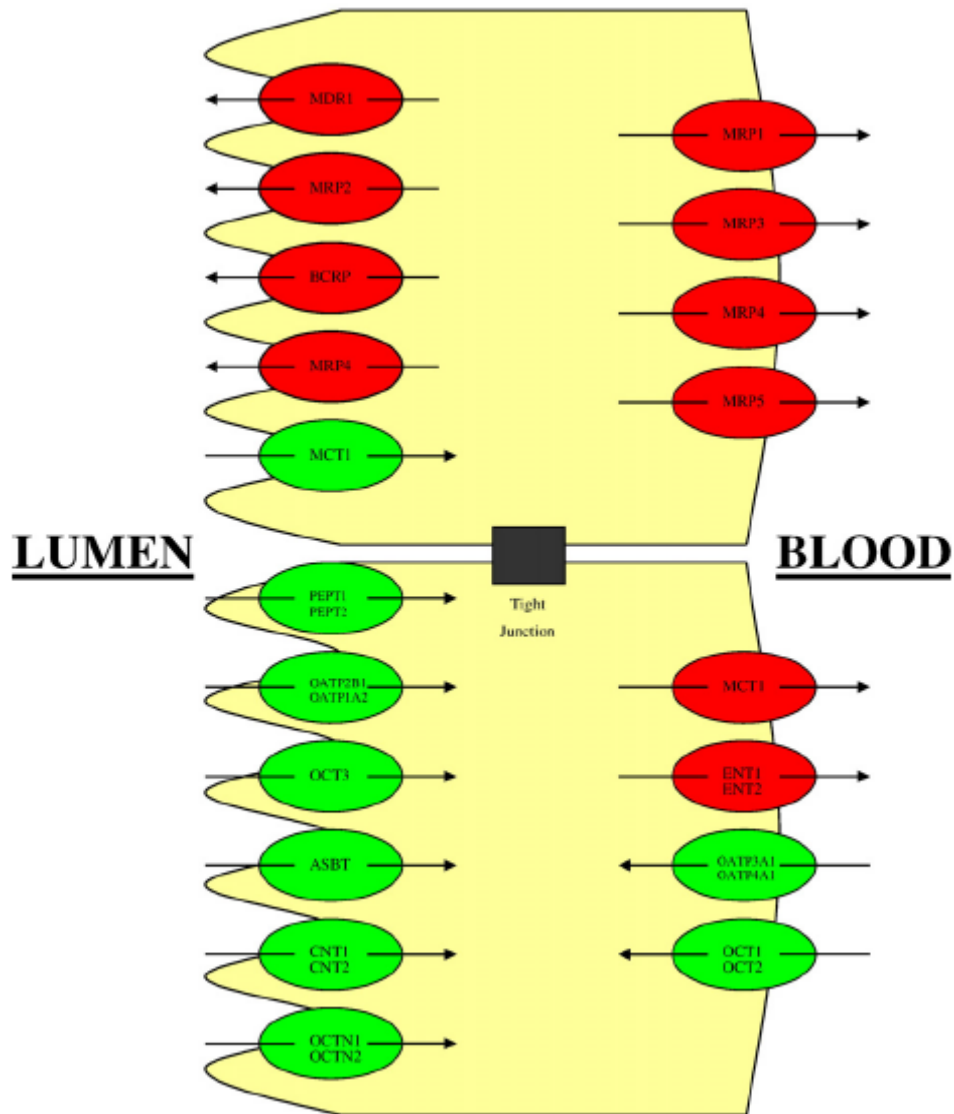


Figure 1.5 Various transporters, both efflux (red) and absorptive (green), that are expressed in the gastrointestinal (GI) tract on both the lumen side and the blood side. The influence of concomitant food intake prompted

the Food and Drug Administration (FDA) to issue a guidance for industry entitled, "Food-Effect

Bioavailability and Fed Bioequivalence Studies.”²⁰ As a result, it is common to find medication labeling containing language denoting that maximum effect is achieved if the drug is administered with a meal. Conversely, some drug products show a decrease in the extent of availability and decreased efficacy with meal coadministration. Of course, there are many drugs for which food-drug interactions are non-existent or negligible. High fat meals are recommended by the FDA for food-effect studies, as such meal conditions (800-1000 calories; 50-65% from fat, 25-30% from carbohydrates, and 15-20% protein) are expected to provide the greatest effects on gastrointestinal physiology so that systemic drug availability is maximally affected. An example of a test meal that would be suitable for a food effect bioavailability and fed bioequivalence study would include the following: two eggs fried in butter, two strips of bacon, two slices of toast with butter, four ounces of hash browns potatoes and eight ounces of whole milk.^{20,21}

Effects on absorption have been characterized as reduced, delayed, increased and accelerated, and those causing no change in absorption.²² The volume of intestinal fluids may increase 2-3 fold following a meal and the levels of phospholipids and bile salts in the gut also may increase 4-5 fold.^{23,24} It is generally believed

that food effects result from changes in drug solubility and other factors as listed by the FDA,²¹ such as food may: "delay gastric emptying; stimulate bile flow; change gastrointestinal pH; increase splanchnic blood flow; change luminal metabolism of a drug substance; and physically or chemically interact with a dosage form or a drug substance." Additional food-drug interactions that may influence the pharmacokinetics of a drug have also been documented. For example, it is known that chelation of a drug to certain food components can result in decreased bioavailability.²⁵ Decreased solubility at higher gastrointestinal pH can occur for poorly soluble weak bases leading to a decrease in bioavailability.²⁶ More rapid splanchnic blood flow is believed to improve the bioavailability of drugs that experience a significant first pass effect.²⁷ Enhanced solubility in the postprandial intestine can markedly improve the bioavailability of a poorly soluble drug.²⁸ Prolonged stomach exposure due to delayed emptying can reduce bioavailability due to drug interaction with the gastric acid secretions or by simply causing increased degradation of an unstable compound.^{29,30}

While evidence as described above, of drug, meal, and formulation interactions, as well as their influences on intestinal absorption and elimination within the GI environment can be readily found in the current

literature, much less is known about such influences and their clinical significance with respect to intestinal transporters. However, when attempting to account for any significant contribution of transporters in food-drug interactions, it is also necessary to consider the fluidic environment and the resulting components present in the GI tract following a meal high in fat.

1.2.3 The postprandial intestine

A myriad of variables are introduced into the gastrointestinal tract upon ingestion and subsequent digestion of a meal. In addition to the actual constituents of a meal, the resulting changes in the volume of intestinal fluids and the fluidic environment are significant. While the total volume may vary by individual, estimated volumes have been reported as follows: 300-500 ml for the fasted state stomach; 800-900 ml for the fed state stomach; 500 ml for the fasted state small intestine; 900-1000 ml for the fed state small intestine.^{18,22} Basal level gastric secretions are estimated to be about 300 ml and may increase up to five times following a meal. The increased gastric secretions introduce bile and alter intestinal pH, which may influence the bioavailability of a given compound.³¹ The larger volume GI environment may influence dissolution by simply presenting more liquid to the drug, as well as

creating a solvent drag effect. For poorly soluble compounds, the higher levels of bile may allow for enhanced wetting of the drug as well as increased micellar solubilization, both of which can increase the dissolution rate.³²

Food constituents have been widely studied with the caloric make-up of various meals being evaluated in humans to determine the pharmacokinetic variations in response to ingestion of meals high in fiber, high in protein, high in carbohydrates, and high in fat, e.g., studies with indinavir following high calorie protein, fat and carbohydrate meals.²⁶ These examples, save for the high fat meal, are outside the scope of this thesis project. This thesis research focuses on the influences of high fat meals because, as recommended by the FDA in food-effect studies,²⁰ such meals are believed to produce maximum effect if any is to be observed.

Triglycerides are predominant in fatty foods, and their digestion and absorption have been widely examined.³³ When fats reach the small intestines, fluid secretion increases with peak bile flow occurring about 30 minutes post meal. The fed state bile concentrations may increase to 10-20 mM from levels of the fasted state of 4-6 mM. Bile acids, their salts and lipases break down fats into monoglycerides and fatty acids that are capable of traversing the intestinal mucosal cell

membrane. In addition, bile salts undergo aggregation into polymolecular micelles that, when emulsified with the breakdown products of lipid hydrolysis, increase in size, which results in improved solubilization capacity. Both bile salts and lipids have been reported to reduce the function of transporters.³⁴⁻³⁶ Konishi and coworkers^{34,35} have documented the increased cellular accumulation of P-gp substrates in the presence of various monoglycerides. Moreover, studies have reported the inhibitory effect of taurocholate on additional transporters.³⁷

The fact that monoglycerides are a product of dietary triglyceride hydrolysis in the digestive tract, combined with the upregulation of bile salts during fatty meal digestion, led us to the hypothesis that drug-transporter interactions (i.e., transporter inhibition) could be an important mechanism for the food effect in addition to the other mechanisms listed above in the FDA guidance. In order to elucidate the food-drug-transporter interplay, it helps to begin by first recognizing the types of drugs most susceptible to significant pharmacokinetic changes when coadministered with a meal. In dealing with drug types, we focus on the drug product's physiochemical properties that dictate its assignment to a particular 'Class' within the FDA's Biopharmaceutics Classification System (BCS) and our

laboratory's Biopharmaceutics Drug Disposition
Classification System (BDDCS), as defined below.

1.3 Drug classification systems

1.3.1 The Biopharmaceutics Classification Systems (BCS)

The oral absorption of a drug is fundamentally dependent on that drug's aqueous solubility and gastrointestinal permeability. Extensive research into these fundamental parameters by Amidon *et al.*³⁸ led to the Biopharmaceutics Classification System (BCS) that categorizes drugs into four groups, Class 1 - Class 4 (Figure 1.6). The BCS classifies compounds based on the critical components related to oral absorption. Centrally embracing permeability and solubility, the objective of the BCS is to allow prediction of *in vivo* pharmacokinetic performance of drug products from *in vitro* measurements of permeability and solubility.

In 2000, the FDA promulgated the BCS as a science based approach to allow waiver of *in vivo* bioavailability and bioequivalence testing for immediate release solid dosage forms for Class 1 compounds, highly soluble and highly permeable drugs, when such drug products also exhibit rapid dissolution.³⁹ In brief, bioequivalence is achieved if the generic product shows the same rate and extent of bioavailability with rate evaluated in terms of C_{\max} and extent measured in terms of AUC. The criteria include a 90% confidence interval around point estimates of the ratios of C_{\max} and AUC, test/reference, falling within 0.8-1.25 on a log normal distribution.

		High Solubility	Low Solubility
Permeability	High	<p><u>Class 1</u></p> <p>High Solubility High Permeability Rapid Dissolution</p>	<p><u>Class 2</u></p> <p>Low Solubility High Permeability</p>
	Low	<p><u>Class 3</u></p> <p>High Solubility Low Permeability</p>	<p><u>Class 4</u></p> <p>Low Solubility Low Permeability</p>

Figure 1.6 The Biopharmaceutics Classification System (BCS).

As depicted in Figure 1.6, the BCS sorts drugs on a scale in terms of solubility versus permeability. A drug substance is considered "highly soluble" when the highest marketed dose strength is soluble in 250 ml of aqueous media over a pH range of 1-7.5 at 37°C.³⁹ A drug substance is considered to be "highly permeable" when the

extent of absorption in humans is determined to be greater or equal to 90% of an administered dose based on a mass balance determination or in comparison to an intravenous reference dose.³⁹ Accordingly, Class 1 compounds possess high properties of both solubility and permeability, while Class 4 compound possess low properties; Class 2 are highly permeable and poorly soluble, while Class 3 possess the opposite characteristics of poor permeability and high solubility. The BCS emphasizes the importance of the physiochemical properties of permeability and solubility much the same way Dr. Christopher Lipinski created his well-recognized "Rule of 5" to evaluate druglikeness. Lipinski's guidelines stipulate that a lead compound being developed for oral administration has no greater than one violation of the criteria listed in the rules in Table 1.1.⁴⁰

Lipinski's Rules:
• Not more than 5 hydrogen bond donors
• Not more than 10 hydrogen bond acceptors
• A molecular weight under 500 g/mol
• A partition coefficient log P less than 5

Table 1.1 Lipinski's "Rule of 5"

While Lipinski's guidelines have proven useful in drug development as well as led to further scientific investigations and, therefore modifications to his "rules," it should be duly noted that a glaring qualification to the "Rule of 5" is that compounds that are substrates for transporters remain an exception to the rule.

The classification framework of the BCS is believed to be useful in the earliest stages of drug discovery research. Its applications improve the prediction of oral absorption and disposition of new molecular entities. In addition, the BCS has proven to be an asset to the FDA by creating a framework that allows a waiver of *in vivo* bioequivalence studies for suitable Class 1

compounds, albeit a limited number. In 2005, Wu and Benet⁸ constructed a Table of 130 compounds in the four BCS classes (Table 1.2). These compounds were predominantly gathered from available literature but judiciously edited.^{38,41-56}

Extensive research into the assembled list of compounds in the four categories has demonstrated that the BCS provides further predictive utility. For example, critical evaluation of drug substances listed in the four BCS classes in Table I allows for prominent trends to become apparent specifically with respect to major routes of elimination. Class 1 and Class 2 compounds are eliminated primarily via metabolism, whereas Class 3 and Class 4 compounds are primarily eliminated unchanged into the urine and the bile (Figure 1.7). This is consistent with the generally held belief that more permeable lipophilic compounds make good substrates for Cytochrome P450 (CYP) enzymes.⁵⁷

		High Solubility	Low Solubility
High Permeability	Class 1		Class 2
	Abacavir	Ketoprofen	Amiodarone
	Acetaminophen	Ketorolac	Atorvastatin
	Acyclovir	Labetolol	Azithromycin
	Amiloride	Levodopa	Carbamazepine
	Amityryptiline	Levofloxacin	Carvedilol
	Antipyrine	Lidocaine	Chlorpromazine
	Atropine	Lomefloxacin	Ciprofloxacin
	Buspirone	Meperidine	Cisapride
	Caffeine	Metoprolol	Cyclosporine
	Captopril	Metronidazole	Danazol
	Chloroquine	Midazolam	Dapsone
	Chlorpheniramine	Minocycline	Diclofenac
	Cyclophosphamide	Misoprostol	Diflunisal
	Desipramine	Nifedipine	Digoxin
	Diazepam	Phenobarbital	Erythromycin
	Diltiazem	Phenylalanine	Flurbiprofen
	Diphenhydramine	Prednisolone	Glipizide
	Disopyramide	Primaquine	Glyburide
	Doxepin	Promazine	Griseofulvin
Doxycycline	Propranolol	Ibuprofen	
Enalapril	Quinidine	Indinavir	
Ephedrine	Rosiglitazone	Indomethacin	
Ergonovine	Salicylic acid		
Ethambutol	Theophylline		
Ethinyl estradiol	Valproic acid		
Fluoxetine	Verapamil		
Glucose	Zidovudine		
Imipramine			
Low Permeability	Class 3		Class 4
	Acyclovir	Fexofenadine	Amphotericin B
	Amiloride	Folic acid	Chlorothiazide
	Amoxicillin	Furosemide	Chlorthalidone
	Atenolol	Ganciclovir	Ciprofloxacin
	Atropine	Hydrochlorothiazide	Colistin
	Bidismide	Lisinopril	Furosemide
	Bisphosphonates	Metformin	Hydrochlorothiazide
	Captopril	Methotrexate	Mebendazole
	Cefazolin	Nadolol	Methotrexate
	Cetirizine	Penicillins	Neomycin
	Cimetidine	Pravastatin	
	Ciprofloxacin	Ranitidine	
	Cloxacillin	Tetracycline	
	Dicloxacillin	Trimethoprim	
	Erythromycin	Valsartan	
Famotidine	Zalcitabine		

Table 1.2 130 compounds by BCS Class

While the theory that metabolism increases as lipid solubility (log P) increases was noted, it had not been previously been recognized in terms of the Biopharmaceutics Classification System.⁸

		High Solubility	Low Solubility
Permeability	High	<p><u>Class 1</u></p> <p>Metabolism</p>	<p><u>Class 2</u></p> <p>Metabolism</p>
	Low	<p><u>Class 3</u></p> <p>Renal and/or Biliary Elimination of Unchanged Drug</p>	<p><u>Class 4</u></p> <p>Renal and/or Biliary Elimination of Unchanged Drug</p>

Figure 1.7 Predominant routes of elimination by BCS class.

It is important to note that the differential permeability characteristics defined in the BCS do not necessarily reflect differences in permeability into hepatocytes. This is evident by the fact that a high

number of Class 3 and Class 4 compounds are eliminated into the bile. The differential permeability characteristics denoted by the high versus low designation appear to reflect the differential access of the compound to the metabolizing enzymes within the hepatocytes.

Recognition of the elimination pathway differences for Class 1 and Class 2 drugs versus Class 3 and Class 4 drugs, combined with the inherent difficulty in quantifying the percent of drug absorbed in humans at a level of 90%, prompted Wu and Benet⁸ to suggest a revised category scheme entitled the Biopharmaceutics Drug Disposition Classification System (BDDCS) (Figure 1.8).

1.3.2. The Biopharmaceutics Drug Disposition Classification System (BDDCS)

The BDDCS replaces the permeability criteria with the major route of elimination because of the belief that it is easier and less ambiguous to determine the assignment of BDDCS for marketed drugs based on the extent of metabolism than using permeability (i.e. extent of absorption) in BCS assignments thereby eliminating many instances of uncertainty in human permeability leading to differences in class designation by different authors.

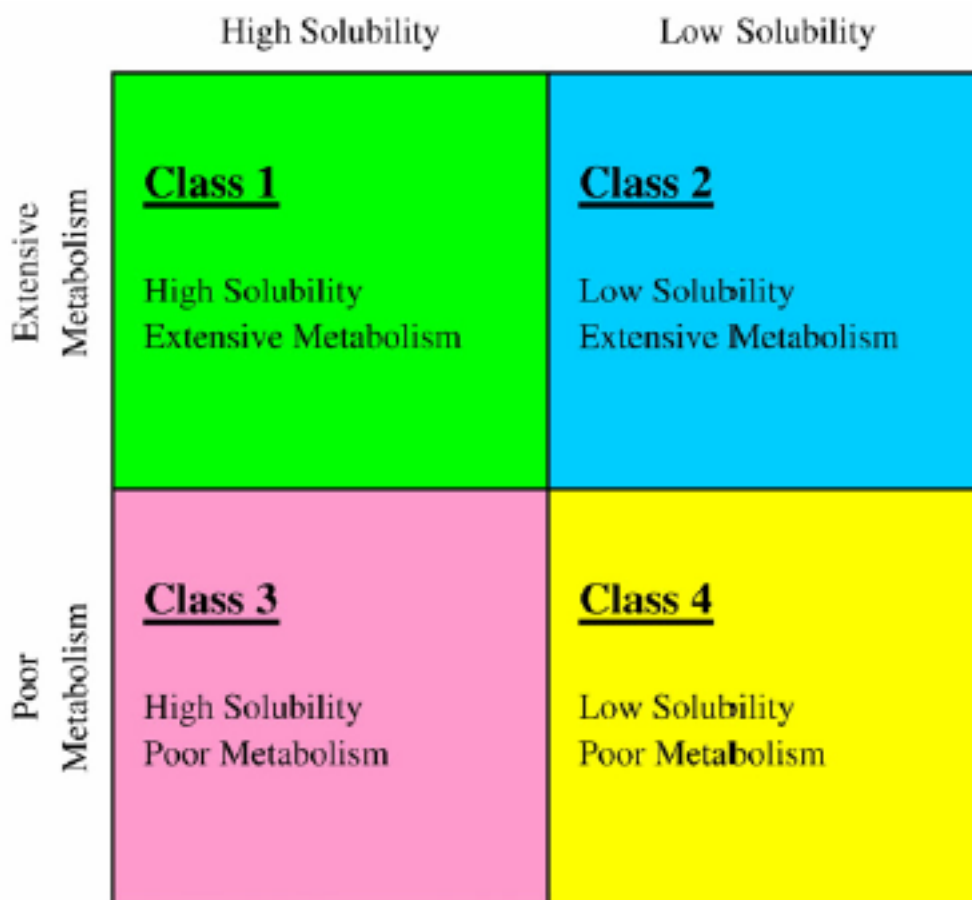


Figure 1.8 The Biopharmaceutics Drug Disposition Classification System.⁸

When initially proposed, "extensive metabolism" was defined as • 50% metabolism of an oral dose *in vivo* in humans. Further consideration of this parameter designation led to the realization that there are very few drugs/compounds that are intermediately metabolized. It is now proposed that the definition of "extensive metabolism" be pushed to • 70% metabolism of an oral dose *in vivo* in humans while the "poor metabolism" be defined as • 50% of the dose be excreted unchanged. Use of the

more stringent BDDCS metabolism criteria versus the BCS permeability characterization resulted in only 10 compounds requiring reclassification and allowed for the inclusion of an additional 38 drugs/compounds. An updated list modified from the BDDCS Table first published by Wu and Benet⁸ is provided in Table 1.3, where Table 1.3a lists the Class 1 and Class 2 compounds and Table 1.3b lists the Class 3 and Class 4 compounds.

1.4 Significance of intestinal transporters

1.4.1. The tools to study transporters.

The investigation of the effects of drug transporters on drug disposition has been ongoing for many years.⁵⁸ The well characterized Madin Darby Canine Kidney (MDCK) cell line has been widely utilized

Table 1.3a

		High Solubility	Low Solubility		
Extensive Metabolism	Class 1		Class 2		
		Abacavir	Ketoprofen	Albendazole	Ketoconazole
		Acetaminophen	Ketorolac	Amiodarone	Lansoprazole
		Albuterol	Labetolol	Atorvastatin	Lopinavir
		Allopurinol	Levamisole	Azathioprine	Lovastatin
		Amitriptyline	Levodopa	Azithromycin	Mebendazole
		Antipyrine	Lidocaine	Carbamazepine	Mefloquin
		Buspirone	Meperidine	Carvedilol	Nalidixic acid
		Caffeine	Metoprolol	Chlorpromazine	Naproxen
		Chloramphenicol	Metronidazole	Cisapride	Nelfinavir
		Chlorpheniramine	Midazolam	Clofazamine	Nevirapine
		Codeine	Minocycline	Cyclosporine	Nifedipine
		Colchicine	Misoprostol	Danazol	Oxaprozin
		Cyclophosphamide	Morphine	Dapsone	Phenytoin
		Desipramine	Phenobarbital	Diclofenac	Piroxicam
		Dexamethasone	Phenylalanine	Diflunisal	Praziquantel
		Diazepam	Prednisolone	Efavirenz	Raloxifene
		Diltiazem	Primaquine	Flurbiprofen	Rifampin
		Diphenhydramine	Promazine	Glipizide	Ritonavir
		Disopyramide	Promethazine	Glyburide	Saquinavir
		Doxepin	Propranolol	Griseofulvin	Sirolimus
		Enalapril	Pyranzinamide	Haloperidol	Spiroinolactone
		Ergonovine	Quinidine	Ibuprofen	Sulfamethoxazole
		Ergotamine	Quinine	Indinavir	Tacrolimus
		Ethinyl estradiol	Rosiglitazone	Indomethacin	Tamoxifen
		Fluoxetine	Salicylic acid	Itraconazole	Terfenadine
		Glucose	Theophylline	Ivermectin	Warfarin
		Hydralazine	Valproic acid		
		Imipramine	Verapamil		
		Isoniazid	Zidovudine		
		Isosorbid dinitrate			

Table 1.3b

		High Solubility	Low Solubility
Poor Metabolism	Class 3		Class 4
	Acyclovir	Ganciclovir	Acetazolamide
	Amiloride	Hydrochlorothiazide	Aluminum hydroxide
	Amoxicillin	Lamivudine	Amphotericin
	Atenolol	Levofloxacin	Chlorothiazide
	Atropine	Lisinopril	Chlorthalidone
	Bidisomide	Lithium	Ciprofloxacin
	Bisphosphonates	Lomefloxacin	Colistin
	Captopril	Metformin	Digoxin
	Cefazolin	Methotrexate	Furosemide
	Cetirizine	Metoclopramide	Neomycin
	Chloroquine	Nadolol	Nystatin
	Cimetidine	Neostigmine	Ofloxacin
	Cloxacillin	Penicillins	Phenazopyridine
	Dicloxacillin	Pravastatin	Talinolol
	Doxycycline	Pyridostigmine	
	Ephedrine	Ranitidine	
	Erythromycin	Riboflavin	
	Ethambutol	Tetracycline	
	Famotidine	Trimethoprim	
	Fexofenadine	Valsartan	
	Fluconazole	Zalcitabine	
	Folinic acid		

Table 1.3 168 compounds categorized by BDDCS Class; (a) Class 1 and Class 2; (b) Class 3 and Class 4.

throughout industry and academia with the most frequent application being the MDCK-MDR1 cell line incorporating the stable expression of the MDR1 gene encoding for the

P-glycoprotein (P-gp) efflux transporter.⁵⁹⁻⁶¹ Compared to various alternative cell monolayers, the MDCK-MDR1 cell system possesses very tight junctions as reflected by their high transepithelial electrical resistance (TEER) values. TEER values are measured by the Millicell electrical resistance system utilizing "chopstick" electrodes (Millipore Corporation, Bedford, MA) and are expressed in units of resistance and surface area. Our laboratory, similar to other research groups, employs semi-porous membranes with a pore size of 0.4 μm and surface area of 4.2 cm^2 upon which a cell monolayer is grown and, therefore, the ohm (\bullet) resistance measured is then multiplied by 4.2 cm^2 . The MDCK-MDR1 cells, mentioned above as having very high TEER, possess values of approximately 5000-6000 $\bullet \cdot \text{cm}^2$. The untransfected parental MDCK cell system possesses TEER values of approximately 200-300 $\bullet \cdot \text{cm}^2$. The commonly used human colonic adenocarcinoma cell system (Caco-2) possesses TEER values of approximately 800-1000 $\bullet \cdot \text{cm}^2$. It should be noted that reported TEER values for the same cell line can vary significantly from laboratory to laboratory. This may be attributed to variables such as the growth media and the frequency of media replacement as well as the passage of the cells at the time of experimentation. For example, Lu *et al.*⁶² reported Caco-2 cells, passage 44, to have TEER values of $664 \pm 42 \bullet \cdot \text{cm}^2$ while the same

cells, but of passage 98, possessed TEER values of $1423 \pm 12 \text{ } \cdot \cdot \text{cm}^2$.

Measurement of the bidirectional transport, apical to basolateral (A•B) and basolateral to apical (B•A), across the MDCK-MDR1 monolayer allows for the calculation of apparent permeability (P_{app}) values as well as net flux ratios (B•A/ A•B). Transport studies by Polli and coworkers⁶⁰ with various drugs in the MDCKII-MDR1 cell system demonstrate that P-gp substrates display a net flux ratio of 2 or higher. It has also been shown using studies in Caco-2 cells that drugs with P_{app} values less than $1 \times 10^{-6} \text{ cm/sec}$ are poorly (0-20%) absorbed; drugs with P_{app} values between $1-10 \times 10^{-6} \text{ cm/sec}$ are moderately (20-70%) absorbed; and drugs with P_{app} values greater than $10 \times 10^{-6} \text{ cm/sec}$ are well (70-100%) absorbed.⁶³

Recent advances in the pharmaceutical sciences have provided new and improved tools for discovering and investigating transporter substrates. Although numerous substrates of the P-gp efflux transporter have been identified, this has not been the case for intestinal uptake transporters. Until now studies have not been able to show which drugs and compounds gain access into the cell by means of carrier mediated uptake transporters. Various studies have documented the utility of Caco-2 cells and that these cells do endogenously express a multitude of uptake transporters.⁶⁴⁻

⁶⁸ Unfortunately, the sensitivity of assays run in Caco-2 cells have proved unsuccessful in consistently identifying uptake transporter substrates. However, isolation and stable transfection of uptake transporter proteins has lead to new lines that allow investigation of substrates for uptake transporters.^{37,69} The MDCK-PepT1 cell system has been used to for permeability screening of classic peptide substrates.⁷⁰ The HEK/OATP2B1 cells have been used to demonstrate the effects of fruit juices on glyburide uptake.⁷¹

It is important to note that unless a drug molecule can passively gain intracellular access, it is not possible to simply investigate whether the molecule is a substrate for efflux transporters. To alleviate this complexity many researchers have employed a double transfection approach. A fine example is represented by recent work by Matsushima *et al.*⁷² with the MDCKII line; one line containing both the OATP1B1 and MDR1 genes and another line containing both OATP1B1 and BCRP. With such tools, it is now feasible to evaluate vectorial transport of drugs and compounds that are substrates for both uptake and efflux transporters.⁷³⁻⁷⁵

It has been the hypothesis of our laboratory that almost all drugs are substrates for some transporter. However, this is not to say that transporter effects will always be clinically relevant. One of the reasons

researchers employ the MDCK-MDR1 cell line is because of its superior TEER values. This exceedingly tight cell system allows for increased sensitivity in identifying P-gp substrates. However, a transporter effect observed in the MDCK-MDR1 cell system may not necessarily be observed in the Caco-2 cell system. The lower TEER values of the Caco-2 cells makes for a leakier system that we believe is far more representative of the human intestine. Consequently, for certain drugs considered to be "model" P-gp substrates it may be difficult to predict their transporter interactions in the gut. In fact, Sahin *et al.* (2007 AAPS Journal 9 (2007) Abstract T3480) have shown that verapamil, which is designated as a model P-gp substrate by the FDA,³⁹ has a net flux ratio close to one in the Caco-2 cell system. Furthermore, Sahin *et al.* (2007 AAPS Journal 9 (2007) Abstract T3480) demonstrated that this ratio remained unchanged in the presence of a P-gp inhibitor suggesting that verapamil absorption is controlled by its passive diffusion and not P-gp. Work such as this has been ongoing in our laboratory for several years and has led us to a number of generalizations regarding transporter effects following oral dosing (Figure 1.9). The upcoming sections 1.4.2 through 1.4.4 provide the rationales proposed by Wu and Benet,⁸ based on our laboratory's findings, for the effects listed in Figure 1.9.

1.4.2 Transporter effects with Class 1 compounds

The gut lumen of the gastrointestinal tract is sufficiently leaky so that small molecular weight, soluble, non-polar compounds (i.e. Class 1 compounds) readily pass through the membrane. Alternatively, the high permeability/high solubility of Class 1 drugs allows high concentrations in the gut to saturate any transporter, both efflux and absorptive. That is, Class 1 compounds may be substrates for both uptake and efflux

		High Solubility	Low Solubility
Metabolism	Extensive	<u>Class 1</u> Transporter effects minimal	<u>Class 2</u> Efflux transporter effects predominate in the gut, while absorptive and efflux transporter effects occur in the liver
	Poor	<u>Class 3</u> Absorptive transporters effects predominate (but may be modulated by efflux transporters)	<u>Class 4</u> Absorptive and efflux transporters effects could be important

Figure 1.9 Transporter effects, following oral dosing, by BDDCS class.

transporters *in vitro* in cellular systems under the right conditions (for example, midazolam⁷⁶ and verapamil³⁹ are substrates for P-glycoprotein), but transporter effects will not be important clinically.

1.4.3 Transporter effects with Class 2 compounds

Similarly, for Class 2 drugs, the high permeability will allow ready access into the gut membranes making intestinal uptake transporters generally unimportant due to the rapid permeation of the drug molecule into the enterocytes. That is, absorption of Class 2 compounds is primarily passive and a function of lipophilicity. However, the low solubility of these compounds will limit the concentrations coming into the enterocytes, thereby preventing saturation of the efflux transporters. Consequently, efflux transporters will affect the extent of oral bioavailability and the rate of absorption of Class 2 drugs. Moreover, there will be little opportunity to saturate intestinal enzymes such as CYP3A4 and UDP-glucuronosyltransferases (UGTs) due to the low solubility. Thus, changes in transporter expression, and inhibition or induction of efflux transporters will cause changes in intestinal metabolism of drugs that are

substrates for the intestinal enzymes. Many Class 2 compounds are primarily substrates for CYP3A as well as substrates or inhibitors of the efflux transporter P-glycoprotein. Work in our laboratory has characterized this interplay in the absorption process for the investigational cysteine protease inhibitor K77^{77,78} and the immunosuppressive sirolimus,⁷⁹ substrates for CYP3A and P-glycoprotein and for raloxifene,⁸⁰ a substrate for UGTs and P-glycoprotein. However, as noted in Figure 1.9, Class 2 compounds may be affected by both uptake and efflux transporters in the liver.⁸¹

1.4.4 Transporter effects with Class 3 and 4 compounds

For Class 3 compounds, sufficient drug will be available in the gut lumen due to good solubility, but an absorptive transporter will be necessary to overcome the poor permeability characteristics of these compounds. However, intestinal apical efflux transporters may also be important for the absorption of such compounds when sufficient enterocyte penetration is achieved via an uptake transporter. That is, since influx of Class 3 compounds will generally be rate limited by an absorptive transporter, the counter effects of efflux transporters will not be saturated and can also be important. In general, these principles also hold for Class 4 compounds, although Class 4 drugs may achieve sufficient

solubility in the natural surfactant containing gut contents so that they act like Class 3 compounds.

1.4.5 Transporter effects in food-drug interactions

Fleisher and coworkers⁴⁴ documented several cases of food effects while taking into account the drug and its formulation classifications as established by the Biopharmaceutics Classification System (BCS).³⁹ The review of Fleisher⁴⁴ showed that in general high fat meals have no effect on the extent of oral drug availability for BCS Class 1 compounds, generally showed increased availability for Class 2 compounds, and generally showed decreased availability for Class 3 compounds. For example, *in vivo* studies such as that reported by Gupta and Benet.⁸² for cyclosporine, a Class 2 drug, demonstrated that when given with a high fat meal to healthy volunteers, bioavailability markedly increased as compared to individuals receiving the drug with a low fat meal. More recently, Ratain *et al.*²⁸ showed that the bioavailability of the new anti-cancer agent, lapatinib, increased 325% when coadministered with a high fat meal when compared with fasting conditions. Lapatinib is a Class 2 drug. In contrast, the angiotensin converting enzyme (ACE) inhibitor captopril, a BCS Class 3 compound, shows a significant decrease in serum drug levels when administered with a meal.⁸³ These observations are consistent with what might be predicted, in terms of our group's Biopharmaceutics Drug Disposition Classification System (BDDCS), if high fat meal ingestion results in an

inhibitory effect on intestinal transporter function (Figure 1.10).

		High Solubility	Low Solubility
Metabolism	Extensive	<p><u>Class 1</u></p> <p>$F_{\text{extent}} \leftrightarrow$</p> <p>$T_{\text{max}} \uparrow$</p>	<p><u>Class 2</u></p> <p>$F_{\text{extent}} \uparrow$</p> <p>$T_{\text{max}} \uparrow\downarrow\leftrightarrow$</p>
	Poor	<p><u>Class 3</u></p> <p>$F_{\text{extent}} \downarrow$</p> <p>$T_{\text{max}} \uparrow$</p>	<p><u>Class 4</u></p> <p>$F_{\text{extent}} \uparrow\downarrow\leftrightarrow$</p> <p>$T_{\text{max}} \uparrow\downarrow\leftrightarrow$</p>

Figure 1.10 Predicted high fat meal effects by BDDCS class.

The predicted effects of food on absorption by BDDCS class is summarized in Figure 1.10, and the rationale for these predictions, based on our laboratory's data, are provided in the upcoming sections 1.4.5.1 through 1.4.5.3 as proposed by Wu and Benet.⁸

1.4.5.1 Class 1 compounds

High fat meals will have no significant effect on the extent of bioavailability for Class 1 compounds. Complete absorption would be expected for high solubility/high permeability compounds. Because the absorption process would be dominated by passive diffusion for Class 1 compounds, no significant transporter drug interactions would be expected. However, high fat meals may delay stomach emptying and therefore cause an increase in peak time.

1.4.5.2 Class 2 compounds

High fat meals will increase the extent of bioavailability for Class 2 compounds. This increased bioavailability with a concomitant high fat meal could be due to inhibition of efflux transporters, such as P-gp, in the intestine. Benet *et al.*^{84,85} have reported that a dynamic interplay exists between P-gp and CYP3A4 demonstrating that P-gp efflux transport prolongs the exposure of drug to CYP3A4 by "cycling" the drug in and out of the cell. Therefore, inhibition of P-gp limits the "cycling," reducing access of drug to the metabolizing enzyme. This mechanism is specifically relevant to compounds that are dual substrates of both metabolizing enzymes and efflux transporters, as is the case for Class 2 drugs. Hence, blocking the efflux transporter decreases the amount of drug metabolized

thereby increasing the bioavailability. Another mechanism that could be acting in concert with the efflux transporter inhibition is increased solubilization of drug in the intestinal lumen (e.g., micelle formation). In addition to change in exposure, peak time could decrease due to inhibition of efflux cycling or increase due to slowing of stomach emptying; a combination of the two will usually be dominated by the delayed emptying.

Formulation changes that markedly increase the solubility of Class 2 compounds will decrease or eliminate the high fat meal effects for these drugs. We believe that this is the reason that the newer cyclosporine microemulsion formulation (Neoral[®]) eliminates the food effects associated with the older olive oil formulation (Sandimmune[®]). In practice, drug formulators attempt to enable a Class 2 compound to function in the body as a Class 1 compound, thereby eliminating food effects on the extent of availability and other transporter-drug interactions.

1.4.5.3 Class 3 and Class 4 compounds

High fat meals will decrease the extent of availability for Class 3 compounds. Class 3 compounds could show lower extent of availability with high fat meals due to inhibition of uptake transporters in the intestine. Recent evidence suggests that intestinal drug

uptake can be decreased by inhibiting organic anion transporting polypeptides (OATPs), as shown by the inhibitory effect *in vitro* of fruits juices on glyburide.⁷¹ Moreover, this inhibition of OATPs by fruit juices is demonstrated *in vivo* by Dresser and colleagues with their work on fexofenadine.⁸⁶ As noted in Figure 1.9, Class 3 compounds will also be substrates for intestinal efflux transporters. Depending upon whether the meal effects are more pronounced on efflux or influx transporters for a Class 3 drug that is a substrate for both, an unexpected increase in the extent of bioavailability or no meal effect can be observed. Wu and Benet⁸ hypothesized that this may be the explanation for the lack of a high fat meal effect on acyclovir and the slight increase observed with ganciclovir.⁸⁷ For Class 3 drugs, peak time would be expected to be increased by a high fat meal due to the combination of delayed stomach emptying and slower absorption.

For Class 4 compounds, it is difficult to predict what will occur, as all of the interacting effects mentioned for Class 2 and Class 3 compounds can be seen here. However, although not shown in Figure 1.10, if high fat meal effects are to occur, an increase of the extent of bioavailability is more likely, resulting from the combination of increased solubilization of drug in the intestine and inhibition of efflux transporters.

1.5 Hypothesis and rationale

The overall goal of this thesis research project is to investigate the hypothesis that intestinal transporters may play a significant role in food-drug interactions. Extensive work has been done to closely represent the upper gastrointestinal (GI) tract by mimicking physiological conditions of a fasted and fed state, yet, these studies have been primarily applied to dissolution testing and have clearly demonstrated that the rate and extent of dissolution is influenced by both the physiological media and the class of drug tested. We seek to extend the application of simulated physiological conditions of the gut lumen to investigate transporter function in cases where intestinal transporters may be important. Furthermore, we seek to utilize the Biopharmaceutics Classification System (BCS) and the metabolism criteria containing, Biopharmaceutics Drug Disposition Classification System (BDDCS), to elucidate the underlying mechanisms in the trends such as those described by Fleisher and colleagues⁴⁴ because, despite our belief that almost all drugs are substrates for some transporter, transporter effects may not always prove to be clinically relevant.

1.6 Specific aims

The objectives of this study are as follows:

1. Evaluate the effects of simulated physiological intestinal media on cellular studies to examine its potential influence on transporter function *in vitro*.
2. Determine whether trends observed in the Biopharmaceutics Classification System (BCS) and the Biopharmaceutics Drug Disposition Classification System (BDDCS) can be explained through *in vitro* cellular transport studies by using model BDDCS Classes 1 and 2 compounds.
3. Evaluate the utility and adequacy of various model systems in determining the role and significance of transporters in select, poorly characterized model Class 3 compounds.

1.7 Summary

The research presented in the thesis focuses on how the BCS and the BDDCS in combination with *in vitro* and *in vivo* model systems are useful in predicting when intestinal transporter function may be clinically relevant. We investigate the role of transporters in food-drug interaction specifically asking the question:

Could high fat meals be inhibiting transporters? In Chapter 2, we examine the effects of simulated physiological intestinal media in cellular studies and *in vitro* transporter function. In Chapter 3, we evaluate the influence of monoolein on the bidirectional transport of select model compounds. In Chapter 4, we discuss the differential transport of Class 1 and 2 compounds in two well-characterized cell systems, the Caco-2 and MDCK cells. In Chapter 5, we investigate the utility and adequacy of various model systems in determining the role and significance of transporters in select, poorly characterized model Class 3 compounds. Finally, our conclusions and perspectives are summarized in Chapter 6.

1.8 References

1. W.L. Jorgensen, E.M. Duffy, Prediction of drug solubility from structure, *Adv. Drug Deliv. Rev.* 54 (2002) 355-366.
2. C.A. Bergström, In silico predictions of drug solubility and permeability: two rate-limiting barriers to oral drug absorption, *Basic Clin. Pharmacol. Toxicol.* 96 (2005) 156-161.
3. C.A. Bergström, Computational models to predict aqueous drug solubility, permeability and intestinal absorption, *Expert Opin. Drug Metab. Toxicol.* 1 (2005) 613-627.
4. G.L. Amidon, P.J. Sinko, D. Fleisher, Estimating human oral fraction dose absorbed: a correlation using rat intestinal membrane permeability for passive and carrier-mediated compounds, *Pharm. Res.* 5 (1988) 651-654.
5. J.R. Kunta, P.J. Sinko, Intestinal drug transporters: in vivo function and clinical importance, *Curr. Drug Metab.* 5 (2004) 109-124.
6. U. Fagerholm, Prediction of human pharmacokinetics - gastrointestinal absorption, *J. Pharm. Pharmacol.* 59 (2007) 905-916.

7. Figure adapted from G.L. Amidon, Oral drug delivery: A mechanistic approach, In: Strategies in Oral Drug Delivery (2008) Course Workbook.
8. C.-Y. Wu, L.Z. Benet, Predicting drug disposition via application of BCS: transport/absorption/elimination interplay and development of a Biopharmaceutics Drug Disposition Classification System, Pharm. Res. 22 (2005) 11-23.
9. L. Kalantzi, K. Goumas, V. Kalioras, B. Abrahamsson, J.B. Dressman, C. Reppas, Characterization of the human upper gastrointestinal contents under conditions simulating bioavailability/bioequivalence studies, Pharm. Res. 23 (2006) 165-176.
10. J. Brouwers, J. Tack, F. Lammert, P. Augustijns, Parallel monitoring of plasma and intraluminal drug concentrations in man after oral administration of fosamprenavir in the fasted and fed state, Pharm. Res. 24 (2007) 1862-1869.
11. Modified from a figure from the US National Library of Medicine:
<http://www.nlm.nih.gov/medlineplus/ency/images/ency/fullsize/19221.jpg>
12. M.F. Paine, D.D. Shen, K.L. Kunze, J.D. Perkins, C.L. Marsh, J.P. McVicar, D.M. Barr, B.S. Gillies,

- K.E. Thummel, First-pass metabolism of midazolam by the human intestine, *Clin. Pharmacol. Ther.* 60 (1996) 14-24.
13. J.M. DeSesso, C.F. Jacobson, Anatomical and physiological parameters affecting gastrointestinal absorption in humans and rats, *Food Chem. Toxicol.* 39 (2001) 209-228.
 14. Y. Shitara, T. Horie T, Y. Sugiyama, Transporters as a determinant of drug clearance and tissue distribution, *Eur. J. Pharm. Sci.* 27 (2006) 425-446.
 15. R.B. Kim, Transporters and drug discovery: why, when, and how, *Mol. Pharmaceut.* 3 (2005) 26-32.
 16. A. Seithel, J. Karlsson, C. Hilgendorf, A. Björquist, A.L. Ungell, Variability in mRNA expression of ABC- and SLC-transporters in human intestinal cells: comparison between human segments and Caco-2 cells, *Eur. J. Pharm. Sci.* 28 (2006) 291-299.
 17. G. Englund, F. Rorsman, A. Rönnblom, U. Karlbom, L. Lazorova, J. Gråsjö, A. Kindmark, P. Artursson, Regional levels of drug transporters along the human intestinal tract: co-expression of ABC and SLC transporters and comparison with Caco-2 cells, *Eur. J. Pharm. Sci.* 29 (2006) 269-277.

18. B.N. Singh, Effects of food on clinical pharmacokinetics, *Clin. Pharmacokinet.* 37 (1999) 213-255.
19. R.Z. Harris, G.R. Jang, S. Tsunoda, Dietary effects on drug metabolism and transport, *Clin. Pharmacokinet.* 42 (2003) 1071-1088.
20. Food and Drug Administration. Guidance for Industry: Food-effect bioavailability and fed bioequivalence studies. Food and Drug Administration, Rockville, MD, 2002. Available at <http://www.fda.gov/cder/guidance/index.htm>.
21. S. Klein, J. Butler, J.M. Hempenstall, C. Reppas, J.B. Dressman, Media to simulate the postprandial stomach I. Matching the physiochemical characteristics of standard breakfasts, *J. Pharm. Pharmacol.* 56 (2004) 605-610.
22. P.G. Welling, Effects of food on drug absorption, *Annu. Rev. Nutr.* 16 (1996) 383-415.
23. E. Galia, E. Nicolaidis, D. Hörter, R. Löbenberg, C. Reppas, J.B. Dressman, Evaluation of various dissolution media for predicting in vivo performance of class I and II drugs, *Pharm. Res.* 15 (1998) 698-705.
24. J.B. Dressman, C. Reppas, In vitro-in vivo correlations for lipophilic, poorly water-soluble drugs, *Eur. J. Pharm. Sci.* 11, S2 (2000) 73-80.

25. J.J. Leyden, Absorption of minocycline hydrochloride and tetracycline hydrochloride. Effect of food, milk, and iron, *J. Am. Acad. Dermatol.* 12 (1985) 308-312.
26. P.L. Carver, D. Fleisher, S.Y. Zhou, D. Kaul, P. Kazanjian, C. Li, Meal composition effects on the oral bioavailability of indinavir in HIV-infected patients, *Pharm. Res.* 16 (1999) 718-724.
27. H. Liedholm, A. Melander, Concomitant food intake can increase the bioavailability of propranolol by transient inhibition of its presystemic primary conjugation, *Clin. Pharmacol. Ther.* 40 (1986) 29-36.
28. M.J. Ratain, E.E. Cohen, The value meal: how to save \$1,700 per month or more on lapatinib, *J. Clin. Oncol.* 25 (2007) 3397-3398.
29. G.L. Amidon, H. Lennernas, V.P. Shah, J.R. Crison, A theoretical basis for a biopharmaceutics drug classification: the correlation of in vitro drug product dissolution and in vivo bioavailability, *Pharm. Res.* 12 (1995) 413-420.
30. L.E. Schmidt, K. Dalhoff, Food-drug interactions, *Drugs* 62 (2002) 1481-1502.
31. C.Y. Lui, G.L. Amidon, R.R. Berardi, D. Fleisher, C. Youngberg, J.B. Dressman, Comparison of gastrointestinal pH in dogs and humans:

- implications on the use of the beagle dog as a model for oral absorption in humans, *J. Pharm. Sci.* 75 (1986) 271-274.
32. W.N. Charman, C.J.H. Porter, S. Mithani, J.B. Dressman, Physiochemical and physiological mechanisms for the effects of food on drug absorption: the role of lipids and pH, *J. Pharm. Sci.* 86 (1997) 269-282.
33. P. Tso, Intestinal lipid absorption, in: R. Johnson (Ed.), *Physiology of the Gastrointestinal Tract*, Raven Press, New York, 1994, pp. 1867-1907.
34. T. Konishi, H. Satsu, Y. Hatsugai, K. Aizawa, T. Inakuma, S. Nagata, S.H. Sakuda, H. Nagasawa, M. Shimizu, Inhibitory effect of a bitter melon extract on the P-glycoprotein activity in intestinal Caco-2 cells, *Br. J. Pharmacol.* 143 (2004) 379-387.
35. T. Konishi, H. Satsu, Y. Hatsugai, K. Aizawa, T. Inakuma, S. Nagata, S.H. Sakuda, H. Nagasawa, M. Shimizu, A bitter melon extract inhibits the P-glycoprotein activity in intestinal Caco-2 cells: monoglyceride as an active compound, *Biofactors* 22 (2004) 71-74.
36. F. Ingels, S. Deferme, E. Destexhe, M. Oth, G. Van den Mooter, P. Augustijns, Simulated

- intestinal fluid as transport medium in the Caco-2 cell culture model, *Int. J. Pharm.* 232 (2002) 183-192.
37. A. Balakrishnan, J.E. Polli, Apical sodium dependent bile acid transporter (ASBT, SLC10A2): a potential prodrug target, *Mol. Pharmaceut.* 3 (2006) 223-230.
38. G.L. Amidon, H. Lennernas, V.P. Shah, J.R. Crison, A theoretical basis for a biopharmaceutics drug classification: the correlation of in vitro drug product dissolution and in vivo bioavailability, *Pharm. Res.* 12 (1995) 413-420.
39. Food and Drug Administration, Guidance for Industry: Waiver of in vivo bioavailability and bioequivalence studies for immediate release solid oral dosage forms based on a Biopharmaceutics Classification System, Food and Drug Administration, Rockville, MD, 2000. Retrieved from www.fda.gov/cder/guidance/index.htm.
40. C.A. Lipinski, Drug-like properties and the causes of poor solubility and poor permeability, *J. Pharmacol. Toxicol. Methods.* 44 (2000) 235-249.
41. H. Lennernas, Human jejunal effective permeability and its correlation with preclinical drug absorption models, *J. Pharm. Pharmacol.* 49 (1997) 627-638.

42. H. van de Waterbeemd, The fundamental variables of the Biopharmaceutics Classification System (BCS): a commentary, *Eur. J. Pharm. Sci.* 7 (1998) 1-3.
43. H. H. Blume, B.S. Schug, The Biopharmaceutics Classification System (BCS): class III drugs—better candidates for BA/BE waiver?, *Eur. J. Pharm. Sci.* 9 (1999) 117-121.
44. D. Fleisher, C. Li, Y. Zhou, L.H. Pao, A. Karim, Drug, meal and formulation interactions influencing drug absorption after oral administration, Clinical implications, *Clin. Pharmacokinet.* 36 (1999) 233-254.
45. R. Löbenberg, G.L. Amidon, Modern bioavailability, bioequivalence and Biopharmaceutics Classification System. New scientific approaches to international regulatory standards, *Eur. J. Pharm. Biopharm.* 50 (2000) 3-12.
46. A. Avdeef, Physicochemical profiling (solubility, permeability and charge state), *Curr. Top. Med. Chem.* 1 (2001) 277-351.
47. B.D. Rege, L.X. Yu, A.S. Hussain, J.E. Polli, Effect of common excipients on Caco-2 transport of low-permeability drugs, *J. Pharm. Sci.* 90 (2001) 1776-1786.
48. C. Tannergren, P. Langguth, K.J. Hoffmann, Compound mixtures in Caco-2 cell permeability

- screens as a means to increase screening capacity, *Pharmazie* 56 (2001) 337-342.
49. I. Kanfer, Report on the International Workshop on the Biopharmaceutics Classification System (BCS): scientific and regulatory aspects in practice, *J. Pharm. Pharm. Sci.* 5 (2002) 1-4.
50. H. Lennernas, L. Knutson, T. Knutson, A. Hussain, L. Lesko, T. Salmonson, G.L. Amidon, The effect of amiloride on the in vivo effective permeability of amoxicillin in human jejunum: experience from a regional perfusion technique, *Eur. J. Pharm. Sci.* 15 (2002) 271-277.
51. M.N. Martinez, G.L. Amidon, A mechanistic approach to understanding the factors affecting drug absorption: a review of fundamentals, *J. Clin. Pharmacol.* 42 (2002) 620-643.
52. M.E. Taub, L. Kristensen, S. Frokjaer, Optimized conditions for MDCK permeability and turbidimetric solubility studies using compounds representative of BCS classes I-IV, *Eur. J. Pharm. Sci.* 15 (2002) 331-340.
53. L. X. Yu, G.L. Amidon, J.E. Polli, H. Zhao, M.U. Mehta, D.P. Conner, V.P. Shah, L.J. Lesko, M.L. Chen, V.H. Lee, A.S. Hussain, Biopharmaceutics Classification System: the scientific basis for

- biowaiver extensions, *Pharm. Res.* 19 (2002) 921-925.
54. C.A. Bergström, M. Strafford, L. Lazorova, A. Avdeef, K. Luthman, P. Artursson, Absorption classification of oral drugs based on molecular surface properties, *J. Med. Chem.* 46 (2003) 558-570.
55. C. Tannergren, T. Knutson, L. Knutson, H. Lennernas, The effect of ketoconazole on the in vivo intestinal permeability of fexofenadine using a regional perfusion technique, *Br. J. Clin. Pharmacol.* 55 (2003) 182-190.
56. M. Lindenberg, S. Kopp, J.B. Dressman. Classification of orally administered drugs on the World Health Organization Model of Essential Medicines according to the Biopharmaceutics Classification System, *Eur. J. Pharm. Biopharm.* 58 (2004) 265-278.
57. D.A. Smith, Design of drugs through a consideration of drug metabolism and pharmacokinetics, *Eur. J. Drug Metab. Pharmacokinet.* 3 (1994) 193-199.
58. K. Ito, H. Suzuki, T. Horie, Y. Sugiyama, Apical/basolateral surface expression of drug transporters and its role in vectorial drug transport, *Pharm. Res.* 22 (2005) 1559-1577.

59. R.B. Kim, M.F. Fromm, C. Wandel, B. Leake, A.J. Wood, D.M. Roden, G.R. Wilkinson, The drug transporter P-glycoprotein limits oral absorption and brain entry of HIV-1 protease inhibitors, *J. Clin. Invest.* 101 (1998) 289-294.
60. J.W. Polli, S.A. Wring, J.E. Humphreys, L. Huang, J.B. Morgan, L.O. Webster, C.S. Serabjit-Singh, Rational use of in vitro P-glycoprotein assays in drug discovery, *J. Pharmacol. Exp. Ther.* 299 (2001) 620-628.
61. M.E. Taub, L. Kristensen, S. Frokjaer, Optimized conditions for MDCK permeability and turbidimetric solubility studies using compounds representative of BCS classes I-IV, *Eur. J. Pharm. Sci.* 15 (2002) 331-340.
62. S. Lu, A.W. Gough, W.F. Bobrowski, B.H. Stewart, Transport properties are not altered across Caco-2 cells with heightened TEER despite underlying physiological and ultrastructural changes, *J. Pharm. Sci.* 85 (1996) 270-273.
63. S. Yee, In vitro permeability across Caco-2 cells (colonic) can predict in vivo (small intestinal) absorption in man--fact or myth, *Pharm. Res.* 14 (1997) 763-766.
64. K. Watanabe, T. Sawano, K. Terada, T. Endo, M. Sakata, J. Sato, Studies on intestinal absorption

- of sulpiride (1): carrier-mediated uptake of sulpiride in the human intestinal cell line Caco-2, *Biol. Pharm. Bull.* 25 (2002) 885-890.
65. K. Watanabe, T. Sawano, T. Endo, M. Sakata, J. Sato, Studies on intestinal absorption of sulpiride (2): transepithelial transport of sulpiride across the human intestinal cell line Caco-2, *Biol. Pharm. Bull.* 25 (2002) 1345-1350.
66. D. Sun, H. Lennernas, L.S. Welage, J.L. Barnett, C.P. Landowski, D. Foster, D. Fleisher, K.D. Lee, G.L. Amidon, Comparison of human duodenum and Caco-2 gene expression profiles for 12,000 gene sequences tags and correlation with permeability of 26 drugs, *Pharm. Res.* 19 (2002) 1400-1416.
67. D.L. Bourdet, G.M. Pollack, D.R. Thakker, Intestinal absorptive transport of the hydrophilic cation ranitidine: a kinetic modeling approach to elucidate the role of uptake and efflux transporters and paracellular vs. transcellular transport in Caco-2 cells, *Pharm. Res.* 23 (2006) 1178-1187.
68. C. Hilgendorf, G. Ahlin, A. Seithel, P. Artursson, A.L. Ungell, J. Karlsson, Expression of thirty-six drug transporter genes in human intestine, liver, kidney, and organotypic cell lines, *Drug Metab. Dispos.* 35 (2007) 1333-1340.

69. A. Balakrishnan, D.J. Sussman, J.E. Polli, Development of stably transfected monolayer overexpressing the human apical sodium-dependent bile acid transporter (hASBT), *Pharm. Res.* 22 (2005) 1269-1280.
70. P.V. Balimane, S. Chong, K. Patel, Y. Quan, J. Timoszyk, Y.H. Han, B. Wang, B. Vig, T.N. Faria, Peptide transporter substrate identification during permeability screening in drug discovery: comparison of transfected MDCK-hPepT1 cells to Caco-2 cells, *Arch. Pharm. Res.* 30 (2007) 507-518.
71. H. Satoh, F. Yamashita, M. Tsujimoto, H. Murakami, N. Koyabu, H. Ohtani, Y. Sawada, Citrus juices inhibit the function of human organic anion-transporting polypeptide OATP-B, *Drug Metab. Dispos.* 33 (2005) 518-523.
72. S. Matsushima, K. Maeda, C. Kondo, M. Hirano, M. Sasaki, H. Suzuki, Y. Sugiyama, Identification of the hepatic efflux transporters of organic anions using double-transfected Madin-Darby canine kidney II cells expressing human organic anion-transporting polypeptide 1B1 (OATP1B1)/multidrug resistance-associated protein 2, OATP1B1/multidrug resistance 1, and OATP1B1/breast cancer resistance protein, *J. Pharmacol. Exp. Ther.* 314 (2005) 1059-1067.

73. M. Sasaki, H. Suzuki, K. Ito, T. Abe, Y. Sugiyama, Transcellular transport of organic anions across a double-transfected Madin-Darby canine kidney II cell monolayer expressing both human organic anion-transporting polypeptide (OATP2/SLC21A6) and Multidrug resistance-associated protein 2 (MRP2/ABCC2), *J. Biol. Chem.* 277 (2002) 6497-6503.
74. K. Letschert, M. Komatsu, J. Hummel-Eisenbeiss, D. Keppler, Vectorial transport of the peptide CCK-8 by double-transfected MDCKII cells stably expressing the organic anion transporter OATP1B3 (OATP8) and the export pump ABCC2, *J. Pharmacol. Exp. Ther.* 313 (2005) 549-556.
75. S. Mita, H. Suzuki, H. Akita, H. Hayashi, R. Onuki, A.F. Hofmann, Y. Sugiyama, Inhibition of bile acid transport across Na⁺/taurocholate cotransporting polypeptide (SLC10A1) and bile salt export pump (ABCB 11)-coexpressing LLC-PK1 cells by cholestasis-inducing drugs, *Drug Metab. Dispos.* 34 (2006) 1575-1581.
76. S. Tolle-Sander, J. Rautio, S. Wring, J.W. Polli, and J.E. Polli, Midazolam exhibits characteristics of a highly permeable P-glycoprotein substrate, *Pharm. Res.* 20 (2003) 757-764.
77. C.L. Cummins, W. Jacobsen, L.Z. Benet, Unmasking the dynamic interplay between intestinal P-

- glycoprotein and CYP3A4, *J. Pharmacol. Exp. Ther.* 300 (2002) 1036-1045.
78. C.L. Cummins, L. Salphati, M.J. Reid, L.Z. Benet, In vivo modulation of intestinal CYP3A metabolism by P-glycoprotein: studies using the rat single-pass intestinal perfusion model, *J. Pharmacol. Exp. Ther.* 305 (2003) 306-314.
79. C.L. Cummins, W. Jacobsen, U. Christians, L.Z. Benet, CYP3A4-transfected Caco-2 cells as a tool for understanding biochemical absorption barriers: studies with sirolimus and midazolam, *J. Pharmacol. Exp. Ther.* 308 (2004) 143-155.
80. J.H. Chang, L.Z. Benet, Glucuronidation and the transport of the glucuronide metabolites in LLC-PK1 cells, *Mol. Pharmaceut.* 2 (2005) 428-434.
81. Y.Y. Lau, Y. Huang, L. Frassetto, L.Z. Benet, Effect of OATP1B transporter inhibition on the pharmacokinetics of atorvastatin in healthy volunteers, *Clin. Pharmacol. Ther.* 81 (2007) 194-204.
82. S.K. Gupta, L.Z. Benet, Effect of food on the pharmacokinetics of cyclosporine in healthy subjects following oral and intravenous administration, *J. Clin. Pharmacol.* 30 (1990) 643-653.

83. Physicians' Desk Reference, 61st ed., Montvale, NJ, Thomson PDR, 2007, pp. 2149-2153.
84. L.Z. Benet, C.L. Cummins, C.Y. Wu, Unmasking the dynamic interplay between efflux transporters and metabolic enzymes, *Int. J. Pharm.* 277 (2004) 3-9.
85. L.Z. Benet, C.L. Cummins, C.Y. Wu, Transporter-enzyme interactions: implications for predicting drug-drug interactions from in vitro data, *Curr. Drug Metab.* 4 (2003) 393-398.
86. G.K. Dresser, D.G. Bailey, B.F. Leake, U.I. Schwarz, P.A. Dawson, D.J. Freeman, R.B. Kim, Fruit juices inhibit organic anion transporting polypeptide-mediated drug uptake to decrease the oral availability of fexofenadine, *Clin. Pharmacol. Ther.* 71 (2002) 11-20.
87. J. Lavelle, S. Follansbee, C.B. Trapnell, W.C. Buhles, K.G. Griffy, D. Jung, A. Dorr, J. Connor, Effect of food on the relative bioavailability of oral ganciclovir, *J. Clin. Pharmacol.* 36 (1996) 238-241.

CHAPTER 2*

- EVALUATION OF THE EFFECTS OF SIMULATED PHYSIOLOGICAL INTESTINAL MEDIA ON CELLULAR STUDIES TO EXAMINE ITS POTENTIAL INFLUENCE ON TRANSPORTER FUNCTION *IN VITRO*

2.1 Introduction

The ability to understand the influence of the gastrointestinal contents on a drug product's permeation through the intestinal epithelia is of great significance to the drug development industry. This chapter focuses on our work to extend the application of simulated physiological intestinal media to cellular studies to assess the role of food-drug interactions in altering the extent of bioavailability via influencing intestinal transporter function. Food-drug interactions have been widely associated with alterations of pharmacokinetic and pharmacodynamic parameters and proven to have significant clinical implications.¹⁻⁴ Extensive research has been done to closely represent the upper gastrointestinal (GI) tract in order to develop an *in vitro-in vivo* correlation (IVIVC).⁵⁻⁸

* This chapter contains material modified from a manuscript in review by Custodio and Benet entitled "Application of dissolution testing simulated physiological intestinal media to in vitro cellular transport studies," *Int. J. Pharm.* (2008).

Dressman and colleagues have developed fluidic models that mimic the physiological media conditions of gastric and intestinal fluids.^{5,9} Two of the most well recognized and characterized media are Fasted State Simulated Intestinal Media (FaSSIF) and Fed State Simulated Intestinal Media (FeSSIF) and their components are listed in Table 2.1.^{5,9}

Fasted state simulated intestinal fluid (FaSSIF)			Fed state simulated intestinal fluid (FeSSIF)		
pH		6.5	pH		5.0
osmolality		270±10 mOsmol	osmolality		635±10 mOsmol
Sodium taurocholate		3 mM	Sodium taurocholate		15 mM
Lecithin		0.75 mM	Lecithin		3.75 mM
KH ₂ PO ₄		3.9 g	Acetic acid		8.65 g
KCl		7.7 g	KCl		15.2 g
NaOH	qs	pH 6.5	NaOH	qs	pH 5.0
Deionized water	qs	1 liter	Deionized water	qs	1 liter

Table 2.1 The composition of two physiological media commonly utilized to simulate fasted (FaSSIF) and fed (FeSSIF) intestinal conditions.

Studies with these media have been predominately applied to evaluating food effects in dissolution testing. An example of a typical protocol for such a dissolution assay can be found in Table 2.2, which includes multiple BCS Class 1 and 2 compounds, various types of media and dissolution apparatus as well as differing paddle rotational speeds.

Drug	BCS	Media	Dissolution tester type	rpm
Acetaminophen	I	water, SIF _{sp} , FaSSIF, FeSSIF, milk	Pharma Test Type PTW SIII-PTW S3C	50,100
Metoprolol	I	SIF _{sp} , SGF, FaSSIF, FeSSIF	Erweka Type DT6	100
Danazol	II	water, SIF _{sp} , FaSSIF, FeSSIF, milk	Pharma Test Type PTW SIII-PTW S3C	50,100
Mefenamic Acid	II	water, SIF _{sp} , FaSSIF, FeSSIF, milk	Pharma Test Type PTW SIII-PTW S3C	50,100
Ketoconazole	II	SGF _{sp} , FaSSIF, FeSSIF	Pharma Test Type PTW SIII-PTW S3C	100

Table 2.2 Examples of typical protocols employed in dissolution testing experiments.

A field of study pioneered by Dr. Dressmans's Group focuses on the study of the dissolution properties of various classes (i.e. BCS/BDDCS Classes 1-4) of drugs as well as various dosage forms (e.g. soft-gels versus hard gelatin capsules, etc). Dressman and colleagues have demonstrated that the rate and extent of dissolution is influenced by both the physiological media and the class of drug tested, clearly showing that the Class 1 drug, metoprolol, is independent of physiological media (Figure 2.1a).⁵

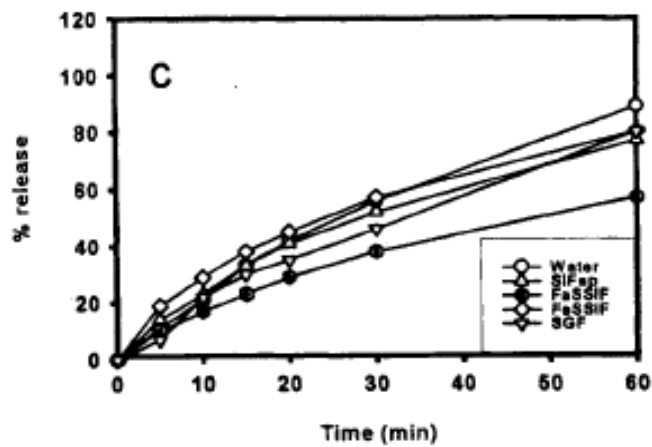
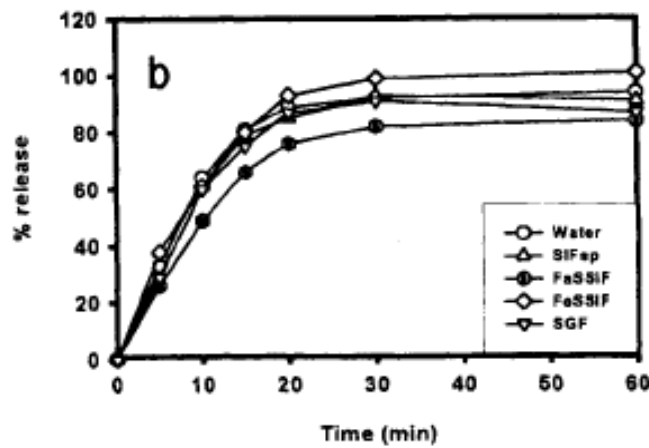
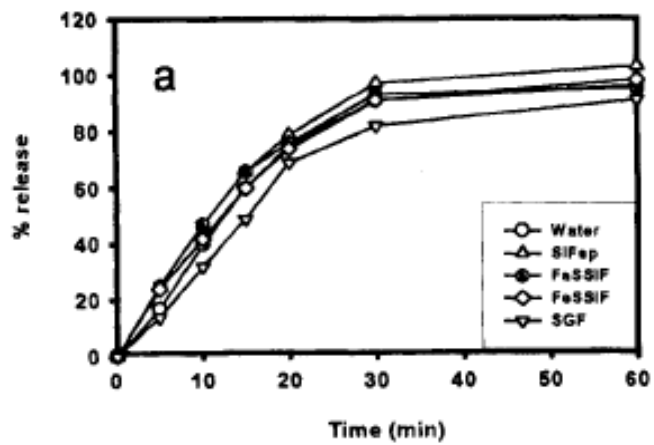


Figure 2.1a Simulated physiological media has no effect on the dissolution for three different tablets of metoprolol, a BCS Class 1 compound.

Contrastingly, the dissolution of the Class 2 drug, danazol is dependent on the type simulated physiological media used (Figure 2.1b).⁵

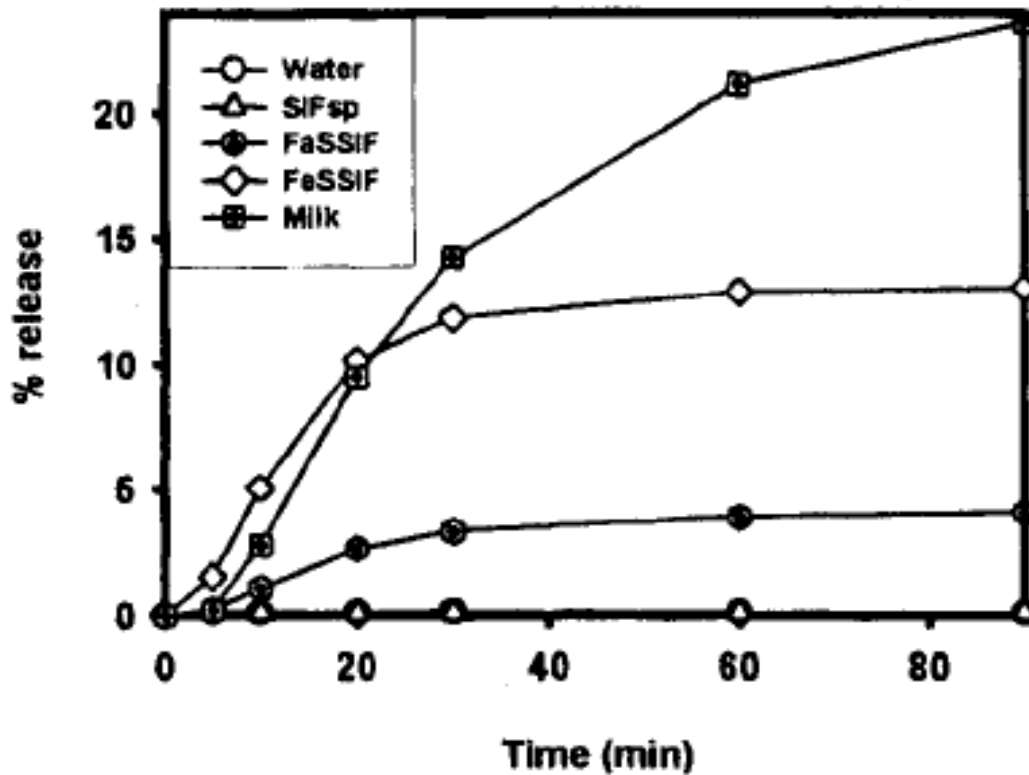


Figure 2.1b The dissolution of capsules of danazol is dependent upon the types of simulated physiological media applied.

Here we seek to extend the application of various established simulated physiological intestinal media to *in vitro* cellular experiments to assess the role of food-drug interactions in altering the extent of drug

availability by influencing intestinal transporter function.

The model *in vitro* cellular systems currently employed in academia and industry to screen the intestinal permeability properties of potential drug candidates have been well characterized.¹⁰⁻¹³ The prediction of absorption characteristics of a compound is exceedingly important in the early stages of drug development.

High throughput screening techniques such as the immobilized artificial membranes (IAM) and the parallel artificial membrane permeability assay (PAMPA) have been increasingly employed.^{14,15} However, these systems cannot adequately account for the role of intestinal transporters in drug absorption.^{11,16,17}

Cellular assays assessing the bidirectional transport of compounds across a monolayer are a widely accepted approach that accounts for passive and active components of absorption by using various cellular systems including, but not limited to, human colonic adenocarcinoma cells (Caco-2), Madin Darby canine kidney cells (MDCK), and Lewis lung carcinoma-porcine kidney cells (LLC-PK). However, these systems are limited in their predictive ability by the transport media commonly used: the standard Hank's buffered salt solution (HBBS) containing 25 mM 4-(2-hydroxyethyl)-1-

piperazineethanesulfonic acid (HEPES) and 1% fetal bovine serum FBS, pH 7.4.^{18,19} While this buffered, aqueous environment is suitable for *in vitro* cellular studies, it does not possess properties characteristic of the GI tract prior to, or following, meal ingestion.^{20,21}

Work has been ongoing for several years to optimize the conditions for cellular transport experiments through the application of biorelevant media.^{18,21-23} Examples of various biorelevant media can be readily found in the literature.^{5,24,25} However, replacing the standard aqueous conditions with biorelevant media has demonstrated the incompatibility of various simulated intestinal fluids when applied to cell-culture based models. Ingels and coworkers have done considerable work documenting the effects of simulated fluids on Caco-2 cells.²¹

Here, we seek to further explore the crossover utility of various simulated media to live cellular assays. We investigated the well recognized and characterized FeSSIF media as well as a variation of another *in vitro* simulation of food effect incorporating oil to simulate dietary fat as described by Al-Behaisi *et al.*²⁵ We evaluated the effects of Ensure Plus[®], which has previously been used by Klein and colleagues as media to simulate the postprandial stomach and shown to closely resemble the FDA standard breakfast.²⁴ In addition, we utilize a simulated media containing monoolein, as

described Konishi and colleagues, to examine the effects of monoglycerides that are expected in the postprandial intestine at high levels.^{26,27}

For our laboratory's study approach, we ran a series of bidirectional transport experiments, in the presence or absence of the various simulated physiological intestinal media, utilizing the MDCK cells and the MDR1-MDCK cell line incorporating the stable expression of the MDR1 gene encoding for the P-glycoprotein (P-gp).²⁸

2.2 Materials and methods

2.2.1 Materials

MDR1-MDCK and MDCK cell lines were generously provided by Dr. Ira Pastan (National Cancer Institute, National Institutes of Health, Bethesda, MD). All components necessary for proper cell culture growth conditions (described below) were purchased from the University of California, San Francisco Cell Culture Facility (San Francisco, CA). [³H]-Vinblastine sulfate was purchased from Moravek Biochemicals and Radiochemicals (Brea, CA). GG918 (GF120918: N-{4-[2-(1,2,3,4-tetrahydro-6,7-dimethoxy-2-isoquinolinyl)-ethyl]-phenyl}-9,10-dihydro-5-methoxy-9-oxo-4-acridine carboxamine) was a kind gift from GlaxoSmithKline (Research Triangle Park, NC). Ensure Plus[®] (Abbott, Abbott Park, IL) and peanut oil (The Hain Celestial

Group, INC., Melville, NY) were purchased from Walgreens (San Francisco, CA). All other chemicals were of reagent grade and purchased from Sigma-Aldrich (St. Louis, MO). Six-well tissue culture treated polystyrene plates were obtained from Corning Life Science (Acton, MA). Falcon polyethylene terephthalate cell culture inserts (pore size 0.4 μm , diameter 4.2 cm^2) were obtained from BD Biosciences (Bedford, MA).

2.2.2 Cell culture

MDCK cells were grown in a humidified 5% CO_2 atmosphere at 37°C using Dulbecco's modified Eagle's medium containing 4.5 g/L glucose, 0.584 g/L *l*-glutamine, 3.7 g/L NaHCO_3 , 10% heat-inactivated FBS, 100 U/mL penicillin and 100 U/mL streptomycin. MDR1-MDCK cell culture medium was the same as above with the addition of 80 ng/mL colchicine as a selective supplement.²⁸ Cells were grown to confluence and harvested. Monolayers were prepared by seeding harvested cells onto polyethylene terephthalate cell culture inserts at a density of approximately 1,000,000 cells/insert. Growth medium was refreshed once every two days and one day prior to the experiment, which was performed 5-6 days postseeding for both cell lines.

2.2.3 Bidirectional transport experiments

The transport assays were performed following a modified protocol previously described by our laboratory.²⁹⁻³¹ In brief, cell monolayers were preincubated in control transport buffer (Hank's buffered salt solution containing 25 mM HEPES and 1% FBS, pH 7.4) at 37°C for 20 minutes. Transepithelial electrical resistance (TEER) values were then measured by the Millicell electrical resistance system utilizing "chopstick" electrodes (Millipore Corporation, Bedford, MA). On average, the MDR1-MDCK cells possessed values of approximately 4000-5000 $\bullet\cdot\text{cm}^2$, while the MDCK cells possessed TEER values of approximately 200-300 $\bullet\cdot\text{cm}^2$. All experiments were performed in triplicate and conducted on at least three separate occasions to ensure reproducibility. Both transfected and parental cells were run on the same day to account for potential between-day variability of radiolabeled counts and TEER values.

The experiment was started by the addition of 10 $\bullet\text{M}$ vinblastine in control transport buffer to the donor compartment and control transport buffer only to the receiver compartment. In the experiments in which Ensure Plus[®], the peanut oil formulation or FeSSIF were applied, the same concentration of vinblastine was used and the test media was substituted for the control transport

buffer. FeSSIF was prepared as previously and extensively described by Dr. Jennifer Dressman's research group.^{5,32} The peanut oil formulation (10% peanut oil, 1% methylcellulose, and 0.130 grams/mL of sucrose) is a modification of a simulation by Al-Behaisi *et al.*²⁵ In the experiments run in the presence of monoolein, the same concentration of vinblastine was used and the control transport buffer was supplemented with monoolein.^{26,27} The final volume in each of the chambers was 1.5 mL on the apical side and 2.5 mL on the basolateral side. Experimental samples were isolated from the receiver compartment at three various time points. At the first two time points, 200 μ L samples were removed and then replaced with fresh media to restore initial starting volumes. At the final time point, following collecting of the last 200 μ L sample, contents of both chambers were removed by suction, each cell culture insert was dipped three times into ice-cold PBS and the cell culture insert membranes were collected. All experiments were run at 37°C with a shaking speed of 25 strokes/minute in the Boekel Shake 'N' Bake Incubator Shaker II (Boekel Scientific, Feasterville, PA).

2.2.4 Analysis of samples

2.2.4.1 Sample preparation

All samples were added to 5 mL Econo-Safe™ Counting Cocktail (Research Products International Corporation, Mount Prospect, IL) and vortexed. Cells monolayers were solubilized by sonication (in an ultrasonic bath) for 15 minutes.

2.2.4.2. Sample analysis

All samples were analyzed using a Beckman LS180 scintillation counter (Beckman Industries, Palo Alto, CA).

2.3 Results

2.3.1 Effect of FeSSIF on the bidirectional transport of vinblastine across MDR1-MDCK cell monolayers

We attempted to investigate the effects of fed state simulated intestinal fluid (FeSSIF) on the bidirectional transport of vinblastine in MDR1-MDCK cells (Table 2.3).

MDR1-MDCK Cells	Transepithelial electrical resistance (TEER) Values (Ω/cm^2)		
	1 Hour	2 Hours	3 Hours
Control Buffer	4834 \pm 290	4574 \pm 399	4208 \pm 185
FeSSIF	1012 \pm 479	-- *	-- *

Table 2.3 Fed State Simulated Intestinal Fluid (FeSSIF) affects MDR1-MDCK monolayer integrity.

* Below limit of detection by the Millipore Millicell electrodes.

The integrity of the cellular monolayer was monitored by measuring the transepithelial electrical resistance (TEER) values. As displayed in Table 2.3, the presence of FeSSIF resulted in decreased TEER values causing the monolayer integrity to become compromised.

2.3.2 Effect of GG918 on the bidirectional transport of vinblastine across MDR1-MDCK cell monolayers

We investigated the effects of a known P-gp inhibitor, GG918, on the bidirectional transport of vinblastine in MDR1-MDCK cells (Figure 2.2). The presence of GG918 (0.5 μ M) resulted in a reduction of the net flux ratio (B to A / A to B) by 88%. Figure 2.2 depicts the observed decrease in the basolateral to apical (B to A) transport and the moderate increase in apical to basolateral (A to B) transport.

2.3.3 Effect of biorelevant media on the bidirectional transport of vinblastine across MDR1-MDCK cell monolayers

We investigated the effects of an oil formulated intestinal simulation on the bidirectional transport of vinblastine in MDR1-MDCK cells (Figure 2.3).

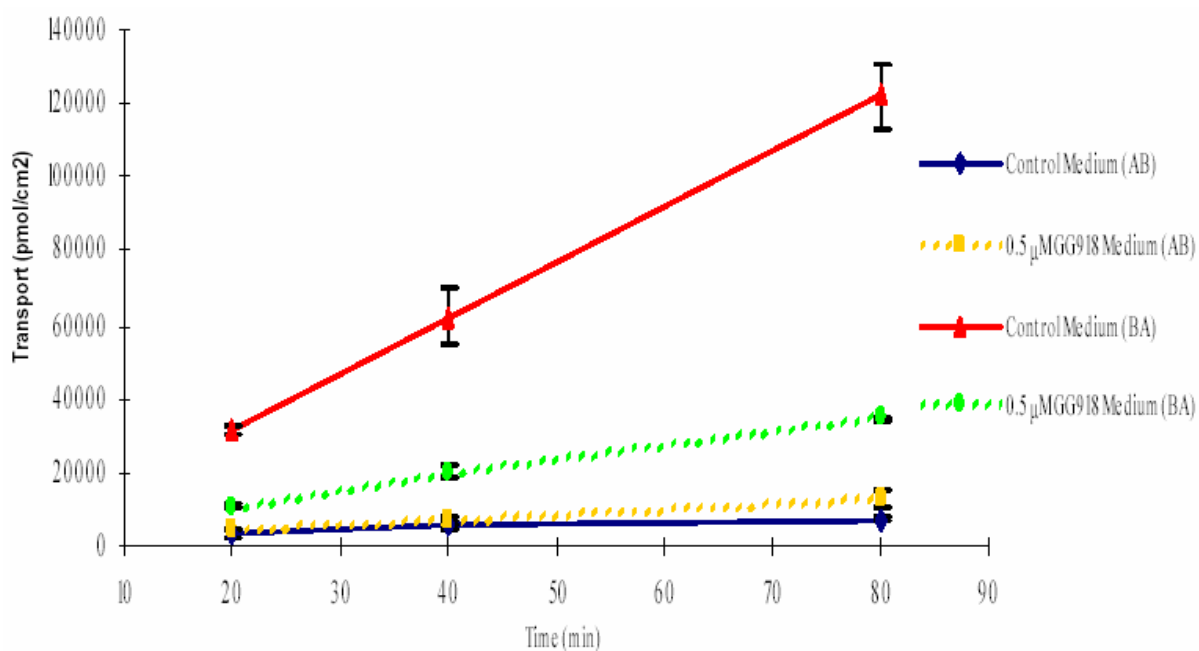


Figure 2.2 Bidirectional transport of vinblastine in MDR1-MDCK cells in the presence or absence of the known P-gp inhibitor, GG918.

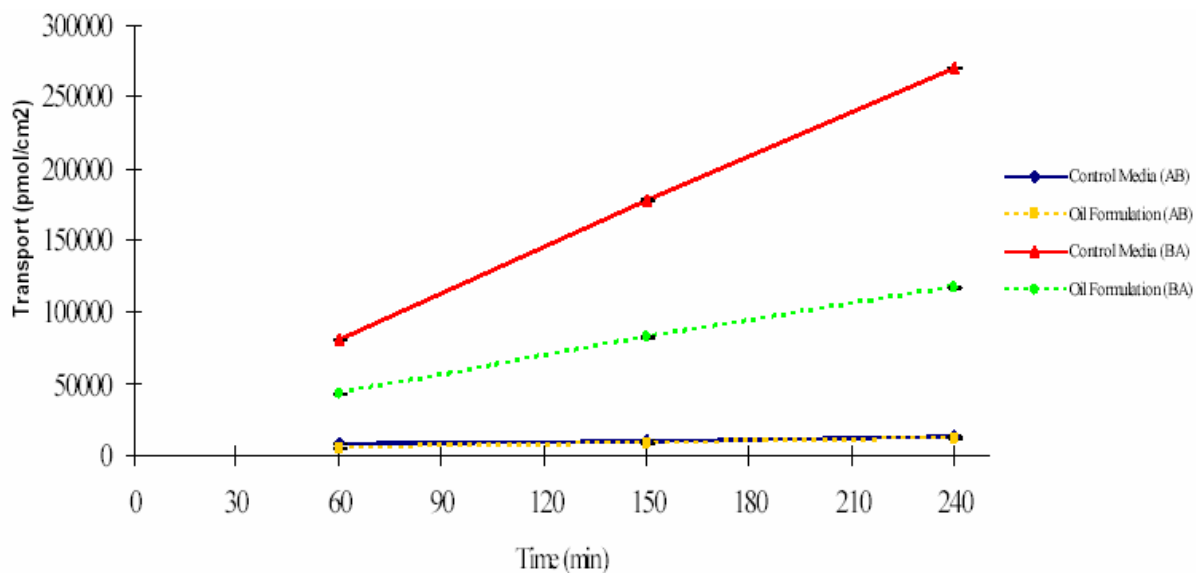


Figure 2.3 Bidirectional transport of vinblastine in MDR1-MDCK cells with or without the simulated physiological oil formulation media.

As depicted in Figure 2.3, the presence of this biorelevant media resulted in a 94% decrease in the next flux ratio, from 43 to 2.5. Figure 2.3 depicts the significant drop in B to A transport in the presence of the oil formulation.

We also investigated the effects of Ensure Plus[®] on the bidirectional transport of vinblastine in MDR1-MDCK cells (Figure 2.4). This set of experiments compared the control transport buffer with full strength Ensure Plus[®] as well as half strength diluted in control buffer. The presence of both the diluted and undiluted Ensure Plus[®] resulted in a significant reduction in the net flux ratio with the half-strength (0.5X) decreasing by 49%, from 17.3 to 8.8. Bidirectional studies run with undiluted (1.0X) Ensure Plus[®] resulted in an 84% decrease in the next flux ratio, from 17.3 to 2.8. Figure 2.4 depicts the effects of 0.5X and 1.0X Ensure Plus[®] on vinblastine transport.

2.3.4 Effect of monoolein supplemented media on the bidirectional transport of vinblastine across MDR1-MDCK cell monolayers

In 2004, Konishi *et al.* reported the inhibitory

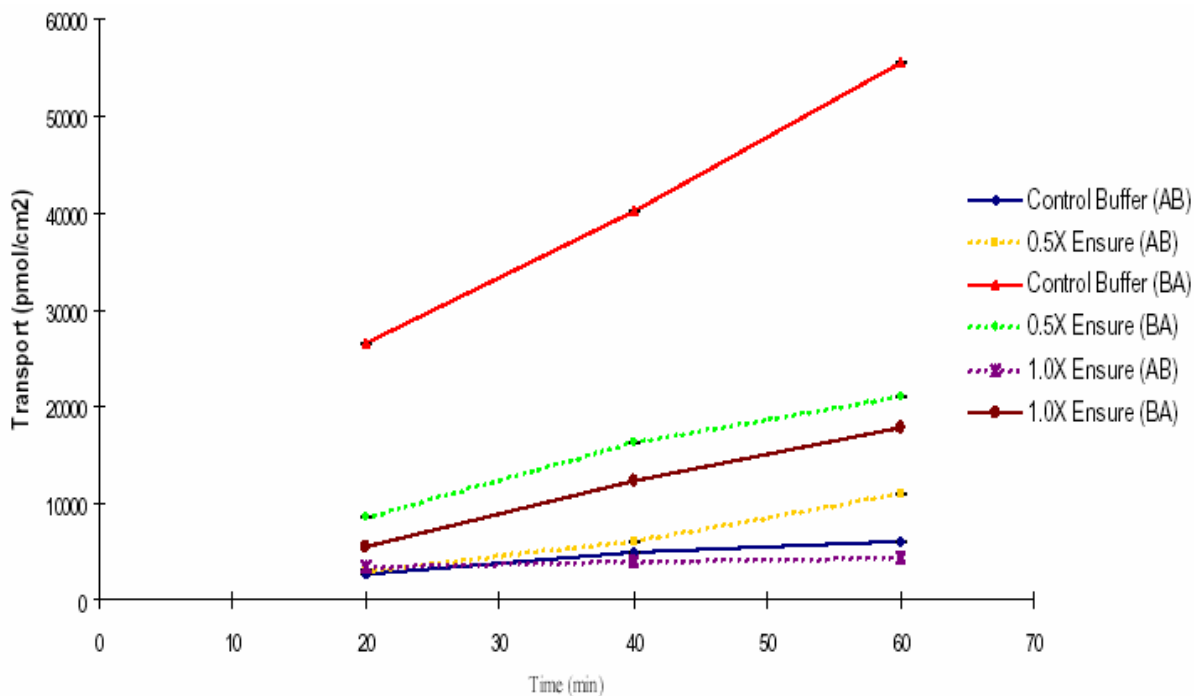


Figure 2.4 Bidirectional transport of vinblastine in MDR1-MDCK cells in the absence or presence of half-strength (0.5X) or full strength (1.0X) Ensure Plus.

effect of various monoglycerides on P-gp function *in vitro*.^{26,27} We therefore investigated the effects of monoolein on the bidirectional transport of vinblastine in MDR1-MDCK cells (Figure 2.5). The presence of monoolein (300 μ M) resulted in a reduction of the net flux ratio by 92%, from 25.9 to 2.1. Figure 2.5 depicts the monoolein effect on vinblastine transport.

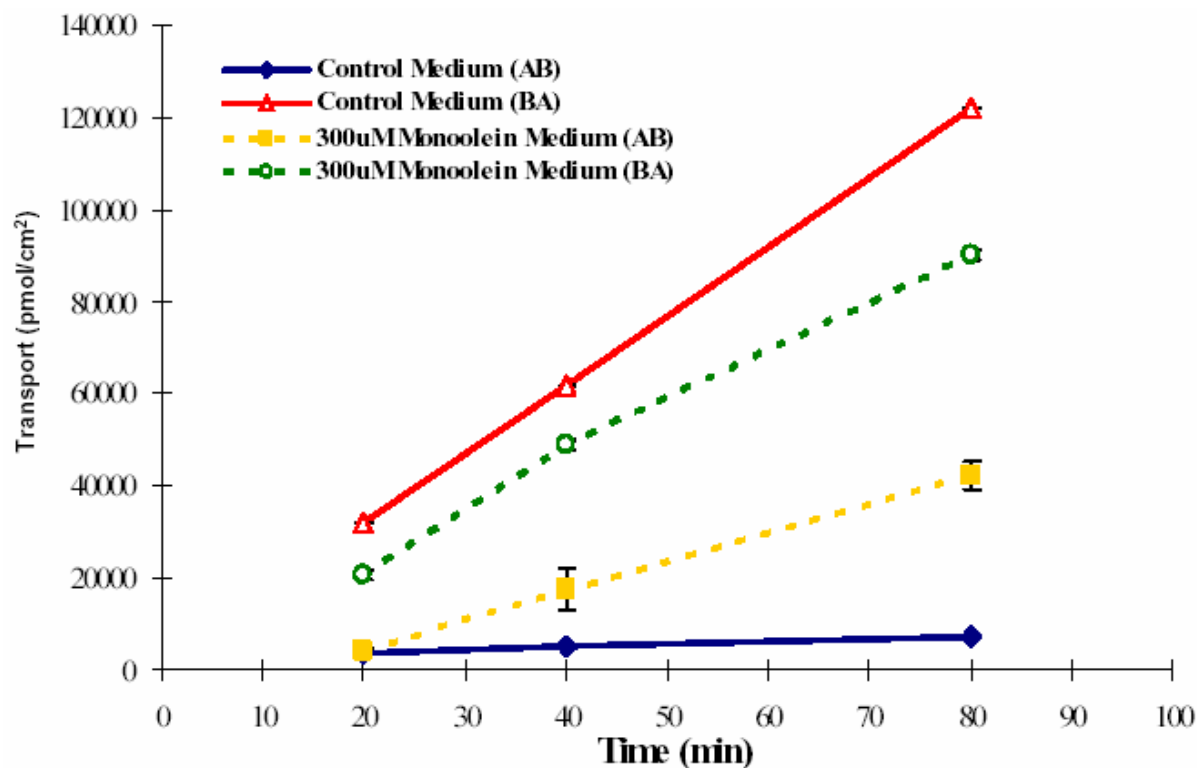


Figure 2.5 Bidirectional transport of vinblastine in MDR1-MDCK cells with or without monoolein supplemented media.

Table 2.5 lists the apparent permeability (P_{app}) values for vinblastine in both the A to B and B to A directions in the presence of control media and monoolein media, as well as the known P-gp inhibitor GG918. Similar to the GG918 results, in the presence of monoolein we observed a decrease in transport and apparent permeability in the B to A direction, as well as an increase transport and apparent permeability in the A to B direction. In the nontransfected parental control MDCK cells, monoolein

(500 \bullet M) has no effect on the B to A or A to B transport of vinblastine (data not shown).

Experimental Media \bullet	Control Media	GG918 Media (0.5 \bullet M)	Monoolein Media (300 \bullet M)
P_{app} Values A \bullet B in MDR1-MDCK Cells (10 ⁻⁶ cm/s)	0.97 \pm 0.02	2.2 \pm 0.4	10.6 \pm 0.6
P_{app} Values B \bullet A in MDR1-MDCK Cells (10 ⁻⁶ cm/s)	25.1 \pm 2.6	6.5 \pm 0.2	19.0 \pm 1.2

Table 2.4 Apparent permeability values (P_{app}) for vinblastine in MDR1-MDCK cells. $P_{app} = (dQ/dt)/(A \bullet C_0)$; where dQ/dt is the amount transported (Q) over time (t), A is the surface area of the insert, and C_0 is the initial concentration of the donor compartment. P_{app} values \pm standard deviation are listed for the both the Apical to Basolateral (A \bullet B) permeability and the Basolateral to Apical (B \bullet A) permeability, each with $n = 3$ transwells.

2.4 Discussion

First, we attempted to investigate the effects of fed state simulated intestinal fluid (FeSSIF) on the bidirectional transport of vinblastine in MDR1-MDCK cells. FeSSIF was developed as a tool in dissolution testing to mimic the postprandial intestine.^{5,9} The acidic conditions of the buffer along with its increased

osmolarity are suitable for solubility studies with formulated compounds (e.g. gencaps and tablets) but are unsuitable for live cellular studies.^{19,22} Attempts to conduct transport assays in the presence of FeSSIF proved toxic to the cells (Table 2.3) and the ability to accurately measure the vectorial transport of vinblastine across the MDR1-MDCK was compromised. The toxicity of FeSSIF on the integrity of the cellular monolayer can be seen by the drastic decline of transepithelial electrical resistance (TEER) values listed in Table 2.3. The TEER value decline may be attributed to the FeSSIF influence on the tight junctions of the cell monolayer as well its influence on the adherence of the cells to the semi-porous membrane. These results are consistent with the toxic effect of FeSSIF on Caco-2 cells demonstrated by Patel et al.²² The loss of resistance we observe correlates well with results reported by Ingels et al.¹⁹ These authors showed an immediate decrease in TEER values on the Caco-2 monolayer in the presence of FeSSIF, compared with control buffer, with values undetectable after 30 minutes. Our data show an 80% drop in monolayer resistance after 1 hour and TEER values below our level of detection thereafter. That MDR1-MDCK monolayers appear to be more resilient to the toxicity of FeSSIF may be attributed to their inherently greater TEER values as compared to Caco-2 cells. The MDR1-MDCK cells possess

values of approximately 4000-5000 $\bullet\cdot\text{cm}^2$ while the Caco-2 cell system possesses TEER values of approximately 800-1000 $\bullet\cdot\text{cm}^2$ (Lu et al., 1996, Custodio et al., 2008).^{4,33}

Next, we investigated the effects of a known P-gp inhibitor, GG918 (0.5 $\bullet\text{M}$), on the bidirectional transport of vinblastine in MDR1-MDCK cells (Figure 2.2). As expected from an efflux transport inhibitor, we observed a decrease in the basolateral to apical (B to A) transport together with a much more moderate increase in apical to basolateral (A to B) transport, effectively reducing the net flux ratio (B to A / A to B) by 88%.

In 2002, Al-Behaisi et al. reported the use of dietary components added to simulated intestinal media to evaluate food effects on dissolution profiles.²⁵ We investigated the effects of an oil formulated intestinal simulation on the bidirectional transport of vinblastine in MDR1-MDCK cells (Figure 2.3). In 2004, Klein et al. reported the use of Ensure Plus[®] as media to simulate the postprandial effects.²⁴ We investigated the effects of Ensure Plus[®] on the bidirectional transport of vinblastine in MDR1-MDCK cells (Figure 2.4) using the full strength as well as half strength diluted in control buffer. We observed a significant decrease in the net flux ratio of vinblastine in both the oil formulation (94%) and Ensure Plus[®] (82%) transport studies. This effect is most

evident by the significant reductions observed in the B to A transport of vinblastine in Figures 2.3 and 2.4.

The bidirectional transport profile of vinblastine depicting a 88% drop in net flux ratio was expected in the presence of the known P-gp inhibitor, GG918 (0.5 μ M), indicative of a transporter inhibition effect. The resulting effects of the oil formulation and Ensure Plus[®], declines in net flux ratios by 94% and 82% respectively, may indicate that these formulations may also be inhibiting the transport of vinblastine. However, we observed transport profiles for the oil formulation and Ensure Plus[®] in the nontransfected parental MDCK cell line that were comparable to the transfected MDR1-MDCK cell line suggesting that the increased viscosity of the two formulations may play a role in the decreased absorption. There is also the potential for shielding effects to occur in the presence of the two formulations thereby reducing the amount of free drug available at the membrane.

Such confounding factors as described above led us to investigate a less complex test media, one that has been previously documented by Konishi and coworkers.^{26,27} We investigated the effects of monoolein on the bidirectional transport of vinblastine in MDR1-MDCK cells (Figure 2.5). The B to A transport of vinblastine in the transfected cell is 26-fold higher than the A to B

transport. When 300 μ M monoolein was added to the transport buffer, B to A transport decreased and A to B transport increased so that the net flux ratio in the presence of monoolein was only 2. Contrastingly, in the control MDCK cells there is no effect of monoolein on the B to A and A to B transport fluxes (data not shown). As P-gp is an apical efflux transporter, we would expect to see a marked decrease in the amount transported in the B to A direction if the transporter function is diminished. The increase in transport observed in the A to B directional may also be attributed to transporter inhibition because the amount of drug effluxed back into the apical compartment may be reduced if the transporter function is diminished thereby increasing the amount that reaches the basolateral component. In the presence of monoolein, the A to B apparent permeability (P_{app}) values increased while the B to A apparent permeability values decreased (Table 2.4). This change in P_{app} values followed the same trend observed with GG918 and is consistent with what we would expect if P-gp function were inhibited. These results suggest a potentially important inhibitory effect of monoglycerides on the transport of vinblastine *in vitro*.

Our findings are of particular interest as Ensure Plus[®] has been shown to closely resemble the FDA Standard Breakfast; the peanut oil, methylcellulose, sucrose

simulation has been shown to mimic fed state intestinal conditions; and the monoolein supplemented media represents the presence of monoglycerides expected in the gut following a high fat meal. The decrease in net flux ratio for vinblastine in MDR1-MDCK cells with addition of the three simulated high fat meal conditions indicate that P-glycoprotein may be inhibited. This is supported by the data demonstrating that monoolein does not influence the net flux ratio of vinblastine in the parental control cells. This *in vitro* effect underscores the utility of biorelevant media in cell culture-based permeability models and on-going work may help elucidate current trends in food-drug interactions seen *in vivo*.

2.5 References

1. B.N. Singh, Effects of food on clinical pharmacokinetics, Clin. Pharmacokinet. 37 (1999) 213-255.
2. R.Z. Harris, G.R. Jang, S. Tsunoda, Dietary effects on drug metabolism and transport, Clin. Pharmacokinet. 42 (2003) 1071-1088.
3. W.N. Charman, C.J.H. Porter, S. Mithani, J.B. Dressman, Physiochemical and physiological mechanisms for the effects of food on drug absorption: the role of lipids and pH, J. Pharm. Sci. 86 (1997) 269-282.
4. J.M. Custodio, C.Y. Wu, L.Z. Benet, Predicting drug disposition, absorption/elimination/transporter interplay and the role of food on drug absorption, Adv. Drug Deliv. Rev. 60 (2008) 717-733.
5. E. Galia, E. Nicolaidis, D. Hörter, R. Löbenberg, C. Reppas, J.B. Dressman, Evaluation of various dissolution media for predicting in vivo performance of class I and II drugs, Pharm. Res. 15 (1998) 698-705.
6. E. Nicolaidis, E. Galia, C. Efthymiopoulos, J.B. Dressman, C. Reppas, Forecasting the in vivo performance of four low solubility drugs from

- their in vitro dissolution data, *Pharm. Res.* 16 (1999) 876-882.
7. J.B. Dressman, C. Reppas, In vitro-in vivo correlations for lipophilic, poorly water-soluble drugs, *Eur. J. Pharm. Sci.* 11 (2000) S73-80.
 8. V.H. Sunesen, B.L. Pedersen, H.G. Kristensen, A. Müllertz, In vivo in vitro correlations for a poorly soluble drug, danazol, using the flow-through dissolution method with biorelevant dissolution media, *Eur. J. Pharm. Sci.* 24 (2005) 305-313.
 9. M. Vertzoni, N. Fotaki, E. Kostewicz, E. Stippler, C. Leuner, E. Nicolaidis, J. Dressman, C. Reppas, Dissolution media simulating the intraluminal composition of the small intestine: physiological issues and practical aspects, *J. Pharm. Pharmacol.* 56 (2004) 453-462.
 10. P.V. Balimane, S. Chong, R.A. Morrison, Current methodologies used for evaluation of intestinal permeability and absorption, *J. Pharmacol. Toxicol. Methods* 44 (2000) 301-312.
 11. P.V. Balimane, S. Chong, Cell culture-based models for intestinal permeability: a critique, *Drug Discov. Today* 10 (2005) 335-343.
 12. P.V. Balimane, Y.H. Han, S. Chong, Current industrial practices of assessing permeability and

- P-glycoprotein interaction, *AAPS J.* 8 (2006) E1-13.
13. H. Bohets, R. Annaert, G. Mannens, L. Van Beijsterveldt, K. Anciaux, P. Verboven, W. Meuldermans, K. Lavrijsen, Strategies for absorption screening in drug discovery and development, *Curr. Top. Med. Chem.* 1 (2001) 367-383.
 14. E.H. Kerns, High throughput physicochemical profiling for drug discovery, *J. Pharm. Sci.* 90 (2001) 1838-1858.
 15. E.H. Kerns, L. Di, Pharmaceutical profiling in drug discovery, *Drug Discov. Today* 8 (2003) 316-323.
 16. E.H. Kerns, L. Di, S. Petusky, M. Farris, R. Ley, P. Jupp, Combined application of parallel artificial membrane permeability assay and Caco-2 permeability assays in drug discovery, *J. Pharm. Sci.* 93 (2004) 1440-1453.
 17. A. Avdeef, S. Bendels, L. Di, B. Faller, M. Kansy, K. Sugano, Y. Yamauchi, PAMPA--critical factors for better predictions of absorption, *J. Pharm. Sci.* 96 (2007) 2893-2909.
 18. F. Ingels, B. Beck, M. Oth, P. Augustijns, Effect of simulated intestinal fluid on drug permeability

- estimation across Caco-2 monolayers, *Int. J. Pharm.* 15 (2004) 221-232.
19. F. Ingels, S. Deferme, E. Destexhe, M. Oth, G. Van den Mooter, P. Augustijns, Simulated intestinal fluid as transport medium in the Caco-2 cell culture model, *Int. J. Pharm.* 232 (2002) 183-192.
 20. V.A. Gray, J.B. Dressman, Change of pH requirements for simulated intestinal fluid TS, *Pharmacoepial Forum.* 22 (1996) 1943-1945.
 21. F.M. Ingels, P.F. Augustijns, Biological, pharmaceutical, and analytical considerations with respect to the transport media used in the absorption screening system, Caco-2, *J. Pharm. Sci.* 92 (2003) 1545-1558.
 22. N. Patel, B. Forbes, S. Eskola, J. Murray, Use of simulated intestinal fluids with Caco-2 cells and rat ileum, *Drug Dev. Ind. Pharm.* 32 (2006) 151-161.
 23. M.L. Lind, J. Jacobsen, R. Holm, A. Müllertz, Development of simulated intestinal fluids containing nutrients as transport media in the Caco-2 cell culture model: assessment of cell viability, monolayer integrity and transport of a poorly aqueous soluble drug and a substrate of efflux mechanisms, *Eur. J. Pharm. Sci.* 32 (2007) 261-270.

24. S. Klein, J. Butler, J.M. Hempenstall, C. Reppas, J.B. Dressman, Media to simulate the postprandial stomach I. Matching the physicochemical characteristics of standard breakfasts, *J. Pharm. Pharmacol.* 56 (2004) 605-610.
25. S. Al-Behaisi, I. Antal, G. Morovján, J. Szúnyog, S. Drabant, S. Marton, I. Klebovich, In vitro simulation of food effect on dissolution of deramciclone film-coated tablets and correlation with in vivo data in healthy volunteers, *Eur. J. Pharm. Sci.* 15 (2002) 157-162.
26. T. Konishi, H. Satsu, Y. Hatsugai, K. Aizawa, T. Inakuma, S. Nagata, S.H. Sakuda, H. Nagasawa, M. Shimizu, Inhibitory effect of a bitter melon extract on the P-glycoprotein activity in intestinal Caco-2 cells, *Br. J. Pharmacol.* 143 (2004) 379-387.
27. T. Konishi, H. Satsu, Y. Hatsugai, K. Aizawa, T. Inakuma, S. Nagata, S.H. Sakuda, H. Nagasawa, M. Shimizu, A bitter melon extract inhibits the P-glycoprotein activity in intestinal Caco-2 cells: monoglyceride as an active compound, *Biofactors* 22 (2004) 71-74.
28. I. Pastan, M.M. Gottesman, K. Ueda, E. Lovelace, A.V. Rutherford, M.C. Willingham, A retrovirus carrying an MDR1 cDNA confers multidrug resistance

- and polarized expression of P-glycoprotein in MDCK cells, *Proc. Natl. Acad. Sci. USA* 85 (1988) 4486-4490.
29. S.D. Flanagan, C.L. Cummins, M. Susanto, X. Liu, L.H. Takahashi, L.Z. Benet, Comparison of furosemide and vinblastine secretion from cell lines overexpressing multidrug resistance protein (P-glycoprotein) and multidrug resistance-associated proteins (MRP1 and MRP2), *Pharmacology*. 64 (2002) 126-134.
 30. C.L. Cummins, W. Jacobsen, U. Christians, L.Z. Benet, CYP3A4-transfected Caco-2 cells as a tool for understanding biochemical absorption barriers: studies with sirolimus and midazolam, *J. Pharmacol. Exp. Ther.* 308 (2004) 143-155.
 31. Y.Y. Lau, H. Okochi, Y. Huang, L.Z. Benet, Multiple transporters affect the disposition of atorvastatin and its two active hydroxy metabolites: application of in vitro and ex situ systems, *J. Pharmacol. Exp. Ther.* 316 (2006) 762-771.
 32. E. Galia, E. Nicolaidis, C. Reppas, J.B. Dressman, New media discriminate dissolution of poorly soluble drugs, *Pharm. Res.* 13 (1996) S262.
 33. S. Lu, A.W. Gough, W.F. Bobrowski, B.H. Stewart, Transport properties are not altered across Caco-2

cells with heightened TEER despite underlying physiological and ultrastructural changes, J. Pharm. Sci. 85 (1996) 270-273.

CHAPTER 3

- INVESTIGATING THE INHIBITORY INFLUENCE OF LIPIDIC CONDITIONS IN THE INTESTINE: *IN VITRO* STUDIES

3.1 Introduction

The previous chapter dealt with the experimental approach of applying simulated physiological media as established in the literature to *in vitro* cellular studies. Chapter 2 also discussed the inherent disadvantages and limitations of such an experimental approach, which ultimately led us to explore a less complex test media. We introduced the application of this less complex, monoglyceride supplemented media in Chapter 2 and in this present chapter we go into further detail of our research that focuses on the investigation of the influence of lipids on drug absorption.

The resulting effects of the oil formulation and Ensure Plus[®], declines in net flux ratios by 94% and 82% respectively (Section 2.3.3), indicate that these simulations may be inhibiting the transport of vinblastine. However, we observed transport profiles for the oil formulation and Ensure Plus[®] in the nontransfected parental MDCK cell line that were comparable to the

transfected MDR1-MDCK cell line suggesting that the increased viscosity of the two simulations may play a role in the decreased absorption. With these complex physiological simulations, there is the potential for shielding effects to occur in the presence of the test media thereby reducing the amount of free drug available at the membrane. Such confounding factors are removed when utilizing a less complex test media, such as the one that has been previously documented by Konishi and coworkers^{1,2} and discussed in this chapter.

High fat meals, as recommended by the FDA in Food-Effect Bioavailability and Fed Bioequivalence Studies,³ result in significantly higher levels of lipidic contents in comparison to a fasting state.^{4,5} Moreover, triglycerides are predominant in our fatty foods, and their digestion and absorption have been widely examined.⁶ When triglycerides reach the small intestines, bile acids, their salts and lipases break down these fats first into diglycerides and then into monoglycerides and fatty acids. It should also be noted that monoglycerides and fatty acids are capable of traversing the intestinal mucosal cell membrane, while triglycerides and diglycerides are not. Persson *et al.*⁷ employed the *in vivo* single-pass perfusion model in the proximal human jejunum to evaluate the GI response to meal and showed that the tri-, di-, monoglyceride and free fatty acid

levels rapidly and markedly increased to 9.5 mM in response to food. Considerable attention has been focused not only on lipids resulting from food ingestion but also on lipids introduced into the GI tract from lipidic excipients, since enhanced bioavailability has been demonstrated for poorly water-soluble drugs when coadministered with a high fat meal or a lipid-based drug formulation.⁸ Increased lipid levels have also been shown to influence the pharmacokinetics of lipid soluble compounds that bind extensively to triglyceride-rich lipoproteins with effects being greater for more lipophilic compounds.^{9,10}

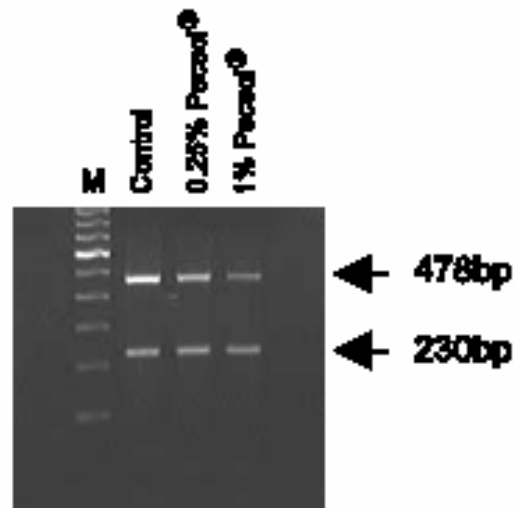
Lipid based delivery systems¹¹ are an ever-growing segment of pharmaceuticals that primarily involves BDDCS Class 2 compounds, as the benefits provided by lipid formulations for BDDCS Class 4 drug are insufficient to overcome their poor permeability characteristics. With the goal of the lipid systems being to improve drug solubilization behavior, the formulation utilized depends on the aqueous solubility of the drug as well as the drug's solubility in lipids. This also holds true when high fat meals are coadministered with the goal of solubility enhancement, as exemplified in a study in which Mueller *et al.*^{12,13} demonstrated that fat-rich meal effects are drug formulation dependent. Moreover, Kaukonen *et al.*¹⁴ demonstrated that triglyceride (TG)

lipid suspension formulations differentially affected various model, poorly soluble compounds, including griseofulvin, danazol and halofantrine, which had previously been shown to exhibit a significant high fat meal effect. The authors examined the effects of various TG formulations on griseofulvin, danazol, halofantrine, diazepam and cinnarizine observing that simple TG solutions offer better solubilization for the more lipophilic compounds while the TG suspensions better enhance the solubility of the less lipid-soluble drugs by increasing the solubilization capacity of the colloidal phase.¹³ The colloidal phase is one example of the various phases that occur in the gastrointestinal tract resulting from the digestion of lipids that are ingested in formulations or food.^{15,16} Accordingly, the role of these intermediate digestion phases, including the lamellar (L₁) liquid crystalline phase and the viscous cubic (C) phase in addition to the aqueous colloidal liquid (L₁) phases, must also be taken into account.^{17,18} Besides the influences on solubilization capacity and intermediate digestion phases, lipids have also been widely reported to influence lymphatic transport of drugs.¹¹

The potential inhibitory influence of lipids is dually highlighted since monoglycerides are found in lipidic excipients. For example, Peceol[®], an excipient

used to enhance absorption of poorly water soluble compounds, is in fact, 2,3-dihydroxypropyl (Z)-octadec-9-enoate, also known as monoolein. Subramanian and Wasan have suggested that Peceol[®] possesses inhibitory properties of P-gp.¹⁹ In order to investigate the influence of Peceol[®] on efflux mechanisms, Wasan and coworkers also employed the Caco-2 cell system. They examined the effect on incubating the cells in the presence of varying concentrations of Peceol[®] for varying times (Figure 3.1).

3.1a



3.1b

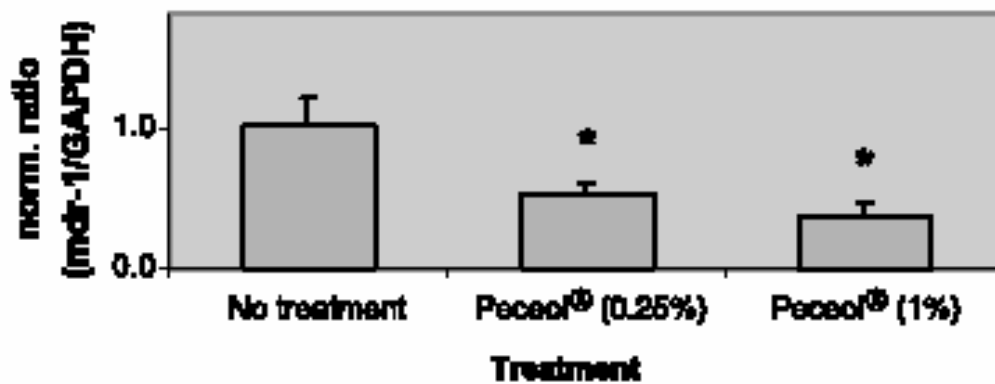


Figure 3.1 (a) mRNA expression profile of mdr-1 (478bp) and GAPDH (230bp) with or without Peceol® (0.25% and 1% v/v) following 1 week incubation with Peceol®. (b) Bar graph of the digital quantification of the mRNA bands from Figure 3.1a.¹⁹

The authors were able to show a P-gp effect at the message level resulting in a reduction in MDR1 mRNA after one day.²⁰ However, following one week treatment of Caco-2 cells with Peceol® (0.25% v/v), the authors not only reported a decrease in P-gp mRNA levels but they also

showed a decrease in protein expression levels of P-gp as well (Figure 3.2).^{20,21}

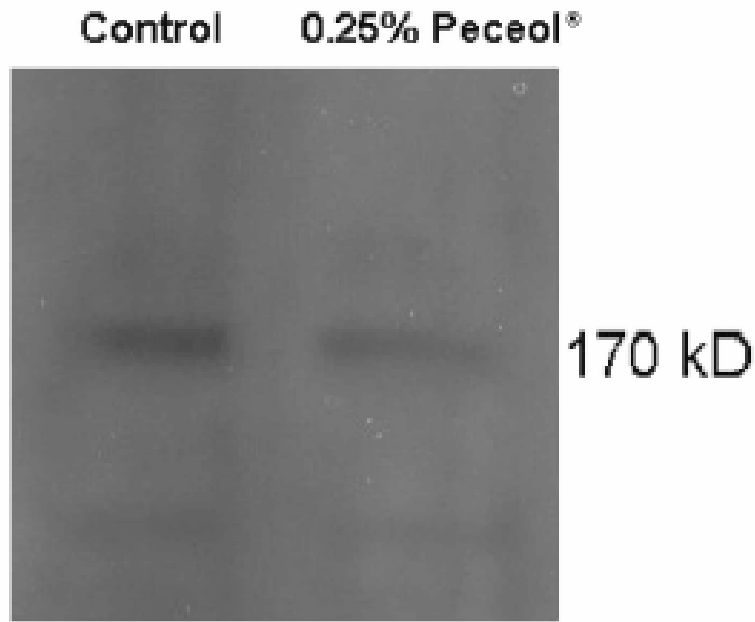


Figure 3.2 Western blot of P-gp (170kD) in Caco-2 cells with or without a 1 week incubation with Peceol®.²⁰

The fact that triglycerides are predominant in high fat meals and that monoglycerides are a product of dietary triglyceride hydrolysis in the digestive tract is of particular relevance when considering the effect of lipids on the intestinal transporter function because, as mentioned above, monoglycerides are capable of traversing the intestinal mucosa cell membrane. Moreover, this increased intestinal level of monoglycerides coincides with the upregulation of bile secretions from the gallbladder. As a result, increased levels of bile salts

accompany high monoglycerides levels. Ingels and coworkers^{22,23} investigated the effect of bile salt, sodium taurocholate, on the known P-gp substrate, cyclosporine. The authors studied the changes in the apical to basolateral (A to B) cyclosporine flux and the basolateral to apical (B to A) cyclosporine flux across Caco-2 cell monolayers demonstrating that an increase in bile salts results in a decreased B to A flux and an increased A to B flux, causing a decrease in net flux ratio from ~16 (control buffer) to ~1 (3 mM sodium taurocholate added to control buffer). A reduction of the net flux ratio to a level where A to B and B to A fluxes are nearly equivalent (i.e. ratio = 1) is consistent with inhibition of an efflux transporter such as P-gp.

Konishi *et al.*^{1,2} previously documented the inhibitory effect of monoglycerides on P-gp activity, employing Caco-2 cells and the known P-gp substrate daunomycin (Figure 3.3).

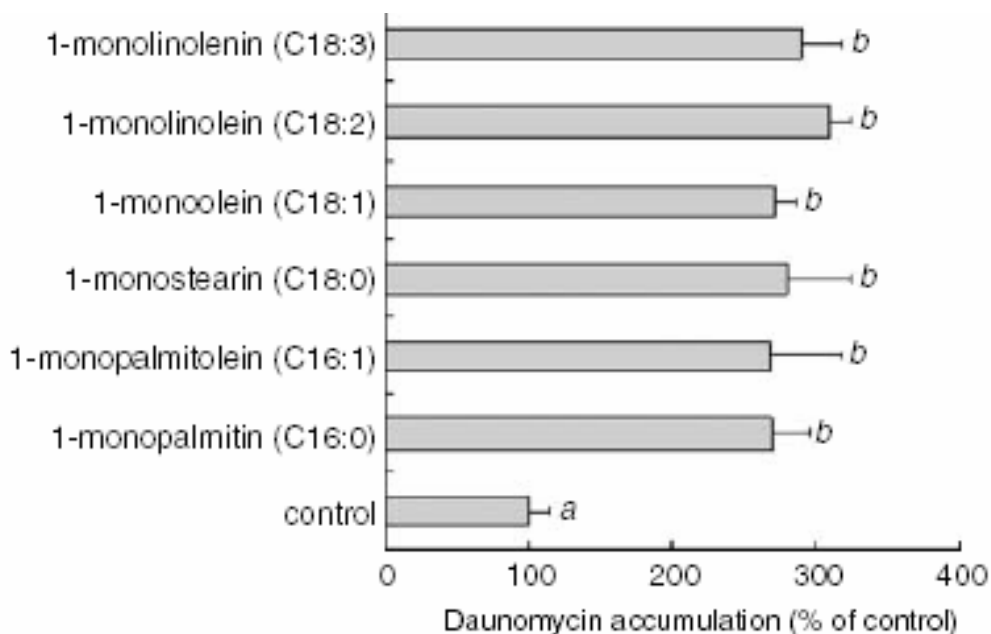


Figure 3.3 Effect of various monoglycerides on the intracellular accumulation of daunomycin in Caco-2 cells.¹

^{ab} The values not sharing common superscript letters (a or b) are significantly different from one another, $P < 0.01$

The authors demonstrated that 6 different monoglycerides were capable of inhibiting P-gp mediated efflux, thereby increasing the cellular accumulation of daunomycin. They also examined the effect of various concentration of 1-monopalmitin on daunomycin accumulation in Caco-2 cells (Figure 3.4) as well as potential cytotoxic effects on the cells (Figure 3.5).

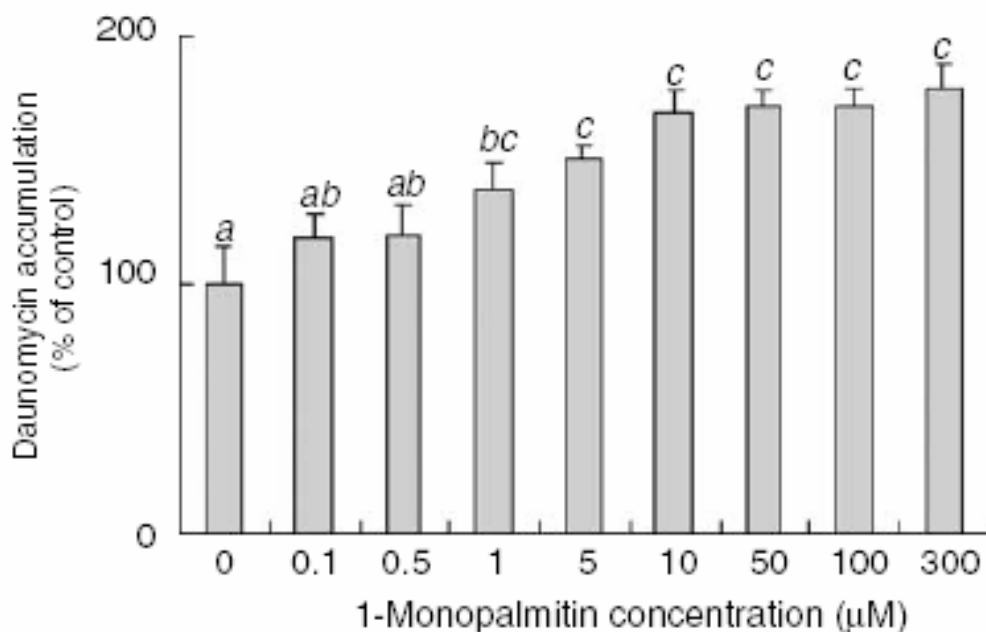


Figure 3.4 The concentration dependent effect of 1-monopalmitin on the intracellular accumulation of daunomycin in Caco-2 cells.¹
^{abc} The values not sharing common superscript letters (a, b, and/or c) are significantly different from one another, $P < 0.01$

Konishi and colleagues^{1,2} used the lactate dehydrogenase (LDH) assay and showed that over the concentration range of 10 mM through 300 mM 1-monopalmitin no effect on the LDH release was observed, thereby ruling out any cell damage caused by the test media. Thus, the authors demonstrated that the inhibitory effect of 1-monopalmitin caused increased accumulation of daunomycin in a

concentration dependent manner, which they attributed to P-gp inhibition.

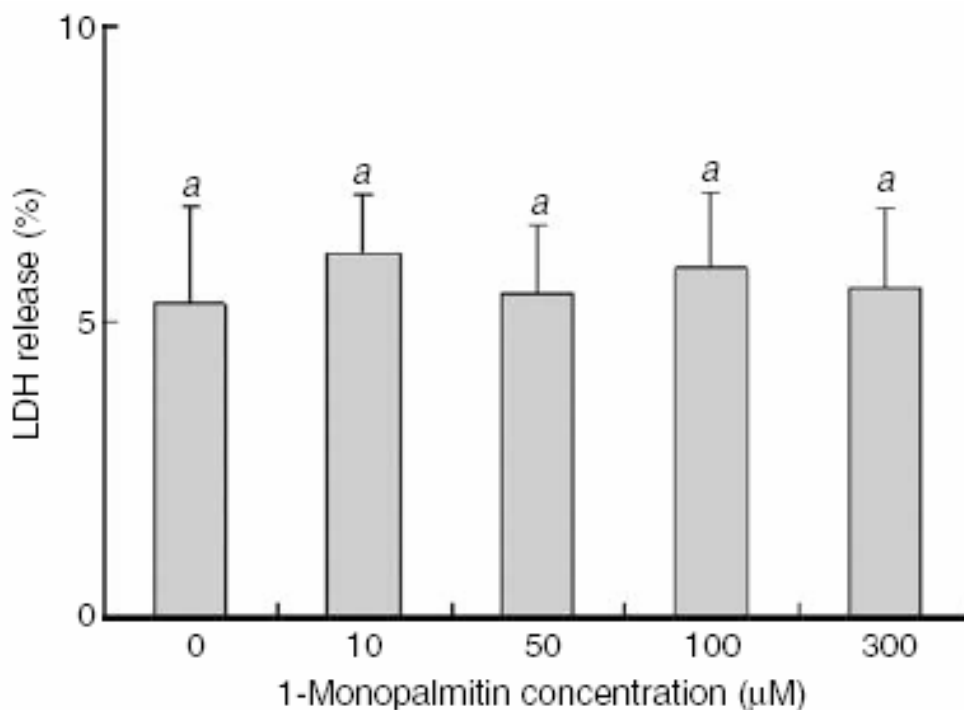


Figure 3.5 Cytotoxicity assay of various concentrations of 1-monopalmitin on Caco-2 cells examined by lactate dehydrogenase (LDH) release.¹
^a The common superscript letter 'a' shared by all values denotes that none are significantly different from one another or control.

The conclusions made by Konishi *et al.*^{1,2} regarding their work with lipids and *in vitro* cellular studies is of particular interest to our project because of the bidirectional transport behavior we observed in the presence of such media as FeSSIF, Ensure Plus[®] and the oil formulation. Accordingly, we concluded that a more appropriately buffered cellular media system was

necessary for our studies as well, and chose Hanks (BSS) (Balanced Salt Solution: 0.4 g/L KCl, 0.6 g/L KH_2PO_4 , 8.0 g/L NaCl, 1.0 g/L glucose, 0.09 g/L $\text{Na}_2\text{HPO}_4 \cdot 7\text{H}_2\text{O}$, 0.35 g/L NaHCO_3), supplemented with the zwitterionic organic chemical buffering agent, HEPES (4-(2-hydroxyethyl)-1-piperazineethanesulfonic acid, 25 mM), 1% FBS, and brought to a pH of 7.4). Therefore, we resumed running our model compounds and test inhibitors utilizing this control transport media, which is recognized throughout the field as the standard for cellular transport assays.

3.2 Materials and methods

3.2.1 Materials

MDR1-MDCK and MDCK cell lines were generously provided by Dr. Ira Pastan (National Cancer Institute, National Institutes of Health, Bethesda, MD). The Caco-2 cell line (HTB-37) was purchased from the American Type Culture Collection (ATCC - Manassas, VA). All components necessary for proper cell culture growth conditions (described below) were purchased from the University of California, San Francisco Cell Culture Facility (San Francisco, CA). [mebmt- \bullet - ^3H]-Cyclosporine was purchased from Amersham Biosciences (Piscataway, NJ). D-[1- ^3H (N)]-Mannitol was purchased from NEN (Boston, MA). [^3H]-Saquinavir was purchased from Moravek Biochemicals and Radiochemicals (Brea, CA). [N-methyl- ^3H]-Verapamil

hydrochloride was purchased from Perkin Elmer (Waltham, MA). GG918 (GF120918: N-{4-[2-(1,2,3,4-tetrahydro-6,7-dimethoxy-2-isoquinolinyl)-ethyl]-phenyl}-9,10-dihydro-5-methoxy-9-oxo-4-acridine carboxamine) was a kind gift from GlaxoSmithKline (Research Triangle Park, NC). All other chemicals were of reagent grade and purchased from Sigma-Aldrich (St. Louis, MO). Poly-D-Lysine Biocoat[®] twelve-well plates were purchased from Becton Dickinson Labware (Bedford, MA). Six-well tissue culture treated polystyrene plates were obtained from Corning Life Science (Acton, MA). Falcon polyethylene terephthalate cell culture inserts (pore size 0.4 μ m, diameter 4.2 cm²) were obtained from BD Biosciences (Bedford, MA).

3.2.2 Cell culture

3.2.2.1 MDR1-MDCK and MDCK cell lines

MDCK cells were grown in a humidified 5% CO₂ atmosphere at 37°C using Dulbecco's modified Eagle's medium (DMEM) containing 4.5 g/L glucose, 3.7 g/L NaHCO₃, 0.584 g/L *l*-glutamine, which was supplemented with 10% heat-inactivated FBS, 100 U/mL penicillin and 100 U/mL streptomycin. MDR1-MDCK cell culture medium was as described above with the addition of 80 ng/mL colchicine as a selective supplement.²⁴ Cells were grown to 90-100% confluence and harvested using 0.05% trypsin EDTA. Monolayers were prepared by seeding harvested cells onto

polyethylene terephthalate cell culture inserts at a density of approximately 1,000,000 cells/insert. Growth medium was refreshed once every two days and one day prior to the experiment, which was performed 5-6 days postseeding for both cell lines.

3.2.2.2 Caco-2 cell line

Caco-2 cells were grown in a humidified 5% CO₂ atmosphere at 37°C using minimum essential medium (MEM) Eagle's with Earle's balanced salt solution (BSS) containing 1.0 g/L glucose, 0.292 g/L l-glutamine, 2.2 g/L NaHCO₃, which was supplemented with 15% heat-inactivated FBS, 1.0 mM sodium pyruvate, 0.1 mM nonessential amino acids, 100 U/mL penicillin and 100 U/mL streptomycin. Cells were grown to 90-100% confluence and harvested using 0.05% trypsin EDTA. Monolayers were prepared by seeding harvested cells onto polyethylene terephthalate cell culture inserts at a density of approximately 60,000 cells/cm². Growth medium for the Caco-2 was refreshed 48 hours post-seeding and then twice weekly, including one day prior to the experiment. Caco-2 cell monolayers were used for bidirectional transport experiments 21-28 days postseeding.

For the intracellular accumulations assays, the Caco-2 cells were grown to 90-100% confluence and

harvested using 0.05% trypsin EDTA. Twelve well plates were prepared by seeding harvested cells into each poly-D-lysine treated well at a density of approximately 500,000 cells/well. Growth medium was refreshed 48 hours post-seeding and then one day prior to the experiment. Cells were used for accumulation studies 4-6 days postseeding.

3.2.3 Intracellular accumulation experiments

The intracellular accumulations assays were performed in a twelve well plate format. Each well containing cells was preincubated in control transport buffer (Hank's buffered salt solution containing 25 mM HEPES and 1% FBS, pH 7.4) at 37°C for 20 minutes. All experiments were performed in triplicate and conducted on at least three separate occasions to ensure reproducibility. The experiment was started by the addition of test compound in control transport buffer to the well. In the experiments run in the presence of various (tri-, di-, and mono-)glycerides, the control transport buffer was supplemented with appropriate triglyceride, diglycerides, or monoglyceride.^{1,2} The final volume in each well was 0.6 ml. Cells were incubated for 2 hours at 37°C at a shaking speed of 25 strokes/minute in a Boekel Shake 'N' Bake Incubator Shaker II (Boekel Scientific, Feasterville, PA). The solution was then

removed by suction and the cells were washed three times with 0.75 ml ice-cold PBS. Following removal of the last wash buffer, 0.4 ml of 0.1% Triton X-100 was added to each well and the plates were allowed to shake at room temperature for 15 minutes. The entire contents of the well was then taken and added to 5 ml scintillation cocktail.

3.2.4 Bidirectional transport experiments

Transport assays were performed following a modified protocol previously described by our laboratory.²⁵⁻²⁸ In brief, cell monolayers were preincubated in control transport buffer (Hank's buffered salt solution containing 25 mM HEPES and 1% FBS, pH 7.4) at 37°C for 20 minutes. Transepithelial electrical resistance (TEER) values were measured by the Millicell electrical resistance system utilizing "chopstick" electrodes (Millipore Corporation, Bedford, MA). On average, the MDR1-MDCK cells possessed values of approximately 4000-5000 $\bullet\cdot\text{cm}^2$, while the MDCK cells possessed TEER values of approximately 200-300 $\bullet\cdot\text{cm}^2$. On average, the Caco-2 cells system possessed TEER values of approximately 800-1000 $\bullet\cdot\text{cm}^2$. All experiments were performed in triplicate and conducted on at least three separate occasions to ensure reproducibility. In the case of the MDR1-MDCK and MDCK cells, both these transfected and parental cell lines

were run on the same day to account for potential between-day variability of radiolabeled counts and TEER values.

The experiment was started by the addition of test compound in control transport buffer to the donor compartment and control transport buffer only to the receiver compartment. In the experiments run in the presence of various (tri-, di-, and mono-)glycerides, the control transport buffer was supplemented with appropriate triglyceride, diglycerides, or monoglyceride.^{1,2} The final volume in each of the chambers was 1.5 mL on the apical side and 2.5 mL on the basolateral side. Experimental samples were taken from the receiver compartment at three time points. At the first two time points, 200 μ L samples were removed and then replaced with fresh media to restore initial starting volumes. At the final time point, following collecting of the last 200 μ L sample, contents of both chambers were removed by suction, each cell culture insert was dipped three times into ice-cold PBS and the cell culture insert membranes were collected. All experiments were run at 37°C at a shaking speed of 25 strokes/minute in a Boekel Shake 'N' Bake Incubator Shaker II (Boekel Scientific, Feasterville, PA).

3.2.5 Analysis of samples

3.2.5.1 Sample preparation

All samples were added to 5 mL Econo-Safe™ Counting Cocktail (Research Products International Corporation, Mount Prospect, IL) and vortexed. Cells monolayers were solubilized by sonication (in an ultrasonic bath) for 15 minutes.

3.2.5.2. Sample analysis

Samples were analyzed using a Beckman LS180 scintillation counter (Beckman Industries, Palo Alto, CA).

3.3 Results

3.3.1 Evaluation of various lipidic conditions on the intracellular accumulation of vinblastine in Caco-2 cells.

Chapter 2 detailed the progression in our experimental approach utilizing various simulated physiological media settling upon the less complex test media of control transport buffer supplemented with monoolein, as described by Konishi and coworkers.¹ We also wanted to determine the ideal monoglyceride to employ while examining the effects of a diglyceride and triglyceride as well. We confirmed the inhibitory effect of 1-monopalmitin in Caco-2 cells and demonstrated a comparable inhibitory effect of 1-monoolein (Figure 3.6), however no change in vinblastine accumulation was

observed in the presence of either 1,2-dipalmitin, 1,3-dipalmitin, or tripalmitin (data not shown).

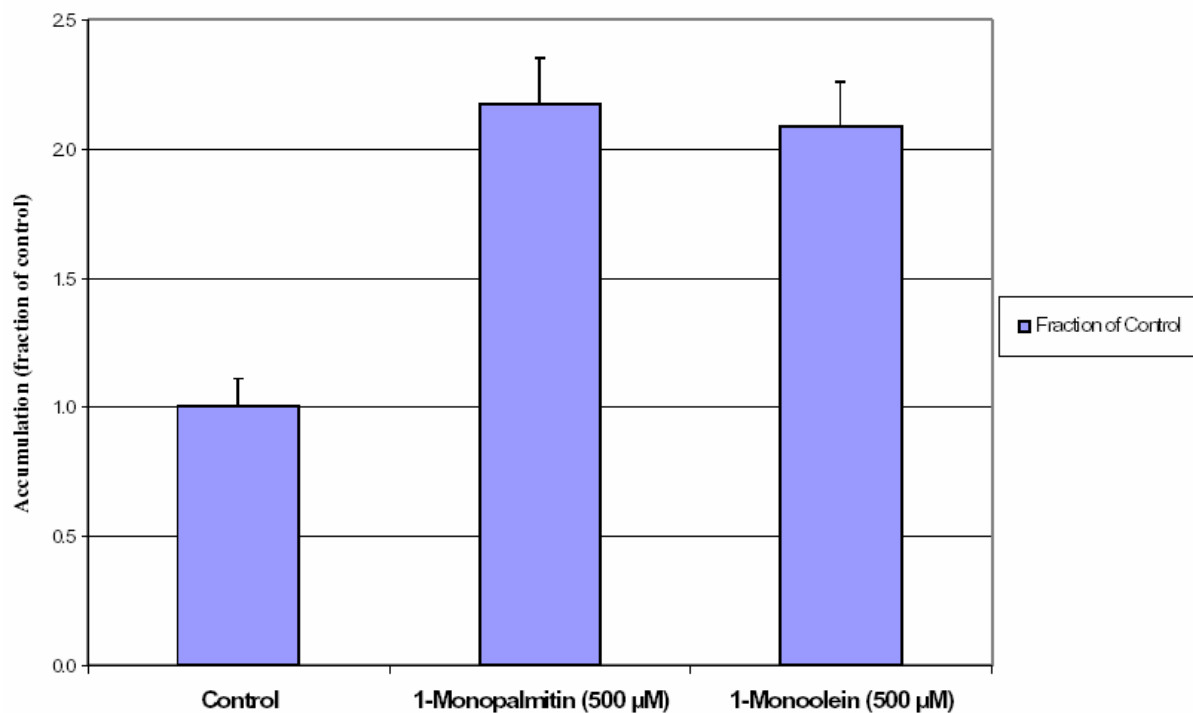


Figure 3.6 Intracellular accumulation of vinblastine in Caco-2 cells in the presence or absence of monoglycerides.

3.3.2 Evaluation of monoolein supplemented media on the intracellular accumulation of cyclosporine in Caco-2 and MDR1-MDCK cells.

Moving forward with 1-monoolein only, we were interested in observing a potential influence on the intracellular accumulation of a Class 2 compound transported by P-gp and shown to possess a known food effect *in vivo* (increase in bioavailability when administered with a high fat meal).²⁹ Choosing cyclosporine as our initial model compound, we observed a

marked increase in intracellular accumulation of apically dosed (A to C direction) cyclosporine in the presence of monoolein (500 μ M) in Caco-2 cells (Figure 3.7). This A to C accumulation was also seen to a lesser extent in the MDR1-MDCK cells, while a basolateral dose results in a decrease in intracellular levels (Figure 3.8).

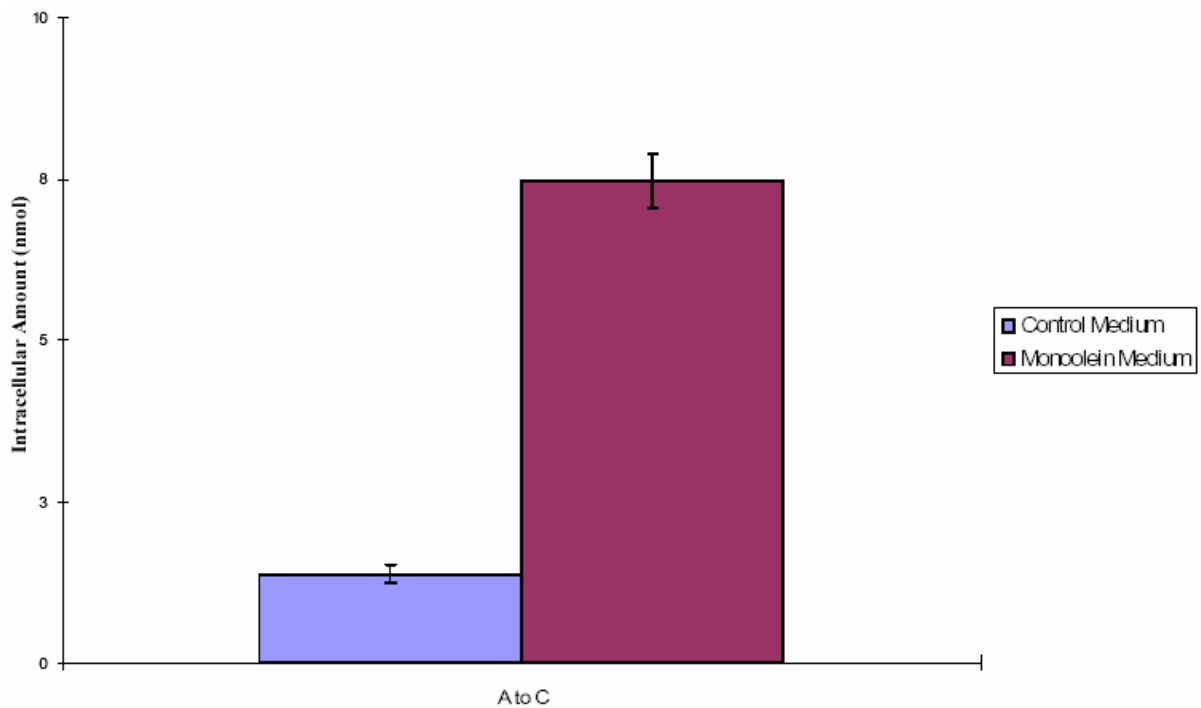


Figure 3.7 Intracellular accumulation of cyclosporine in Caco-2 cells in the presence or absence of 1-monoolein.

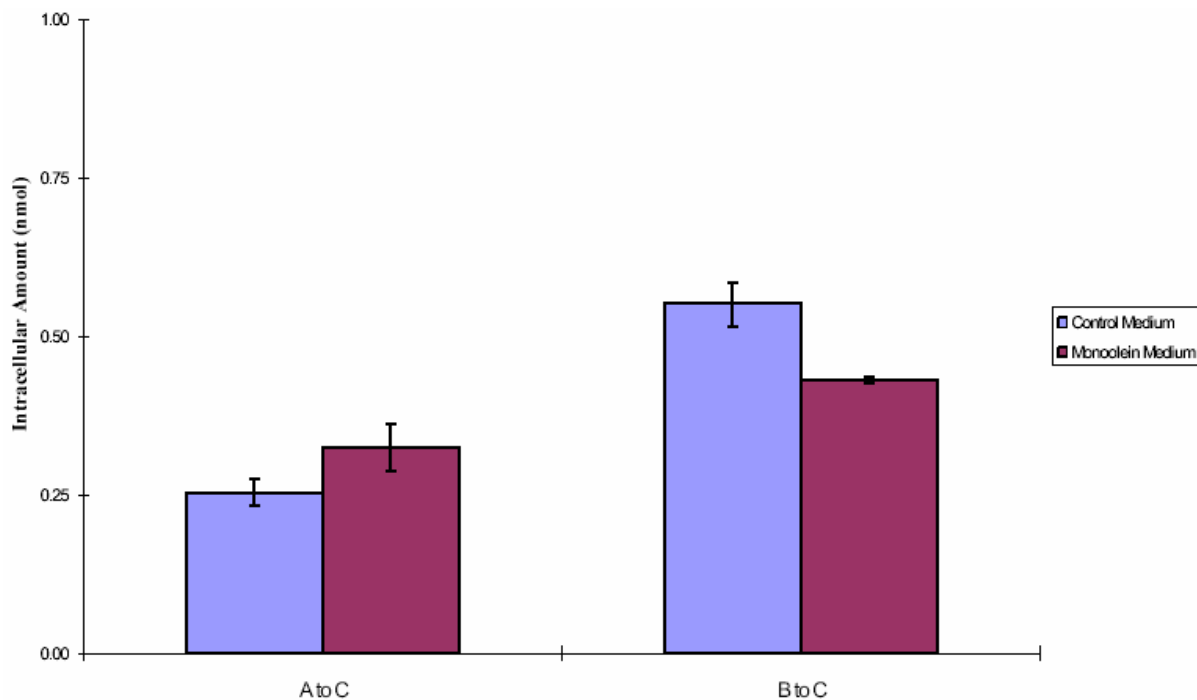


Figure 3.8 Accumulation of cyclosporine in the apical to intracellular (A to C) direction and the basolateral to intracellular (B to C) direction in MDR1-MDCK cells in the presence or absence of 1-monoolein.

3.3.3 Effect of monoolein supplemented media on the bidirectional transport of cyclosporine across MDR1-MDCK and MDCK cell monolayers

We investigated the effect of monoolein supplemented media on the flux of the known P-gp substrate, cyclosporine across MDR1-MDCK cell monolayers in comparison to that observed in the parental MDCK cell monolayers (Figures 3.9 and 3.10).

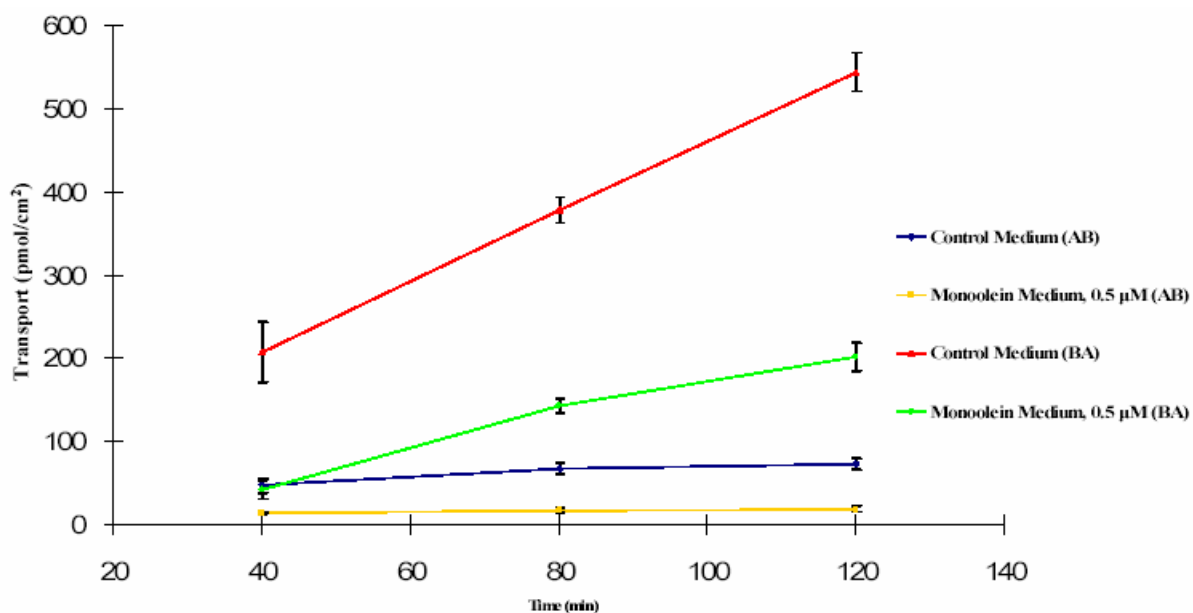


Figure 3.9 Bidirectional transport of cyclosporine in MDR1-MDCK cells with or without 1-monoolein supplemented media.

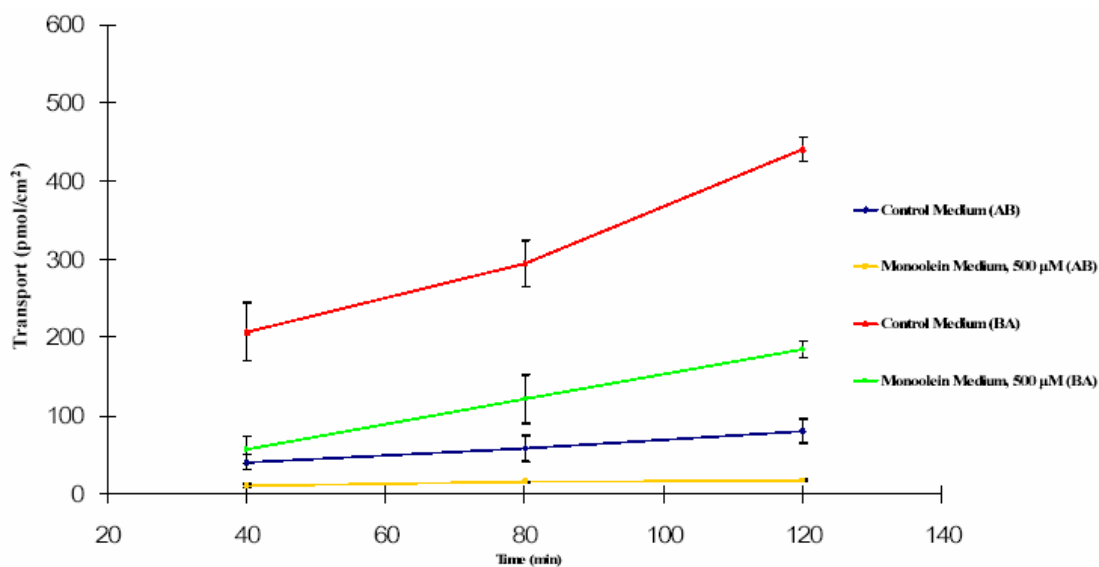


Figure 3.10 Bidirectional transport of cyclosporine in MDCK cells with or without 1-monoolein supplemented media.

The presence of monoolein (500 μ M) resulted in a significant decrease in both the B to A and A to B transport of cyclosporine in the transfected cells as well as the nontransfected parental cells.

3.3.4 Effect of GG918 on the bidirectional transport of saquinavir across MDR1-MDCK cell monolayers

We investigated the effects of a known P-gp inhibitor, GG918, on the bidirectional transport of saquinavir in MDR1-MDCK cells (Figure 3.11). The presence of GG918 (0.5 μ M) resulted in a reduction of the net flux ratio (B to A / A to B) by 98%, from 153 to 1.8. Figure 3.11 depicts the observed decrease in the basolateral to apical (B to A) transport coupled with an increase in apical to basolateral (A to B) transport.

3.3.5 Effect of monoolein supplemented media on the bidirectional transport of saquinavir across MDR1-MDCK and MDCK cell monolayers

We investigated the effects of the monoglyceride, monoolein on the bidirectional transport of saquinavir in MDR1-MDCK cells (Figure 3.12) as well as the nontransfected parental MDCK cells (Figure 3.13). In the

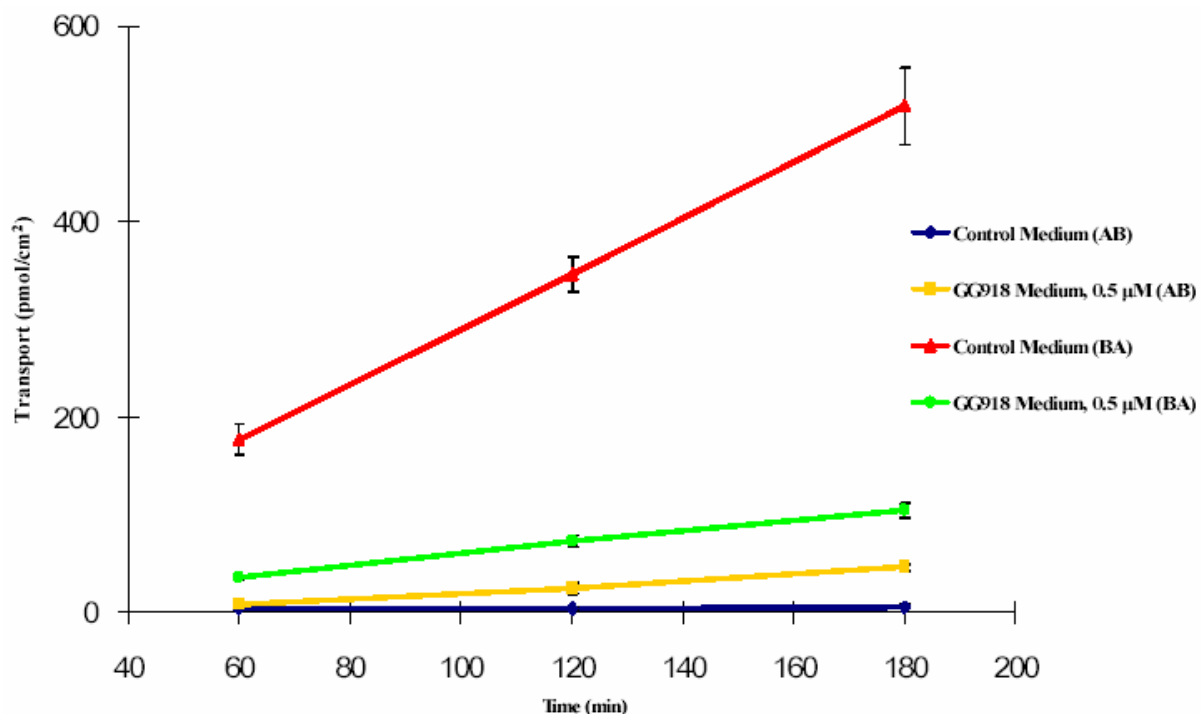


Figure 3.11 Bidirectional transport of saquinavir in MDR1-MDCK cells in the presence or absence of known P-gp inhibitor, GG918.

MDR1-MDCK cells, the presence of the monoolein (500 μM) supplemented media resulted in a significant decrease in the basolateral to apical saquinavir flux and no change in the apical to basolateral flux. Figure 3.12 depicts the drop in B to A transport in the presence of the monoolein formulation, as compared to control, which results in a decrease of 43% in the net flux ratio in the transfected cell line.

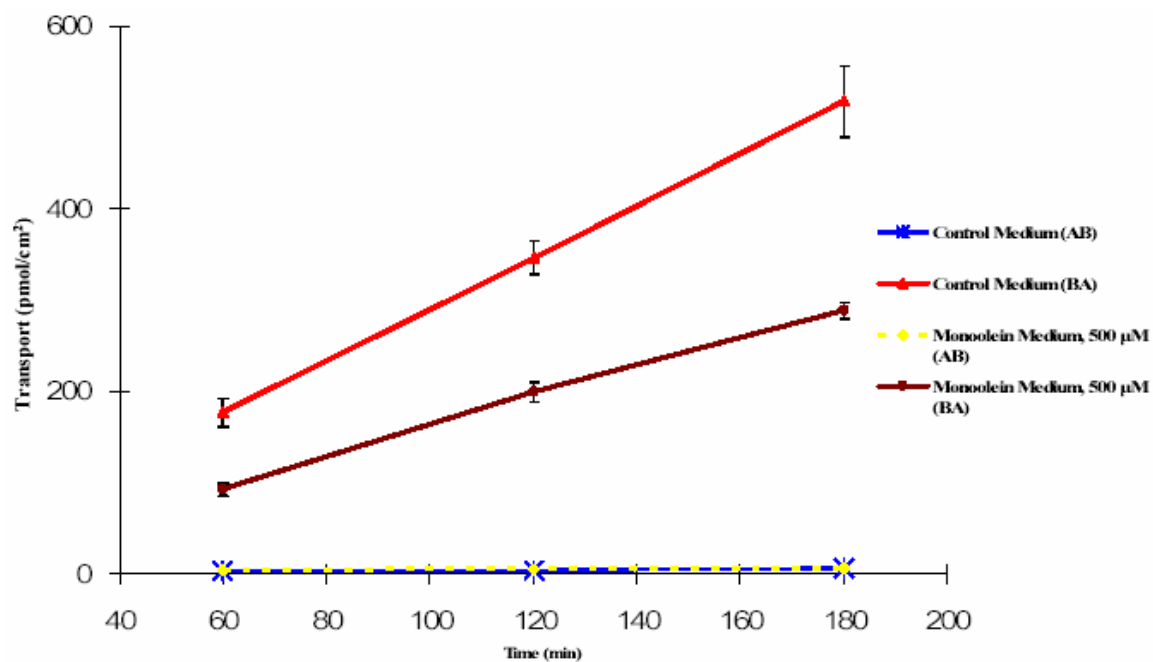


Figure 3.12 Bidirectional transport of saquinavir in MDR1-MDCK cells with or without 1-monoolein supplemented media.

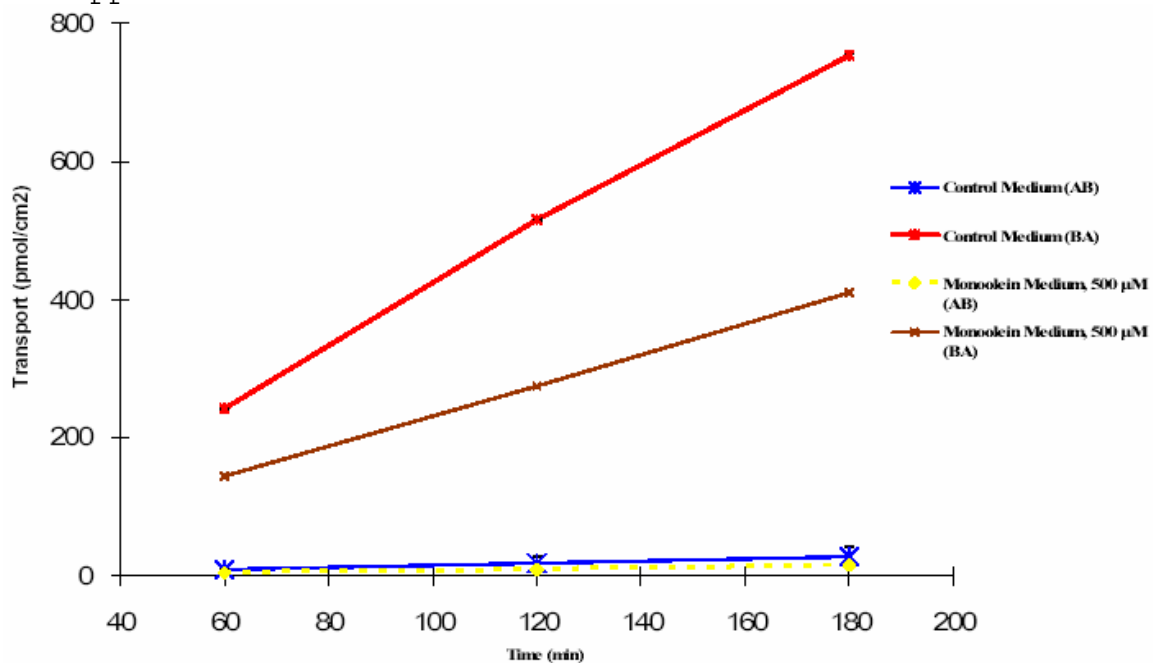


Figure 3.13 Bidirectional transport of saquinavir in MDCK cells with or without 1-monoolein supplemented media.

In the nontransfected cell line, the presence of the monoolein (500 μ M) resulted in a 10% decrease in the net flux ratio in the transfected cell line. Figure 3.13 depicts the significant drop in B to A transport in the presence of the monoolein formulation coupled with a moderate decrease in the A to B transport.

3.3.6 Effect of GG918 on the bidirectional transport of saquinavir across Caco-2 cell monolayers

We investigated the effects of a GG918 on the bidirectional transport of saquinavir in Caco-2 cells (Figure 3.14). The net flux ratio in control transport buffer was 2.25. The presence of GG918 (0.5 μ M) resulted in a reduction of the net flux ratio to 1.22, a decrease of 46%. Figure 3.14 depicts the decrease in the basolateral to apical (B to A) transport and the increase in apical to basolateral (A to B) transport.

3.3.7 Effect of monoolein supplemented media on the bidirectional transport of saquinavir across Caco-2 cell monolayers

We investigated the influence of monoolein on the

bidirectional transport of saquinavir in Caco-2 cells (Figure 3.15). The presence of the monoolein (500 μ M) supplemented media resulted in a marked decrease in the flux across the cellular monolayer in both directions. Figure 3.15 depicts the significant drop in B to A transport as well as a significant decrease in transport from the apical to basolateral compartment.

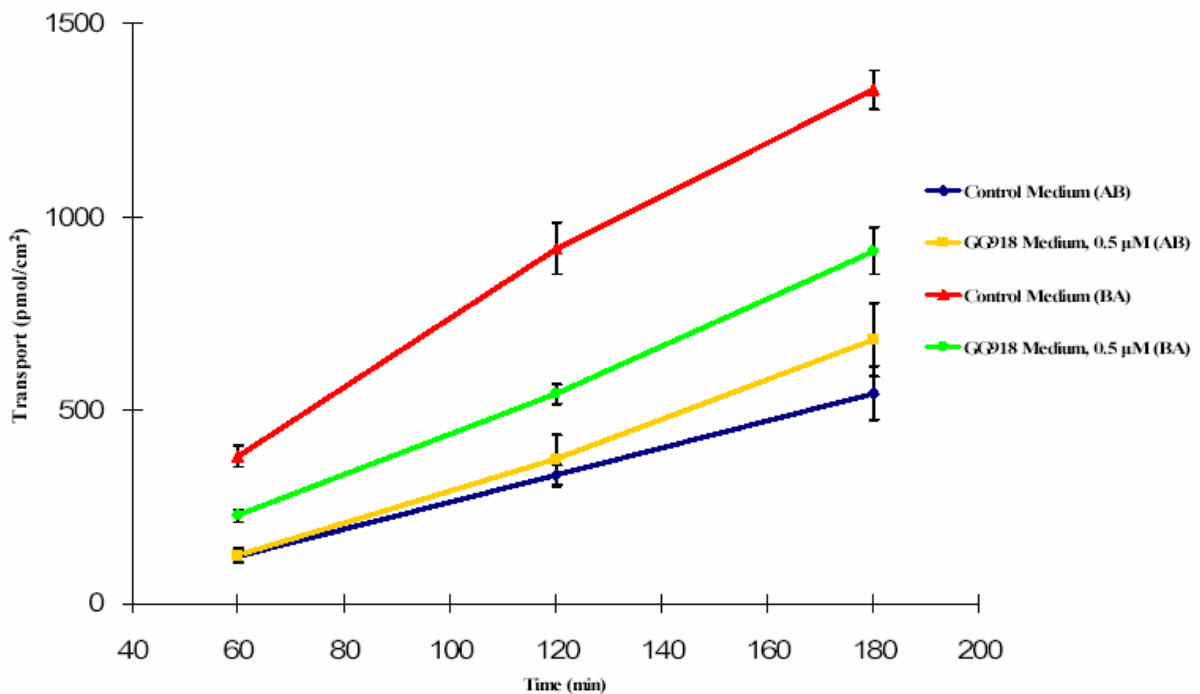


Figure 3.14 Bidirectional transport of saquinavir in Caco-2 cells in the presence or absence of known P-gp inhibitor, GG918.

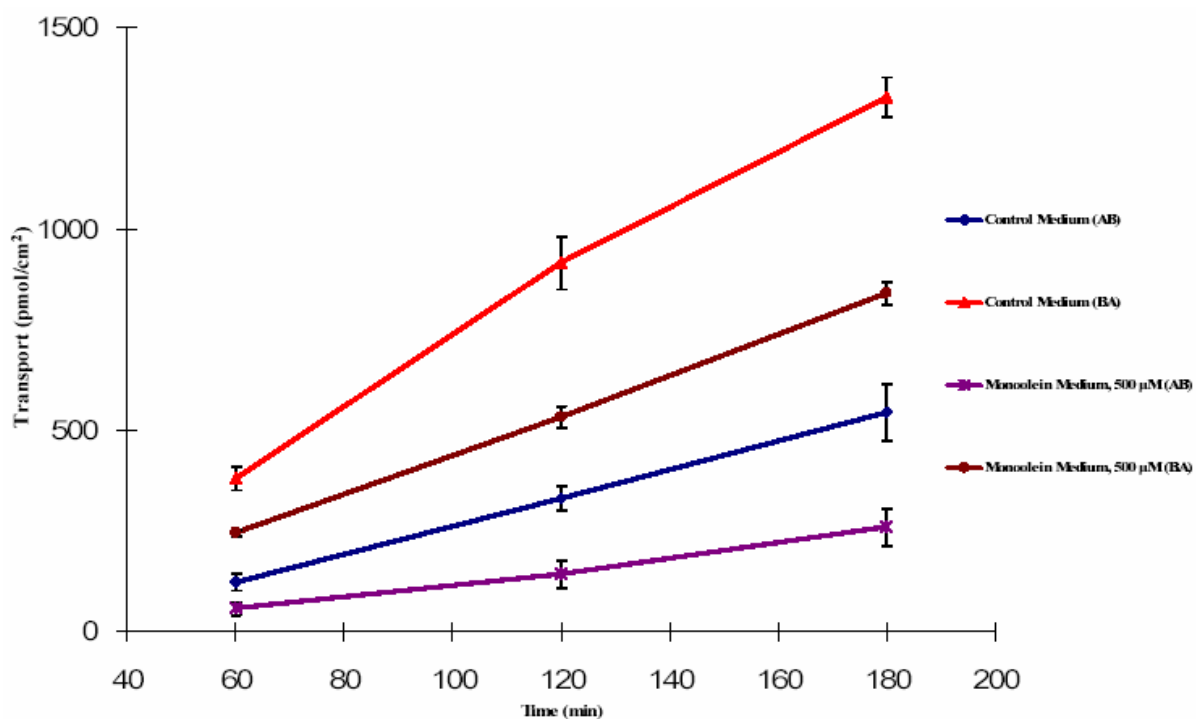


Figure 3.15 Bidirectional transport of saquinavir in Caco-2 cells with or without 1-monoolein supplemented media.

3.3.8 Net flux and apparently permeability changes in MDR1-MDCK, MDCK and Caco-2 cell monolayers.

In addition to evaluating the transport profiles of saquinavir in the presence or absence of a known efflux inhibitor and a potential efflux inhibitor, we were also interested in determining the net change in flux (Table 3.1) as well as any influence on apparent permeability values (Table 3.2). The net flux ratios in resulting from each experimental condition are included in Table

3.1 and the resulting apparent permeability values (P_{app}) are included in Table 3.2.

Cell Line	Control Media	GG918 Media (0.5 μ M)	Monoolein Media (500 μ M)
Net Flux Ratio in MDR1-MDCK Cells	153	1.82	87
Net Flux Ratio in Caco-2 Cells	2.2	1.2	2.9

Table 3.1 Net flux ratios (B to A / A to B) for saquinavir (20 μ M) in MDR1-MDCK and Caco-2 cells in the presence or absence of potential inhibitors, each with n = 3 transwells.

3.4 Discussion

First, we wanted to follow up on the influence of glyceride additives that we previously introduced in Chapter 2. In Section 2.3.4 we demonstrated the inhibitory effect of monoolein supplemented media on the transport of vinblastine across MDR1-MDCK cell monolayers. Monoolein was of particular interest to our studies because of the high concentrations of monoglyceride expected in the intestine following meal

Experimental Media ●	Control Media	GG918 Media (0.5 ●M)	Monoolein Media (300 ●M)
P_{app} Values A ● B in MDR1-MDCK Cells (nm·sec ⁻¹)	1.54 ± 0.3	26.4 ± 3.7	1.57 ± 0.5
P_{app} Values A ● B in MDCK Cells (nm·sec ⁻¹)	12.1 ± 0.9	49 ± 5.5	7.5 ± 1.1
P_{app} Values A ● B in Caco Cells (nm·sec ⁻¹)	29.2 ± 2.7	38.8 ± 4.1	14.1 ± 2.2

Table 3.2 Apparent permeability values (P_{app}) for saquinavir (20 ●M) in MDR1-MDCK, MDCK, and Caco-2 cells. P_{app} values ± standard deviation are listed for the Apical to Basolateral (A to B) direction, each with n = 3 transwells. $P_{app} = (dQ/dt)/(A \cdot C_0)$; where dQ/dt is the amount transported (Q) over time (t), A is the surface area of the insert, and C_0 is the initial concentration of the donor compartment.

ingestion and digestion. Since monoglycerides are a product of dietary triglyceride hydrolysis in the gut and are subsequent to diglyceride levels as well, we tested the effects of tripalmitin, 1,2-dipalmitin, 1,3-dipalmitin, 1-monopalmitin, and 1-monoolein. Utilizing the Caco-2 cell system in an intracellular accumulation assay, we evaluated the ability of the cells to efflux the known P-gp substrate, vinblastine under various

conditions. Monoglycerides but not di- or tri-glycerides, were capable of significantly inhibiting vinblastine efflux thereby resulting in a marked accumulation of the efflux transporter substrate within the cell (Figure 3.6). These results are consistent with the P-gp substrate behavior demonstrated in Caco-2 cells shown by Konishi et al.^{1,2} 1-Monoolein was signaled out for use as our model monoglyceride not only because of its confirmed inhibitory effect on efflux but also because it is employed as an excipient in formulations.¹⁹

Vinblastine was selected as the first model compound (Sections 2.3.1 through 2.3.4; Section 3.3.1) because it is a Class 2 compound and known P-gp substrate and is readily available for purchase in radiolabeled form. However, this is a drug that is only administered intravenously (IV) and, hence, does not possess a food effect. The selection criteria for our next model compound was that it be an orally administered Class 2 P-gp substrate, with a known food effect. The known P-gp and CYP3A4 dual substrate, cyclosporine, when administered in the presence of a high fat meal, has delayed and decreased absorption resulting in a decrease in peak concentration and area under the curve (AUC).³⁰

We investigated the effects of a monoolein supplemented media on the intracellular accumulation of cyclosporine in Caco-2 cells and MDR1-MDCK cells (Figures

3.7 and 3.8). In both Caco-2 and MDR1-MDCK cells, we observed an accumulation of cyclosporine in the presence of monoolein (500 μ M) with a greater accumulation occurring in the Caco-2 cells. This increase in intracellular levels is expected if the cells are unable to properly pump the drug out due to the reduction in function of the efflux transporter. We also examined the effect of monoolein on the intracellular accumulation when cyclosporine is dosed from the basolateral compartment, which resulted in a decrease in intracellular levels of cyclosporine (Figure 3.8). This result was unexpected because an inhibition of an apical efflux mechanism should lead to a buildup of drug within the cell, however, monoolein may be preventing the drug from permeating through both the semi-porous membrane of the insert in addition to the basolateral membrane of the Caco-2 cells. Despite this result we were interested in the bidirectional transport of cyclosporine across MDR1-MDCK and MDCK cell monolayers (Figures 3.9 and 3.10). We previously demonstrated an inhibitory effect of monoolein on vinblastine (Section 2.3.4), which mimicked the known P-gp inhibitor GG918 in that a reduction in the net flux ratio was observed in the transfected cells but not in the parental control cells. However, the effect on cyclosporine did not follow the same pattern suggesting a mechanism other than a transporter effect on the drug.

Figure 3.9 depicts a decrease in B to A flux along with a decrease in A to B flux in the MDR1-MDCK cells and Figure 3.10 depicts the same decline in both directions in the untransfected parental control cells suggesting adsorption and not transport inhibition.

This led us to select the model compound saquinavir, also an orally administered Class 2 P-gp and CYP3A4 dual substrate, with a known food effect. When coadministered with a high fat meal, the bioavailability of saquinavir may increase up to six fold.³¹

In order to confirm that saquinavir is indeed an appropriate compound for these studies, we first looked at its bidirectional transport in the presence of GG918 (0.5 μ M). As expected from inhibition of P-gp in MDR1-MDCK cells, we observed a decrease in the B to A transport coupled with an increase in the A to B transport, effectively reducing the net flux ratio by 98% (Figure 3.11). The net flux ratio also approached unity in the presence of GG918 in Caco-2 cells (Figure 3.14).

Next, we continued investigating the effects of monoolein supplemented media on the bidirectional transport of saquinavir in MDR1-MDCK cells (Figure 3.12). Figure 3.12 depicts the transport in MDR1-MDCK cells showing that the B to A transport of saquinavir is significantly decreased in the presence of monoolein (500 μ M) while the and A to B transport remained unchanged so

that the next flux ratio is nearly halved.

Contrastingly, in the control MDCK cells the presence of monoolein supplemented media resulted in a decrease in net flux ratio of only 10%, from 27.4 to 24.6 (Figure 3.13). Interestingly, in the assays performed in the Caco-2 cell system, the monoolein media resulted in a marked decrease in the flux across the cellular monolayer in both directions (Figure 3.15).

The net flux ratios and apparent permeability values (P_{app}) are listed in Tables 3.1 and 3.2. As expected, the known P-gp inhibitor GG918 reduces the net flux ratio. Addition of GG918 to the transport buffer also results in an increase in the apparent permeability in the apical to basolateral direction. This is expected because removing the apical efflux pump would result in more rapid access of drug to the basolateral side.

The reduction in net flux ratio of saquinavir in MDR1-MDCK cells in the presence of monoolein follows the trend we observed previously with vinblastine. However, unlike vinblastine, we do not observe a decrease in the B to A transport coupled with an A to B increase. As a result, we do not observe any increase in the apparent permeability ($P_{app (A \text{ to } B)}$) with monoolein. The results from the bidirectional studies run across Caco-2 cell monolayers show the expected decrease in the basolateral to apical direction, yet again, there is no increase in

the A to B transport. Instead, we observe a decrease in the apical to basolateral direction in the presence of monoolein (500 μ M). This results in a 30% increase in the net flux ratio (Table 3.1). The A to B decrease equates to a ~50% slower permeation rate in the A to B direction ($P_{app(A \text{ to } B)}$) (Table 3.2).

There are various potential explanations for the reduction in the P_{app} value for saquinavir with monoolein in Caco-2 cells. First, the reduction we see in the P_{app} value in the Caco-2 cell system is not seen in the MDR1-MDCK cells. This is due to the inherent properties differentiating the two cell types. The MDR1-MDCK cells are a canine kidney epithelial cell line with transepithelial electrical resistance (TEER) of 4000-5000 $\Omega \cdot \text{cm}^2$ while the Caco-2 cells are a human colon carcinoma cell line with TEER values of 800-1000 $\Omega \cdot \text{cm}^2$. The Caco-2 cells are a "leakier" system that is more representative of the intestine.

The differences between the two cells are emphasized when evaluating the transport of Class 2, P-gp substrates such as saquinavir. In the MDR1-MDCK cells we observe a net flux ratio greater than 150, as compared to a 2.2 ratio in the Caco-2 cells (Table 3.1). In each case, we have bidirectional transport profile characteristics indicative of a P-gp substrate (ratio 2 or greater).³² However, in the Caco-2 system the higher A to B

permeability results in the lower net flux ratio. It must also be noted that, unlike MDR1-MDCK cells, Caco-2 cells endogenously express various uptake transporters. Various studies have documented the utility of Caco-2 cells and that these cells do endogenously express a multitude of uptake transporters.³³⁻³⁷ The increase in the A to B flux and permeation may be attributed to a carrier mediated uptake mechanism of saquinavir's absorption and this uptake cannot be detected in the MDR1-MDCK cell system. Our hypothesis that components of high fat meals may be inhibiting transporters is not limited to efflux transporters. Results from our cellular systems suggest and support that in addition to an efflux transporter inhibitory effect, monoolein may be influencing a mechanism of saquinavir absorption, such as an apical uptake transporter. Our work focusing specifically on the role of intestinal uptake transporters will be covered in further detail in the following Chapter 4.

3.5 References

1. T. Konishi, H. Satsu, Y. Hatsugai, K. Aizawa, T. Inakuma, S. Nagata, S.H. Sakuda, H. Nagasawa, M. Shimizu, Inhibitory effect of a bitter melon extract on the P-glycoprotein activity in intestinal Caco-2 cells, *Br. J. Pharmacol.* 143 (2004) 379-387.
2. T. Konishi, H. Satsu, Y. Hatsugai, K. Aizawa, T. Inakuma, S. Nagata, S.H. Sakuda, H. Nagasawa, M. Shimizu, A bitter melon extract inhibits the P-glycoprotein activity in intestinal Caco-2 cells: monoglyceride as an active compound, *Biofactors* 22 (2004) 71-74.
3. Food and Drug Administration. Guidance for Industry: Food-effect bioavailability and fed bioequivalence studies. Food and Drug Administration, Rockville, MD, 2002. Available at <http://www.fda.gov/cder/guidance/index.htm>.
4. D.R. Brocks, K.M. Wasan, The influence of lipids on stereoselective pharmacokinetics of halofantrine: Important implications in food-effect studies involving drugs that bind to lipoproteins, *J. Pharm. Sci.* 91 (2002) 1817-1826.
5. A.J. Humberstone, C.J. Porter, G.A. Edwards, W.N. Charman, Association of halofantrine with

- postprandially derived plasma lipoproteins decreases its clearance relative to administration in the fasted state, *J. Pharm. Sci.* 87 (1998) 936-942.
6. P. Tso, Intestinal lipid absorption, in: R. Johnson (Ed.), *Physiology of the Gastrointestinal Tract*, Raven Press, New York, 1994, pp. 1867-1907.
 7. E.M. Persson, R.G. Nilsson, G.I. Hansson, L.J. Löfgren, F. Libäck, L. Knutson, B. Abrahamsson, H. Lennernäs, A clinical single-pass perfusion investigation of the dynamic in vivo secretory response to a dietary meal in human proximal small intestine, *Pharm. Res.* 23 (2006) 742-751.
 8. A.J. Humberstone, W.N Charman, Lipid-based vehicles for the oral delivery of poorly water soluble drugs, *Adv. Drug Deliv. Rev.* 25 (1997) 103-128.
 9. P. Gershkovich, D. Shtainer, A. Hoffman, The effect of a high-fat meal on the pharmacodynamics of a model lipophilic compound that binds extensively to triglyceride-rich lipoproteins, *Int. J. Pharm.* 333 (2007) 1-4.
 10. P. Gershkovich, A. Hoffman, Effect of a high-fat meal on absorption and disposition of lipophilic compounds: The importance of degree of association

- with triglyceride-rich lipoproteins, *Eur. J. Pharm. Sci.* 32 (2007) 24-32.
11. C.J. Porter, N.L. Trevaskis, W.N. Charman, Lipids and lipid-based formulations: optimizing the oral delivery of lipophilic drugs, *Nat. Rev. Drug Discov.* 6 (2007) 231-248.
 12. E.A. Mueller, J.M. Kovarik, J.B. van Bree, J. Grevel, P.W. Lückner, K. Kutz, Influence of a fat-rich meal on the pharmacokinetics of a new oral formulation of cyclosporine in a crossover comparison with the market formulation, *Pharm. Res.* 11 (1994) 151-155.
 13. E.A. Mueller, J.M. Kovarik, K. Kutz, Minor influence of a fat-rich meal on the pharmacokinetics of a new oral formulation of cyclosporine, *Transplant. Proc.* 26 (1994) 2957-2958.
 14. A.M. Kaukonen, B.J. Boyd, W.N. Charman, C.J. Porter, Drug solubilization behavior during in vitro digestion of suspension formulations of poorly water-soluble drugs in triglyceride lipids, *Pharm. Res.* 21 (2004) 254-260.
 15. W.N. Charman, C.J.H. Porter, S. Mithani, J.B. Dressman, Physiochemical and physiological mechanisms for the effects of food on drug

- absorption: the role of lipids and pH, *J. Pharm. Sci.* 86 (1997) 269-282.
16. M.C. Carey, D.M. Small, C.M. Bliss, Lipid digestion and absorption, *Annu. Rev. Physiol.* 45 (1983) 651-677.
 17. G.A. Kossena, W.N Charman, B.J. Boyd, D.E. Dunstan, C.J. Porter, Probing drug solubilization patterns in the gastrointestinal tract after administration of lipid-based delivery systems: a phase diagram approach, *J. Pharm. Sci.* 93 (2004) 332-348.
 18. G.A. Kossena, W.N Charman, B.J. Boyd, C.J. Porter, Influence of the intermediate digestion phases of common formulation lipids on the absorption of a poorly water-soluble drug, *J. Pharm. Sci.* 94 (2005) 481-492.
 19. R. Subramanian, K.M. Wasan, Effect of lipid excipients on in vitro pancreatic lipase activity, *Drug Dev. Ind. Pharm.* 29 (2003) 885-890.
 20. V. Risovic, K. Sachs-Barrable, M. Boyd, K.M. Wasan, Potential mechanisms by which Peceol increases the gastrointestinal absorption of amphotericin B, *Drug Dev. Ind. Pharm.* 30 (2004) 767-774.
 21. K.M. Wasan, K. Sachs-Barrable, S.D. Lee, Potential mechanisms by which lipid excipients increase the

- oral gastrointestinal absorption of drugs: a case study using amphotericin B, *Bulletin Technique Gattefossé*. (2006) 31-42.
22. F. Ingels, S. Deferme, E. Destexhe, M. Oth, G. Van den Mooter, P. Augustijns, Simulated intestinal fluid as transport medium in the Caco-2 cell culture model, *Int. J. Pharm.* 232 (2002) 183-192.
23. F.M. Ingels, P.F. Augustijns, Biological, pharmaceutical, and analytical considerations with respect to the transport media used in the absorption screening system, Caco-2, *J. Pharm. Sci.* 92 (2003) 1545-1558.
24. I. Pastan, M.M. Gottesman, K. Ueda, E. Lovelace, A.V. Rutherford, M.C. Willingham, A retrovirus carrying an MDR1 cDNA confers multidrug resistance and polarized expression of P-glycoprotein in MDCK cells, *Proc. Natl. Acad. Sci. USA* 85 (1988) 4486-4490.
25. W.S. Putnam, L. Pan, K. Tsutsui, L. Takahashi, L.Z. Benet, Comparison of bidirectional cephalixin transport across MDCK and caco-2 cell monolayers: interactions with peptide transporters, *Pharm. Res.* 19 (2002) 27-33.
26. S.D. Flanagan, C.L. Cummins, M. Susanto, X. Liu, L.H. Takahashi, L.Z. Benet, Comparison of

- furosemide and vinblastine secretion from cell lines overexpressing multidrug resistance protein (P-glycoprotein) and multidrug resistance-associated proteins (MRP1 and MRP2), *Pharmacology* 64 (2002) 126-134.
27. C.L. Cummins, W. Jacobsen, U. Christians, L.Z. Benet, CYP3A4-transfected Caco-2 cells as a tool for understanding biochemical absorption barriers: studies with sirolimus and midazolam, *J. Pharmacol. Exp. Ther.* 308 (2004) 143-155.
28. Y.Y. Lau, H. Okochi, Y. Huang, L.Z. Benet, Multiple transporters affect the disposition of atorvastatin and its two active hydroxy metabolites: application of in vitro and ex situ systems, *J. Pharmacol. Exp. Ther.* 316 (2006) 762-771.
29. S.K. Gupta, L.Z. Benet, Effect of food on the pharmacokinetics of cyclosporine in healthy subjects following oral and intravenous administration, *J. Clin. Pharmacol.* 30 (1990) 643-653.
30. A.M. Krensky, F. Vincenti, W.M. Bennett, Immunosuppressant, tolerogens, and immunostimulants. In: L.L. Brunton, J.S. Lazo, K.L. Parker (Eds.), *Goodman and Gilman's The*

- Pharmacologic Basis of Therapeutics. 11th Edition. McGraw-Hill, New York, 2006, pp. 1408-1412.
31. C. Flexner, Antiretroviral agents and treatment of HIV infection. In: L.L. Brunton, J.S. Lazo, K.L. Parker (Eds.), Goodman and Gilman's Pharmacologic Basis of Therapeutics. 11th Edition. McGraw-Hill, New York, 2006, pp. 1299-1301.
 32. J.W. Polli, S.A. Wring, J.E. Humphreys, L. Huang, J.B. Morgan, L.O. Webster, C.S. Serabjit-Singh, Rational use of in vitro P-glycoprotein assays in drug discovery, *J. Pharmacol. Exp. Ther.* 299 (2001) 620-628.
 33. K. Watanabe, T. Sawano, K. Terada, T. Endo, M. Sakata, J. Sato, Studies on intestinal absorption of sulpiride (1): carrier-mediated uptake of sulpiride in the human intestinal cell line Caco-2, *Biol. Pharm. Bull.* 25 (2002) 885-890.
 34. K. Watanabe, T. Sawano, T. Endo, M. Sakata, J. Sato, Studies on intestinal absorption of sulpiride (2): transepithelial transport of sulpiride across the human intestinal cell line Caco-2, *Biol. Pharm. Bull.* 25 (2002) 1345-1350.
 35. D. Sun, H. Lennernas, L.S. Welage, J.L. Barnett, C.P. Landowski, D. Foster, D. Fleisher, K.D. Lee, G.L. Amidon, Comparison of human duodenum and Caco-2 gene expression profiles for 12,000 gene

- sequences tags and correlation with permeability of 26 drugs, *Pharm. Res.* 19 (2002) 1400-1416.
36. D.L. Bourdet, G.M. Pollack, D.R. Thakker, Intestinal absorptive transport of the hydrophilic cation ranitidine: a kinetic modeling approach to elucidate the role of uptake and efflux transporters and paracellular vs. transcellular transport in Caco-2 cells, *Pharm. Res.* 23 (2006) 1178-1187.
37. C. Hilgendorf, G. Ahlin, A. Seithel, P. Artursson, A.L. Ungell, J. Karlsson, Expression of thirty-six drug transporter genes in human intestine, liver, kidney, and organotypic cell lines, *Drug Metab. Dispos.* 35 (2007) 1333-1340.

CHAPTER 4

- APPLICATION OF VARIOUS MODEL SYSTEMS IN DETERMINING THE ROLE OF TRANSPORTERS IN THE ABSORPTION OF SELECT MODEL CLASS 3 COMPOUNDS

4.1 Introduction

4.1.1 Rationale

Our research documented thus far in the preceding chapters has concentrated primarily on highly permeable, highly metabolized compounds. But what about the compounds with poor permeability and metabolism? That is an important question; and it is a question that many pharmaceutical scientists are considering. In this chapter we shift our focus to the Class 3 category of the Biopharmaceutics Classification System and the Biopharmaceutics Drug Disposition Classification System (Figure 4.1). It should also be noted that we believe that Class 4 compounds may achieve sufficient solubility in the natural surfactant containing gastrointestinal (GI) contents so that they behave like Class 3 compounds

and, hence, are susceptible to the similar physiological mechanisms governing absorption.

Fig. 4.1a

Biopharmaceutics Classification System (BCS)

	High Solubility	Low Solubility
High Permeability	<p>Class 1</p> <p>High Solubility High Permeability Rapid Dissolution</p>	<p>Class 2</p> <p>Low Solubility High Permeability</p>
Low Permeability	<p>Class 3</p> <p>High Solubility Low Permeability</p>	<p>Class 4</p> <p>Low Solubility Low Permeability</p>

Fig. 4.1b

Biopharmaceutics Drug Disposition Classification System (BDDCS)

	High Solubility	Low Solubility
Extensive Metabolism	<p>Class 1</p> <p>High Solubility Extensive Metabolism</p>	<p>Class 2</p> <p>Low Solubility Extensive Metabolism</p>
Poor Metabolism	<p>Class 3</p> <p>High Solubility Poor Metabolism</p>	<p>Class 4</p> <p>Low Solubility Poor Metabolism</p>

Figure 4.1 (a) The Biopharmaceutics Classification System as defined by the FDA¹ after Amidon *et al.*² (b) The Biopharmaceutics Drug Disposition Classification System.³

According to the Food and Drug Administration (FDA), a drug substance is considered "highly soluble" when the highest marketed dose strength is soluble in 250 ml of aqueous media over a pH range of 1-7.5 at 37°C.¹ A drug substance is considered to be "highly permeable" when the extent of absorption in humans is determined to be

greater or equal to 90% of an administered dose based on a mass balance determination or in comparison to an intravenous reference dose.¹ Accordingly, Class 3 compounds only meet one of these criteria, as they possess characteristics of poor permeability and high solubility. In addition, these compounds are poorly metabolized and their main route of elimination is through renal and/or biliary excretion of unchanged drug.

The limitations of the low permeability characteristics of Class 3 compounds does not necessarily result in an ineffective drug product. A fine example of an effective Class 3 drug is the oral hypoglycemic medication, metformin. In fact, since its approval by the FDA in 1995, metformin has remained among the most highly prescribed drugs in the United States; its pharmacokinetics were initially characterized here at UCSF.⁴⁻⁶ Despite metformin's poorly permeability, it still gains access to the systemic circulation. Moreover, this ability to enter the blood despite the structural challenges is a property shared broadly by Class 3 compounds currently on the market. In the case of metformin, the ability to overcome the gastro-

intestinal barrier results in an oral bioavailability of 40-55%,⁷ certainly not unacceptably poor.

That metformin is a very small molecule (MW 129.2 g/mol), it follows that a component of its absorption may be via a paracellular route.⁸ However, as discussed earlier in Section 1.4.4, we believe that another mechanism that significantly contributes to the intestinal absorption of metformin, and Class 3 drugs in general, is a mechanism of carrier mediate uptake. With high solubility, sufficient drug will be available in the gut lumen but an absorptive transporter will be necessary to overcome the low permeability of these compounds. In this chapter, we discuss the involvement of carrier mediated uptake transport of various Class 3 compounds.

4.1.2 Selecting Class 3 model compounds

It is our laboratory's hypothesis that almost all drugs are substrates for some transporter. Yet for Class 3 compounds, there are many challenges that must be dealt with in order to examine this hypothesis. While a myriad of intestinal uptake transporters have been previously reported, and with new transporters currently being identified, the substrate profile for many of these carriers has not been fully elucidated. This may be attributed to the lack of tools in the past to determine the substrate specificity and affinity. Fortunately,

there are novel tools becoming increasingly more available.⁹⁻¹²

In the case of investigating efflux as well as permeability screening, the Caco-2 cellular system has long been the industry standard. However, the application of this cell line to research on Class 3 compounds has not been as reliable and this issue will be discussed further in this chapter. Various studies have documented the utility of Caco-2 cells and that these cells do endogenously express a multitude of uptake transporters.¹³⁻¹⁷ Unfortunately, the sensitivity of assays run in Caco-2 cells have proven unsuccessful in consistently identifying uptake transporter substrates. However, isolation and stable transfection of uptake transporter proteins has led to new lines that allow investigation of substrates for uptake transporters.^{9,10} For example, the MDCK-PEPT1 cell system has been used for permeability screening of classic peptide substrates.¹¹ In fact, and in contrast to other intestinal absorptive transporters, the peptide transporter 1 (PEPT1) has been well examined because it was one of the first uptake transporters to demonstrate a proven ability to enhance oral absorption; it is an effective target for the nonpeptide prodrug, valacyclovir.¹⁸⁻²²

The extensive characterization of PEPT1 in the literature led to our selection of the angiotensin

converting enzyme (ACE) inhibitor captopril as a model Class 3 compounds for our research. The first reason being that captopril is a known substrate for PEPT1.²³ The second reason being that captopril shows a significant decrease in serum drug levels when administered with a meal.²⁴

In addition to captopril, we chose the histamine H₂-receptor antagonist drug ranitidine as a model Class 3 compound despite being aware that a carrier mediated uptake mechanism has not been fully identified for this drug. It should also be noted that a food drug effect has not been reported for ranitidine. However, another interesting interaction was presented at the 2005 AAPS meeting by FDA scientists and others and later published in 2007 (Figure 4.2)²⁵

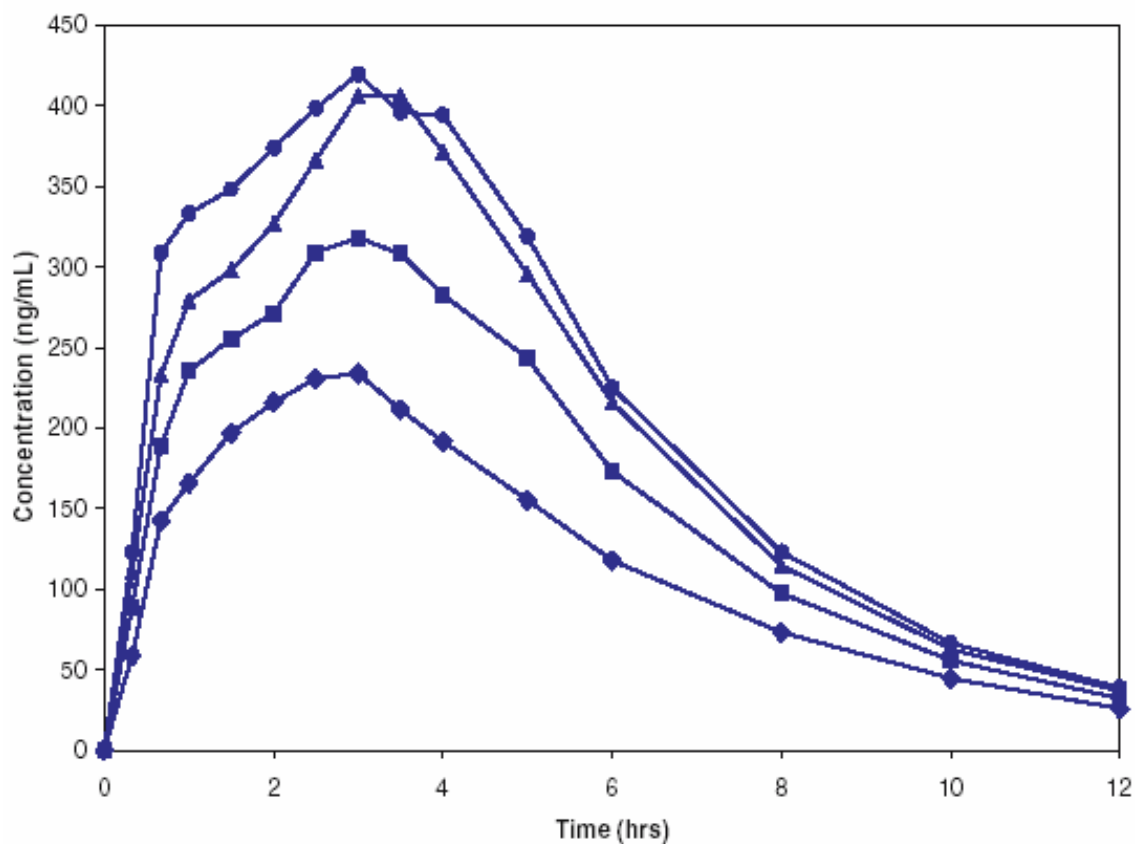


Figure 4.2 Ranitidine plasma concentrations in 24 healthy volunteers after administration of 150 mg ranitidine solution with or without sorbitol; control without sorbitol (closed circle); plus 1.25 grams (triangle); plus 2.5 grams (square); plus 5.0 grams (diamond).

In Figure 4.2, the authors demonstrate a significant reduction in the exposure of ranitidine in the presence of varying amounts of the excipient, sorbitol. We believe a possible explanation for this interaction could

be related to inhibition of unidentified intestinal uptake carriers for ranitidine.

As discussed above, metformin is also a BCS and BDDCS Class 3 compound. We selected metformin for study as well because we believe its absorption involves an uptake transporter. In addition, when metformin is coadministered with a meal, its extent of absorption is decreased with a resulting lowering of its serum concentrations.^{26,27} This food-drug interaction may be explained, in part, by an influence on metformin's uptake transport into enterocytes. One such uptake transporter in the human intestine called the Plasma Membrane Monoamine Transporter (PMAT) was recently reported by Wang and colleagues (Figure 4.3).²⁸ In addition to the human intestine, PMAT has also been reported to be expressed in the mouse and rat intestine.²⁹

Wang and coworkers show in Figure 4.3 that the recently cloned PMAT transporter message and protein are detectable in the human small intestine. More importantly, they utilized immunohistochemistry to clearly depict the localization of PMAT (Figure 4.4),

Fig. 4.3a

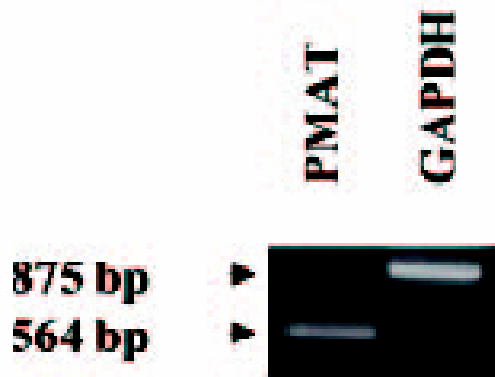


Fig. 4.3b

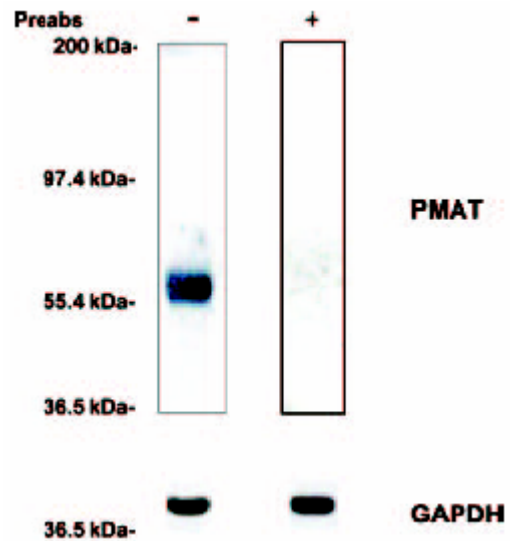


Figure 4.3 PMAT expression in human small intestine by (a) RT-PCR and (b) Western blotting.²⁸

which is highly expressed at the tips of the enterocytes in the small intestine.²⁸ This is precisely where we would expect to find an apical uptake transporter.

An fine example of newer technology and tools in the pharmaceutical sciences is well represented by the PMAT-MDCK cell line engineered by Dr. Wang's group to further study the properties of the uptake transporter and its potential contribution to the absorption of its substrates (Figure 4.5).³⁰

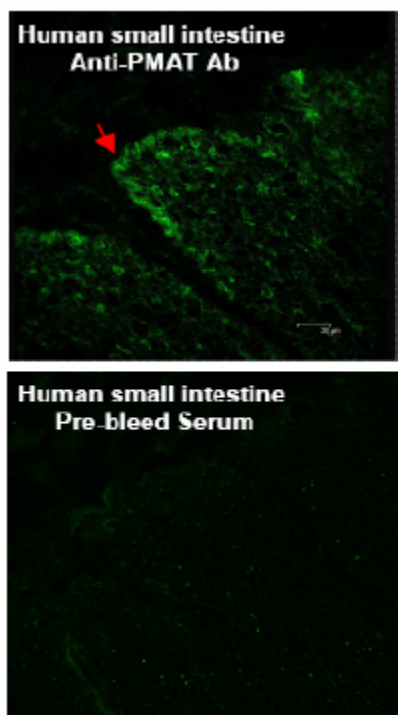


Figure 4.4 PMAT expression in human small intestine by immunohistochemistry performed with an anti-PMAT antibody. Slides containing human small intestine tissue were permeabilized and stained with either anti-PMAT antibody or prebleed serum (control).²⁸

Fig. 4.5a

Fig. 4.5b

Fig. 4.5c

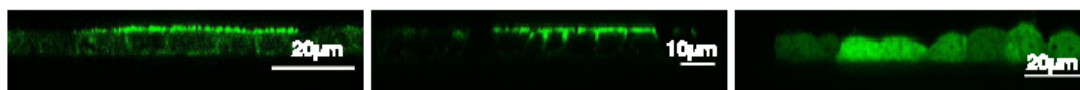


Figure 4.5 Localization of (a) PMAT, (b) YFP-PMAT, or (c) YFP only in polarized PMAT-MDCK cellular monolayers grown on semiporous filter inserts.³⁰ Confocal microscopy of (a) PMAT-MDCK cells were stained with anti-PMAT antibody. Confocal fluorescence microscopy of (b) PMAT-MDCK cells expressing YFP-PMAT; (c) and YFP (yellow fluorescent protein) alone.

In Figure 4.5, Xia *et al.* use confocal microscopy to demonstrate that their PMAT-MDCK cell system expresses the uptake transporter on the apical side of the polarized cells.³⁰ The use of the PMAT antibody does show background staining (Figure 4.5a) but the use of the YFP-PMAT tag indicated the specificity to the apical membrane (Figure 4.5b). This not only confirms that PMAT is properly localized but it also confirms that it is specific.

With the addition of the PMAT transporter into the MDCK cell line, Zhou *et al.* were able to determine the effect of various compounds on the PMAT-mediated uptake of the cation, MPP⁺, thereby demonstrating the similarity of the plasma membrane monoamine transporter to the family of organic cation transporters (OCTs) (Figure 4.6).^{28,31} Moreover, Xia *et al.* were able to show a marked increase metformin uptake, which is further augmented in acidic conditions due to the proton stimulated nature of the transporter (Figure 4.7).²⁸

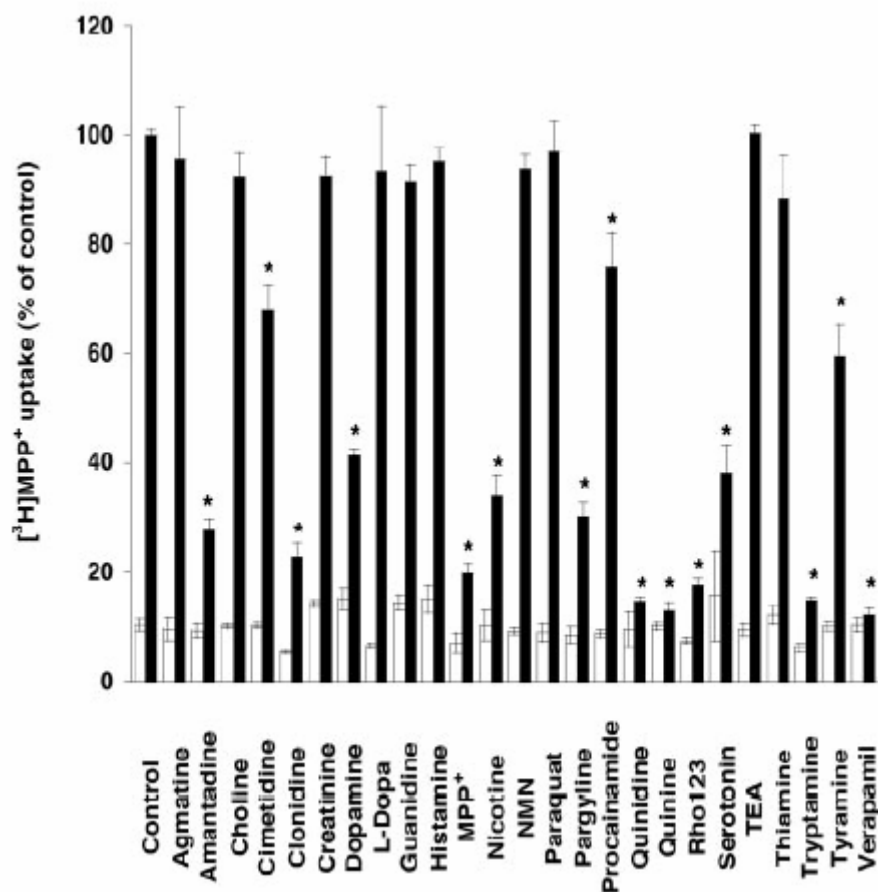


Figure 4.6 The varying levels of uptake of MPP⁺ into PMAT-MDCK (solid bars) cells in the presence of a range of compounds as compared to control MDCK cells (open bars).³¹

Combined with the confirmation that there is proper location and expression of the transporter as well as a negative control, this PMAT-mediated uptake clearly indicates the utility and adequacy of this cell

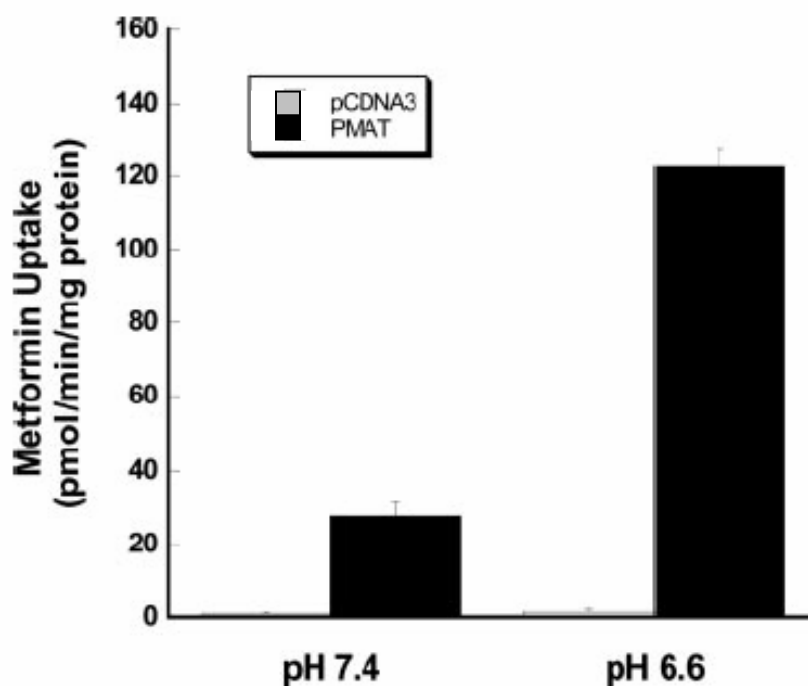


Figure 4.7 The uptake of metformin in PMAT-MDCK cells (black bars) in comparison to MDCK cell transfected with the empty vector only (grey bars). Also, the influence of pH on metformin uptake.

system. Accordingly, and as a result of a gracious gift of cells from Dr. Wang, we evaluated the bidirectional transport of metformin *in vitro*. Adhering to the precedence of the experimental approach of our laboratory, we followed our *in vitro* cellular assays with *in vivo* studies in the rat model. The *in vitro* and *in vivo* results are presented and discussed herein.

4.2 Materials and methods

4.2.1 Materials

PMAT-MDCK and VECTOR-MDCK cell lines were graciously provided by Dr. Joanne Wang (University of Washington, Seattle, WA). The Caco-2 cell line (HTB-37) was purchased from the American Type Culture Collection (ATCC - Manassas, VA). All components necessary for proper cell culture growth conditions (described below) were purchased from the University of California, San Francisco Cell Culture Facility (San Francisco, CA) except for the selective antibiotic, Geneticin[®] (G418), which was purchased as a liquid (50mg/ml) from Invitrogen (Carlsbad, CA). D-[1-³H(N)]-Mannitol was purchased from NEN (Boston, MA). [biguanidine-¹⁴C]-Metformin hydrochloride was purchased from Moravek Biochemicals and Radiochemicals (Brea, CA). L-[methyl-³H]-Carnitine hydrochloride was purchased from American Radiolabeled Chemicals, Inc (St. Louis, MO). GG918 (GF120918: N-{4-[2-(1,2,3,4-tetrahydro-6,7-dimethoxy-2-isoquinolinyl)-ethyl]-phenyl}-9,10-dihydro-5-methoxy-9-oxo-4-acridine carboxamine) was a kind gift from GlaxoSmithKline (Research Triangle Park, NC). All other chemicals were of reagent grade and purchased from Sigma-Aldrich (St. Louis, MO). Poly-D-Lysine Biocoat[®] twelve-well plates were purchased from Becton Dickinson Labware (Bedford, MA). Six-well tissue culture treated polystyrene plates

were obtained from Corning Life Science (Acton, MA). Falcon polyethylene terephthalate cell culture inserts (pore size 0.4 μm , diameter 4.2 cm^2) were obtained from BD Biosciences (Bedford, MA).

4.2.2 Cell culture

4.2.2.1 Caco-2 cell line

Caco-2 cells were grown in a humidified 5% CO_2 atmosphere at 37°C using minimum essential medium (MEM) Eagle's with Earle's balanced salt solution (BSS) containing 1.0 g/L glucose, 0.292 g/L l-glutamine, 2.2 g/L NaHCO_3 , which was supplemented with 15% heat-inactivated FBS, 1.0 mM sodium pyruvate, 0.1 mM nonessential amino acids, 100 U/mL penicillin and 100 U/mL streptomycin. Cells were grown to 90-100% confluence and harvested using 0.05% trypsin EDTA. Monolayers were prepared by seeding harvested cells onto polyethylene terephthalate cell culture inserts at a density of approximately 60,000 cells/ cm^2 . Growth medium for the Caco-2 was refreshed 48 hours post-seeding and then twice weekly, including one day prior to the experiment. Caco-2 cell monolayers were used for bidirectional transport experiments 21-28 days postseeding.

For the intracellular accumulation assays, the Caco-2 cells were grown to 90-100% confluence and harvested

using 0.05% trypsin EDTA. Twelve well plates were prepared by seeding harvested cells into each poly-D-lysine treated well at a density of approximately 500,000 cells/well. Growth medium was refreshed 48 hours post-seeding and then one day prior to the experiment. Cells were used for accumulation studies 4-6 days postseeding.

4.2.2.2 PMAT-MDCK and MDCK cell lines

Both PMAT-MDCK and VECTOR-MDCK were grown in a humidified 5% CO₂ atmosphere at 37°C using minimum essential medium (MEM) Eagle's with Earle's balanced salt solution (BSS) containing 1.0 g/L glucose, 0.292 g/L l-glutamine, 2.2 g/L NaHCO₃, which was supplemented with 10% heat-inactivated FBS, 100 U/mL penicillin and 100 U/mL streptomycin. The selective marker Geneticin (200 •g/ml) was also added to growth medium, as both lines contain the G418 resistant gene. Cells were grown to 90-100% confluence and harvested using 0.05% trypsin EDTA. Monolayers were prepared by seeding harvested cells onto polyethylene terephthalate cell culture inserts at a density of approximately 1,000,000 cells/insert. Growth medium was refreshed once every two days and one day prior to the experiment, which was performed 5-6 days postseeding for both cell lines.

4.2.3 Intracellular accumulation experiments

The intracellular accumulations assays were performed in a twelve well plate format. Each well containing cells was preincubated in control transport buffer (Hank's buffered salt solution containing 25 mM HEPES and 1% FBS, pH 7.4) at 37°C for 20 minutes. All experiments were performed in triplicate and conducted on at least three separate occasions to ensure reproducibility. The experiment was started by the addition of test compound in control transport buffer to the well. The final volume in each well was 0.6 ml. The cell were incubated for 1 hour at 37°C with a shaking speed of 25 strokes/minute in the Boekel Shake 'N' Bake Incubator Shaker II (Boekel Scientific, Feasterville, PA). The solution was then removed by suction and the cells were washed three times with 0.75 ml ice-cold PBS. Following removal of the last wash buffer, 0.4 ml of 0.1% Triton X-100 was added to each well and the plates were allowed to shake at room temperature for 15 minutes before the cells were collected.

4.2.4 Bidirectional transport experiments

The transport assays were performed following a modified protocol previously described by our laboratory.³²⁻³⁵ In brief, cell monolayers were preincubated in control transport buffer (Hank's buffered salt solution containing 25 mM HEPES and 1% FBS, pH 7.4) at

37°C for 20 minutes. Transepithelial electrical resistance (TEER) values were then measured by the Millicell electrical resistance system utilizing "chopstick" electrodes (Millipore Corporation, Bedford, MA). On average, the PMAT-MDCK cells possessed values of approximately 600-800 $\bullet\cdot\text{cm}^2$, while the VECTOR-MDCK cells possessed TEER values of approximately 500-750 $\bullet\cdot\text{cm}^2$. On average, the Caco-2 cells system possessed TEER values of approximately 800-1000 $\bullet\cdot\text{cm}^2$. All experiments were performed in triplicate and conducted on at least three separate occasions to ensure reproducibility. In the case of the PMAT-MDCK and VECTOR-MDCK cells, both transfected and parental cell lines were run on the same day to account for potential between-day variability of radiolabeled counts and TEER values.

The experiment was started by the addition of test compound in control transport buffer to the donor compartment and control transport buffer only to the receiver compartment. The final volume in each of the chambers was 1.5 mL on the apical side and 2.5 mL on the basolateral side. Experimental samples were isolated from the receiver compartment at three time points. At the first two time points, 200 $\bullet\text{L}$ samples were removed and then replaced with fresh media to restore initial starting volumes. At the final time point, following collecting of the last 200 $\bullet\text{L}$ sample, contents of both

chambers were removed by suction, each cell culture insert was dipped three times into ice-cold PBS and the cell culture insert membranes were collected. All experiments were run at 37°C with a shaking speed of 25 strokes/minute in the Boekel Shake 'N' Bake Incubator Shaker II (Boekel Scientific, Feasterville, PA).

4.2.5 *In situ* rat intestinal studies

4.2.5.1 Animals

All animal experiments were conducted using protocols approved by the Institutional Animal Care and Use Committee (IACUC) of the University of California San Francisco. Separate approval was additionally obtained by the University Committee for Use and Care of Animals (UCUCA), University of Michigan. In San Francisco, all animals were housed and handled according to University of California IACUC and Laboratory Animal Resource Center (LARC) guidelines and were maintained on a 12-hour light/dark cycle at the UCSF Animal Care Facility. In Ann Arbor, all animals were housed and handled according to the University of Michigan Unit for Laboratory Animal Medicine guidelines. Male albino Wistar rats (Charles River, IN) weighing 250-280 grams were used for all perfusion studies. Prior to each experiment, the rats were fasted overnight (12-18 hr) with free access to

water. Animals were randomly assigned to the different experimental groups.

4.2.5.2 Single-pass intestinal perfusion procedure

The experimental design for the *in situ* single-pass rat intestinal perfusion was based on procedures documented by Cummins et al.³⁶ as well as Amidon and colleagues.^{37,38} Male albino Wistar rats (250-280 grams) were anesthetized with an intra-muscular injection of 1 ml/kg of ketamine:xylazine solution (9%:1%) and placed on a heated surface maintained at 37°C (Harvard Apparatus Inc., Holliston, MA). The abdomen was opened by a midline incision of 3-4 cm. A proximal jejunal segment (4 cm below the ligament of Treitz) of approximately 10 cm was carefully exposed and cannulated on two ends with flexible PVC tubing (2.29 mm i.d., inlet tube 40 cm, outlet tube 20 cm, Fisher Scientific Inc., Pittsburgh, PA).

Care was taken to avoid disturbance of the circulatory system, and the exposed segment was kept moist with 37°C normal saline solution. The perfusate was incubated in a 37°C water bath to maintain temperature, and a perfusion solution containing 10 mM MES buffer, pH 6.5, 135 mM NaCl, 5 mM KCl, and 0.1 mg/ml phenol red with an osmolarity of 290 mosm/l was pumped through the intestinal segment (Watson Marlow Pumps 323S, Watson-

Marlow Bredel Inc, Wilmington, MA). The isolated segment was rinsed with blank perfusion buffer, pH 6.5, at a flow rate of 0.5 ml/min in order to clean out any residual debris.

At the start of the study, perfusion solution containing metformin (50 μ M) was perfused through the intestinal segment at a flow rate of 0.2 ml/min. In addition, the perfusion buffer contained the nonabsorbable marker, phenol red, to allow quantitation of water flux throughout the experiment. The perfusion buffer was first perfused for 1 hr, in order to assure steady state conditions (as also assessed by the inlet over outlet concentration ratio of phenol red that approached 1 at steady state). Following reaching steady state, samples were taken at 10 min intervals for 1 hour (10, 20, 30, 40, 50, and 60 min).

All samples including perfusion samples at different time points, original drug solution, and inlet solution taken at the exit of the syringe were immediately assayed for metformin and phenol red content. Following the termination of the experiment, the length of the perfused intestinal segment was accurately measured.

4.2.5.3 Single-pass intestinal perfusion data analysis

The net water flux in the single-pass intestinal perfusion studies, resulting from both water absorption

and efflux in the intestinal perfused segment, was determined by measurement of phenol red, a nonabsorbed, nonmetabolized marker. The phenol red (0.1 mg/ml) was included in the perfusion buffer and co-perfused with the tested compound. The measured C_{out}/C_{in} ratio of metformin was corrected for water transport (to obtain the corrected ratio C'_{out}/C'_{in}) according to the following equation:

$$\frac{C'_{out}}{C'_{in}} = \frac{C_{out}}{C_{in}} \times \frac{C_{in \text{ phenol-red}}}{C_{out \text{ phenol-red}}}$$

where $C_{in \text{ phenol red}}$ is equal to the concentration of phenol red in the inlet sample, and $C_{out \text{ phenol red}}$ is equal to the concentration of phenol red in the outlet sample.

The effective permeability (P_{eff}) through the rat gut wall in the single-pass intestinal perfusion studies was determined assuming the "plug flow" model.³⁹ The value

for P_{eff} was calculated by the following equation:

$$P_{eff} \text{ (cm/sec)} = \frac{-Q \ln(C'_{out} / C'_{in})}{2\pi RL}$$

where Q is the perfusion buffer flow rate (0.2 ml/min), C'_{out}/C'_{in} is the ratio of the outlet concentration and the inlet or starting concentration of metformin that has been adjusted for water transport, R is the radius of the intestinal segment (set to 0.2 cm), and L is the length of the perfused intestinal segment.

4.2.6 Analysis of the samples

4.2.6.1 Non-radiolabeled samples

4.2.6.1.1 Sample preparation

For the 200 \bullet l samples obtained at the time points throughout the bidirectional transport studies, the internal standard was added to each tube. For the cells harvested following the accumulation experiments, as well as those at the end of the bidirectional transport experiments, 0.4 ml of methanol/water (50:50) was added to each well or insert, allowed to shake at room temp for at least 30 minutes, and then transferred to a 1.5 ml tube for centrifugation at maximum speed for 10 min. An aliquot (200 \bullet l) of the supernatant was transferred to a clean tube and the internal standard was added to each

tube. The final sample mixtures were then mixed briefly followed by centrifugation at 4000 rpm for 10 min. An aliquot (150 μ l) of the supernatant was transferred into HPLC screw cap vials with 250- μ l inserts (Hewlett Packard, Palo Alto, CA).

4.2.6.2.2 Sample analysis

Samples were analyzed by LC/MS following a modified protocol based on work previously described by Lau *et al.*⁴⁰ and Christians *et al.*⁴¹ from our laboratory. We used a liquid chromatography-mass selective detector system (Hewlett Packard) consisting of the 1100 HPLC components HPLCI and HPLCII connected via a 7240 Rheodyne six-port switching valve mounted on a step motor (Rheodyne, Cotati, CA). The system was controlled and data were processed using ChemStation Software revision A.06.01 (Hewlett Packard).

Samples (50 μ l) were injected onto a 10 x 2-mm extraction column (Keystone Scientific, Bellefonte, PA) filled with Hypersil ODS-1 of 10- μ m particle size (Shandon, Chadwick, UK). The samples were washed with a mobile phase that consisted of 13 mM trifluoroacetic acid in ACN:H₂O (40:60). The flow was 2 ml/min, and the temperature for the extraction column was set to 65°C. After 0.75 min, the switching valve was activated, and the analytes were eluted in the backflush mode from the

extraction column onto a 150mm X 4.6 mm C18 Xterra 5•m analytical column (Waters, Milford, MA). The mobile phase consisted of 13mM trifluoroacetic acid in ACN:H₂O (40:60). The flow rate was 1.5 ml/min with a splitter resulting in 0.5 ml/min to the detector. The analytical column was also maintained at 65°C. Two minutes after sample injection, the mass-selective detector was activated.

4.2.6.2 Radiolabeled samples

4.2.6.2.1 Sample preparation

All samples were added to 5 mL Econo-Safe™ Counting Cocktail (Research Products International Corporation, Mount Prospect, IL) and vortex mixed. Cells monolayers were solubilized by sonication (in an ultrasonic bath) for 15 minutes.

4.2.6.2.2 Sample analysis

All samples were analyzed using a Beckman LS180 scintillation counter (Beckman Industries, Palo Alto, CA).

4.3 Results

4.3.1 Studies with captopril in Caco-2 cells

We began our investigation of BCS and BDDCS Class 3 compounds with Caco-2 cells and the

angiotensin converting enzyme (ACE) inhibitor captopril. We performed uptake assays as well as inhibition studies with various inhibitors including rifampicin, indocyanine green, glycyl-L-sarcosine, cephalixin, benzoic acid, sodium taurocholate, and monoolein. We analyzed our samples by LC/MS and successfully created a method to detect captopril and our internal standard, enalapril (Figure 4.8). However, experiments run in our Caco-2 cellular system resulted in minimal intracellular levels of drug, no different than background levels, and constant under all conditions tested (data not shown).

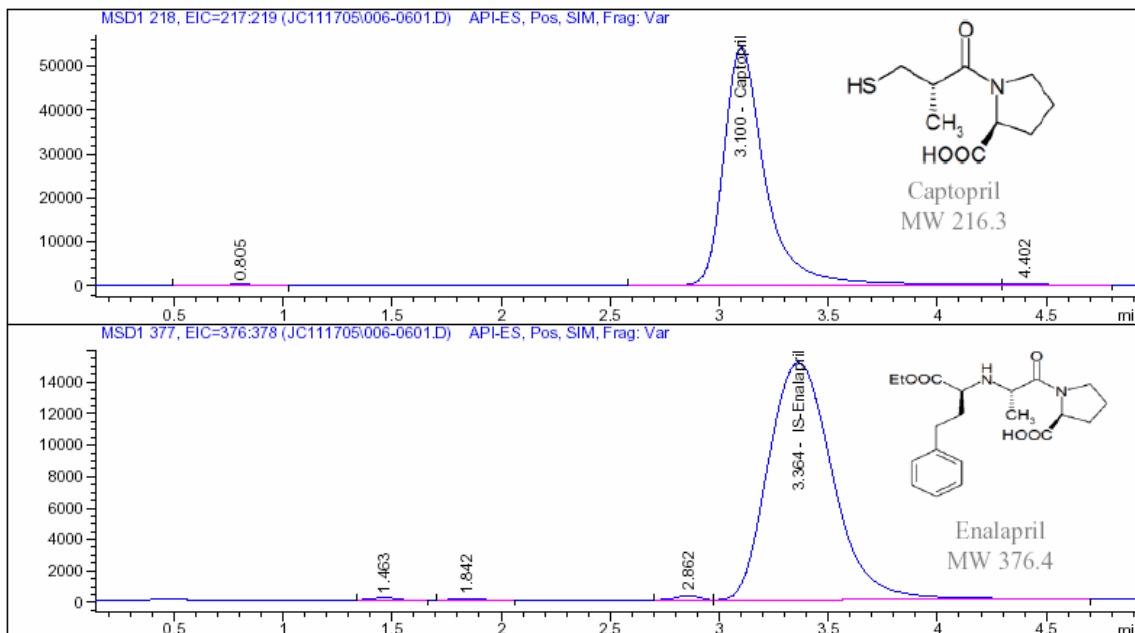


Figure 4.8 LC/MS chromatograms of captopril (MW 216.3) and the internal standard, enalapril (MW 376.4).

4.3.2 Studies with metformin in Caco-2 cells

Prior to receiving the PMAT-MDCK and VECTOR-MDCK cells, we performed various uptake and inhibitor studies in our Caco-2 cell system because of reported evidence of endogenous expression of absorptive transporters (Figure 4.9).¹³⁻¹⁷ Figure 4.9a compares the uptake of varying concentrations of metformin at 37°C and 4°C clearly demonstrating the involvement of a saturable, carrier-mediate uptake process in the absorption of metformin. Figure 4.9b depicts the

inhibitory profile of metformin in the presence of various known transporter substrates and inhibitors including 1-methyl-4-phenylpyridinium (MPP+), tetraethylammonium (TEA), and the zwitterion L-carnitine. Intracellular accumulation was measured in the presence or absence of the known P-gp inhibitor, GG918 and resulted in no change (data not shown). Figure 4.9c depicts the concentration dependent inhibitory effect of L-carnitine on the uptake of metformin and the significant inhibition by monoolein is shown in Figure 4.9d, a decrease of 42%. The uptake of metformin was also evaluated over a range of pH 5 to pH 9 and no difference was detected (data not shown).

4.3.3 Bidirectional transport assays and intracellular accumulation studies of metformin in PMAT-MDCK and VECTOR-MDCK cells

Once it was determined that metformin is avidly transported by the recently cloned plasma membrane monoamine transporter (PMAT),²⁸ we obtained the PMAT-MDCK and VECTOR-MDCK cells and performed bidirectional transport assays and intracellular accumulation studies (Figures 4.10 - 4.14).

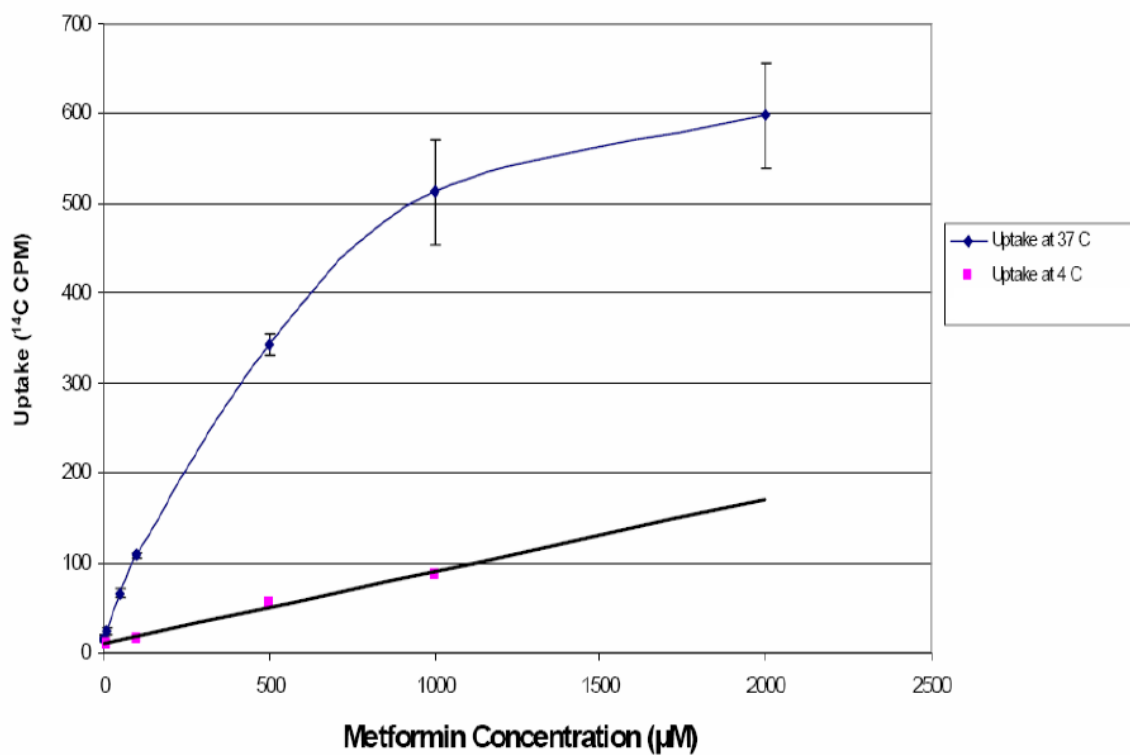


Figure 4.9a Uptake of varying concentrations of metformin in Caco-2 cells at 37°C and 4°C.

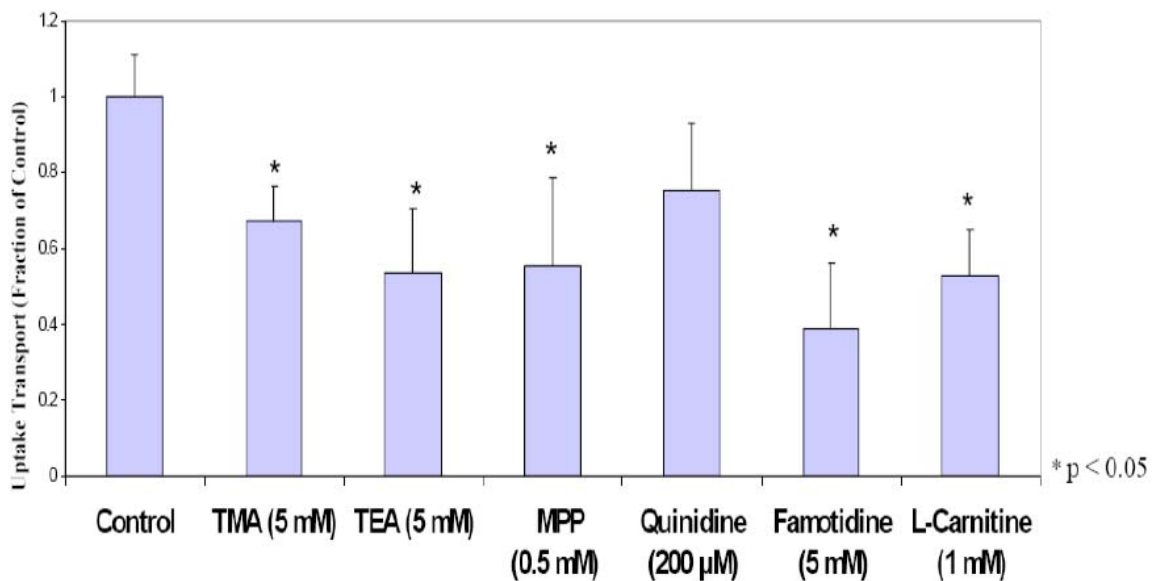


Figure 4.9b The inhibitory profile of metformin in Caco-2 cells in the presence of various compounds.

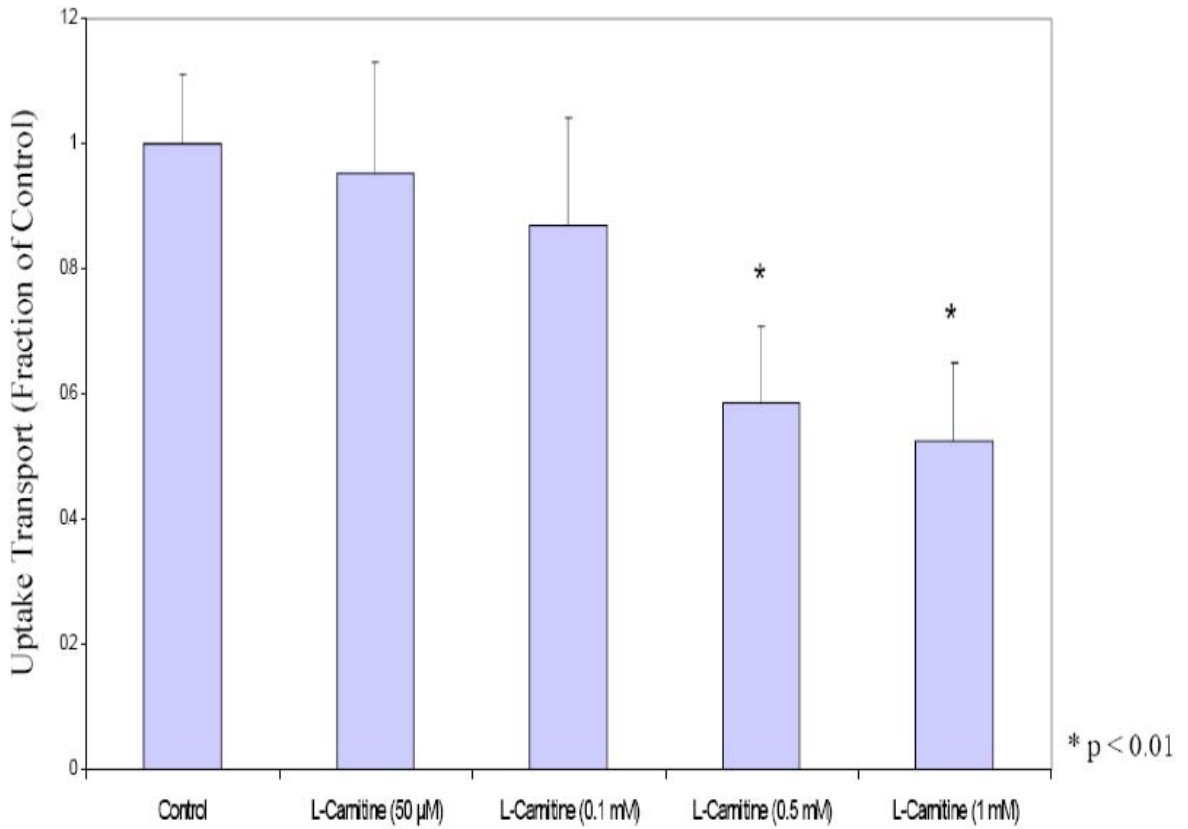


Figure 4.9c The concentration dependent inhibition of metformin uptake in Caco-2 cells by L-carnitine.

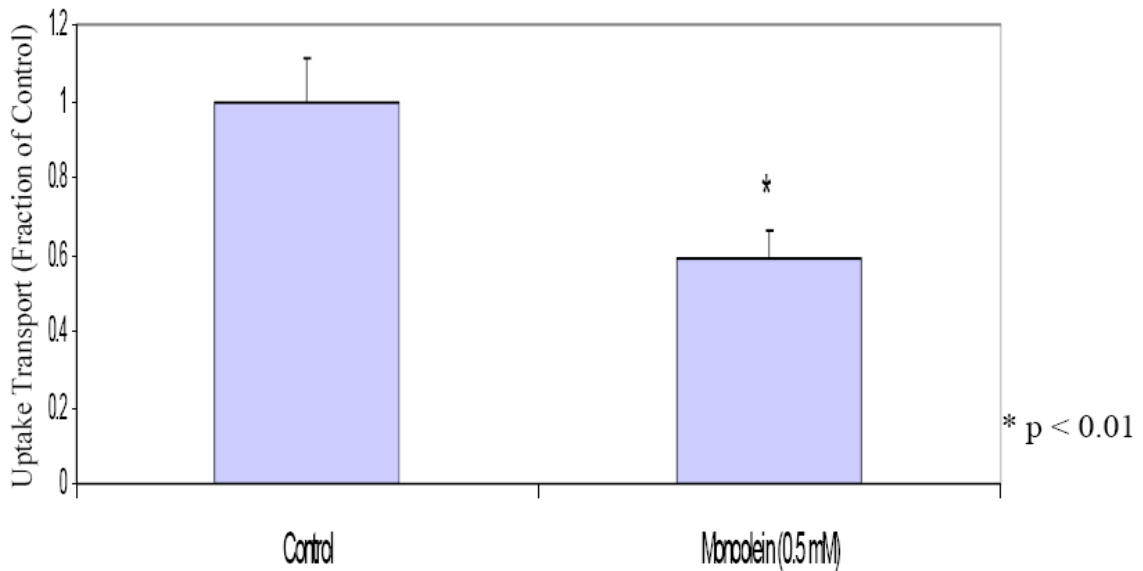


Figure 4.9d The inhibition of metformin uptake in Caco-2 cells by monoolein.

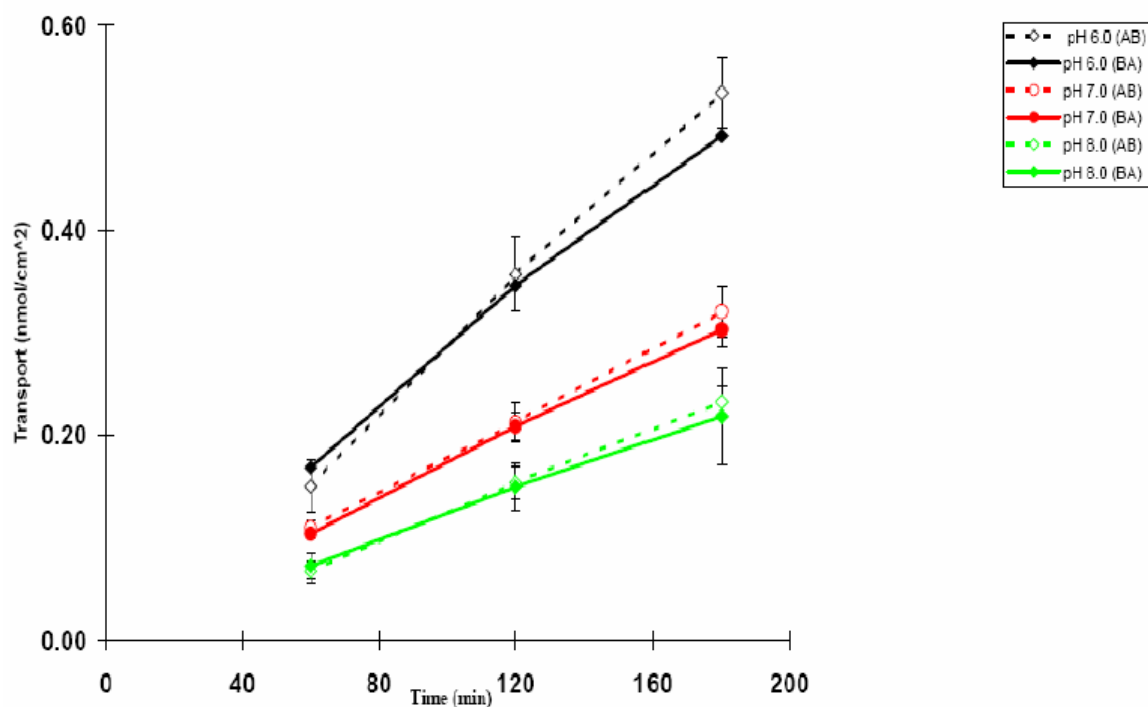


Figure 4.10a Bidirectional transport of metformin (10 μM) in PMAT-MDCK cells at pH 6 (black); pH 7 (red); pH 8 (green).

To test the system and confirm previously reported pH data by Zhou *et al.*,^{28,31} we evaluated the transport of metformin over a range of pH 6 to pH 8. Figure 4.10a depicts in PMAT-MDCK cells the increasing flux in both direction with increasing acidity while Figure 4.10b show no pH effect in the VECTOR-MDCK parental control cells. The subsequent experiments were performed at the control pH of 7.2.

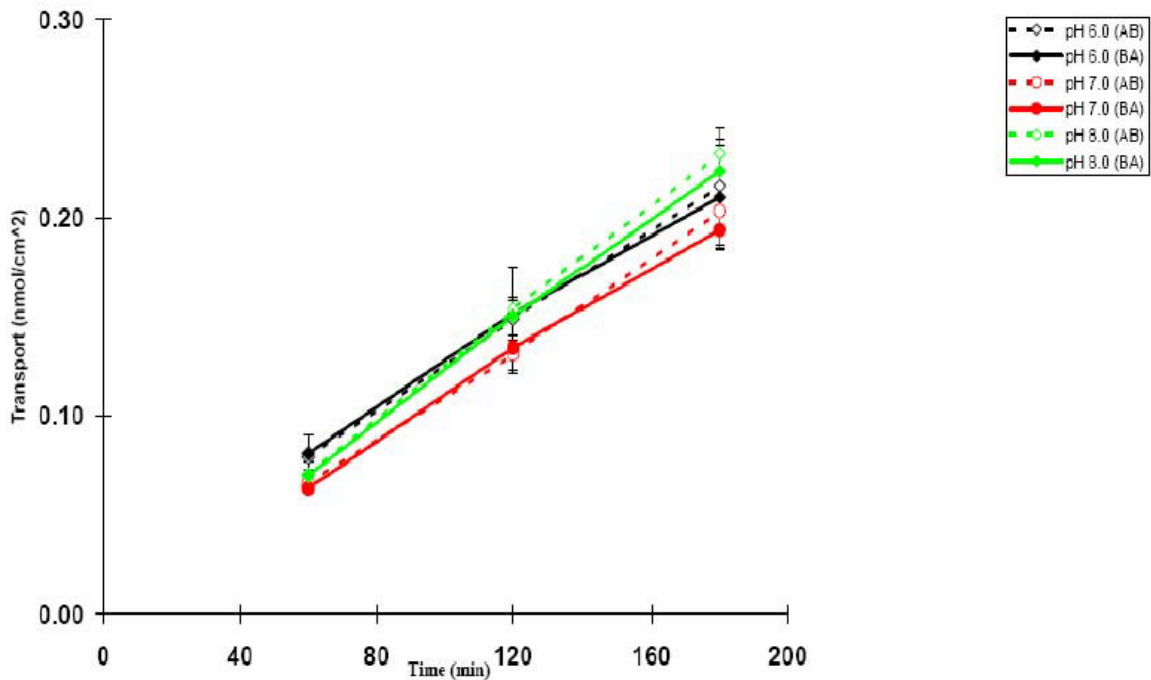


Figure 4.10b Bidirectional transport of metformin (10 μM) in VECTOR-MDCK cells at pH 6 (black); pH 7 (red); pH 8 (green).

Figure 4.11a depicts the transport profile of metformin in PMAT-MDCK cells in the presence or absence of the known PMAT inhibitor MPP⁺ (1.0 mM). Here we observed greater apical to basolateral (A to B) transport than in the basolateral to apical (B to A) direction, and both the A to B and B to A fluxes were significantly reduced with the addition of MPP⁺.

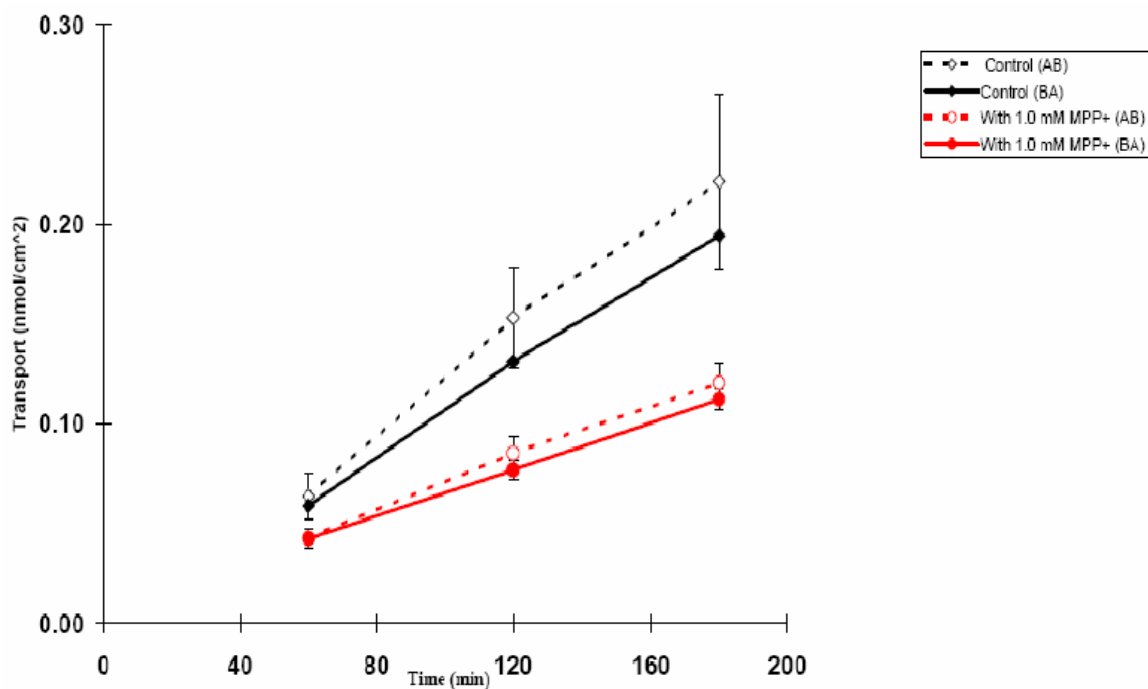


Figure 4.11a Bidirectional transport of metformin (10•M) PMAT-MDCK cells in the presence (red lines) or absence (black lines) of the known PMAT inhibitor, MPP⁺.

These effects are not observed in parental VECTOR-MDCK cells (Figure 4.11b). No change in transport in either direction in transfected or nontransfected cells was observed in the presence of monoolein (0.5 mM) (data not shown).

The intracellular accumulation resulting from an apical dose (A to C) decreased significantly in the presence MPP⁺ while the intracellular accumulation

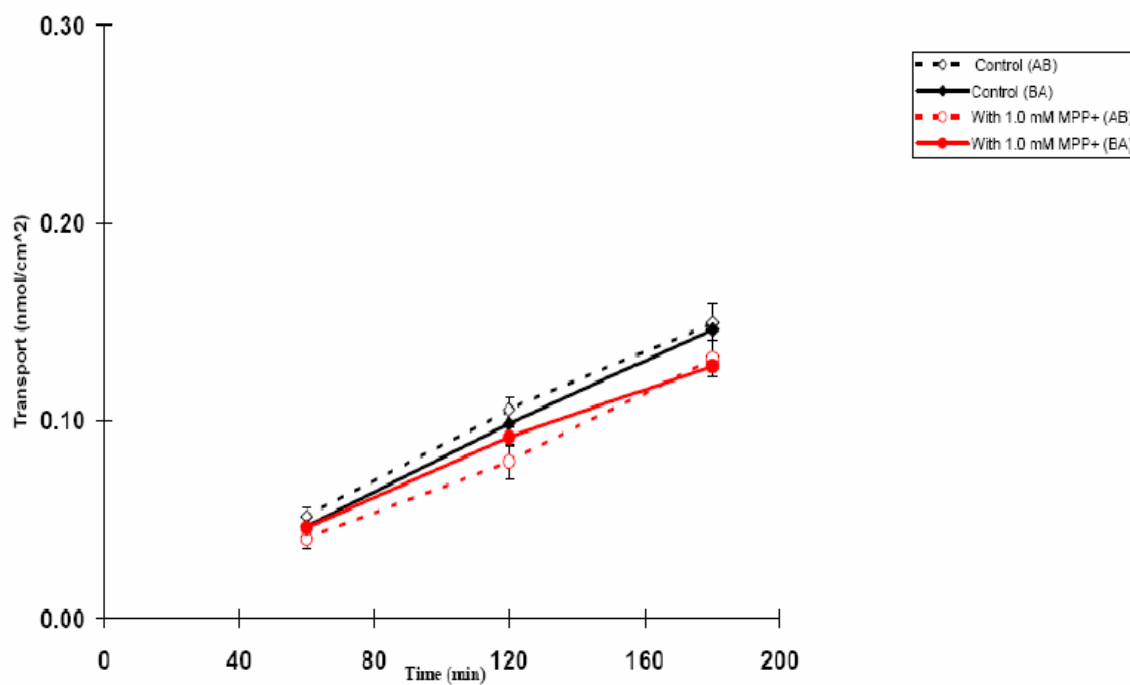


Figure 4.11b Bidirectional transport of metformin (10 μM) VECTOR-MDCK cells in the presence (red lines) or absence (black lines) of the known PMAT inhibitor, MPP⁺.

resulting from a basolateral dose (B to C) was reduced by greater than 90% with MPP⁺ (Figure 4.12a). The A to C effect is insignificant in the VECTOR-MDCK cells, however, there remains a marked inhibition of metformin accumulation in control cells in the B to C direction with the addition of MPP⁺ (Figure 4.12b).

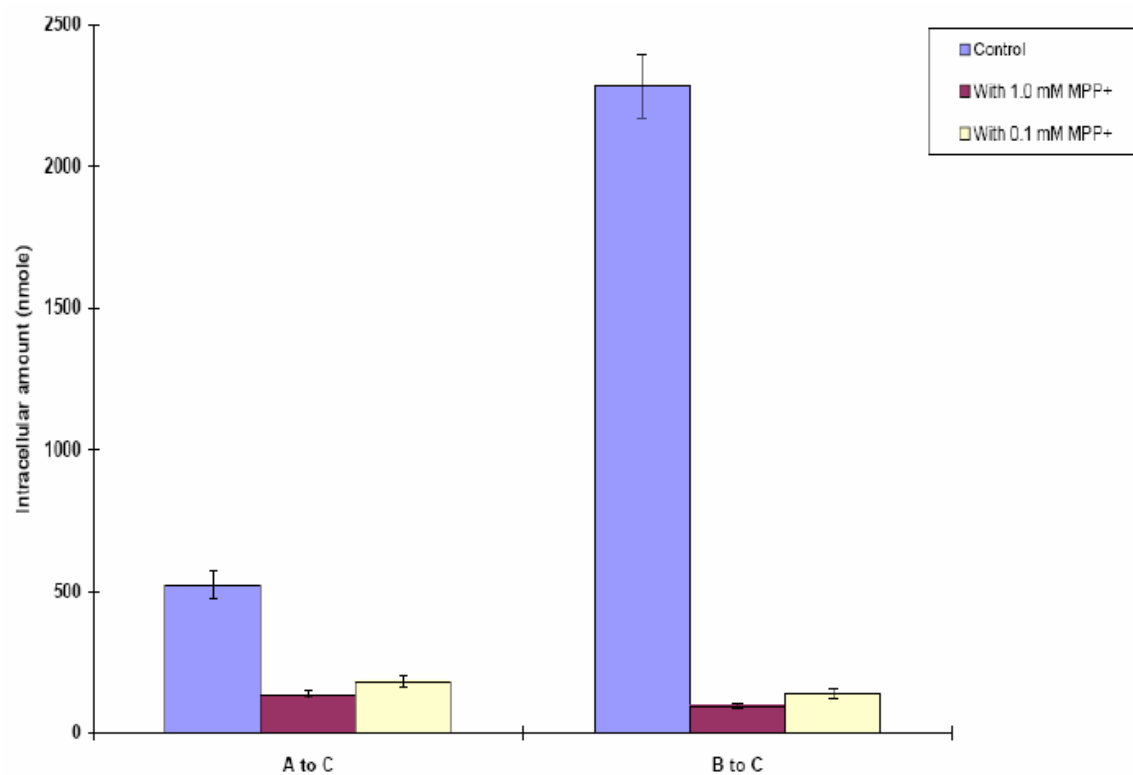


Figure 4.12a Intracellular accumulation of metformin (10 μM) in PMAT-MDCK cells in the presence or absence of MPP⁺.

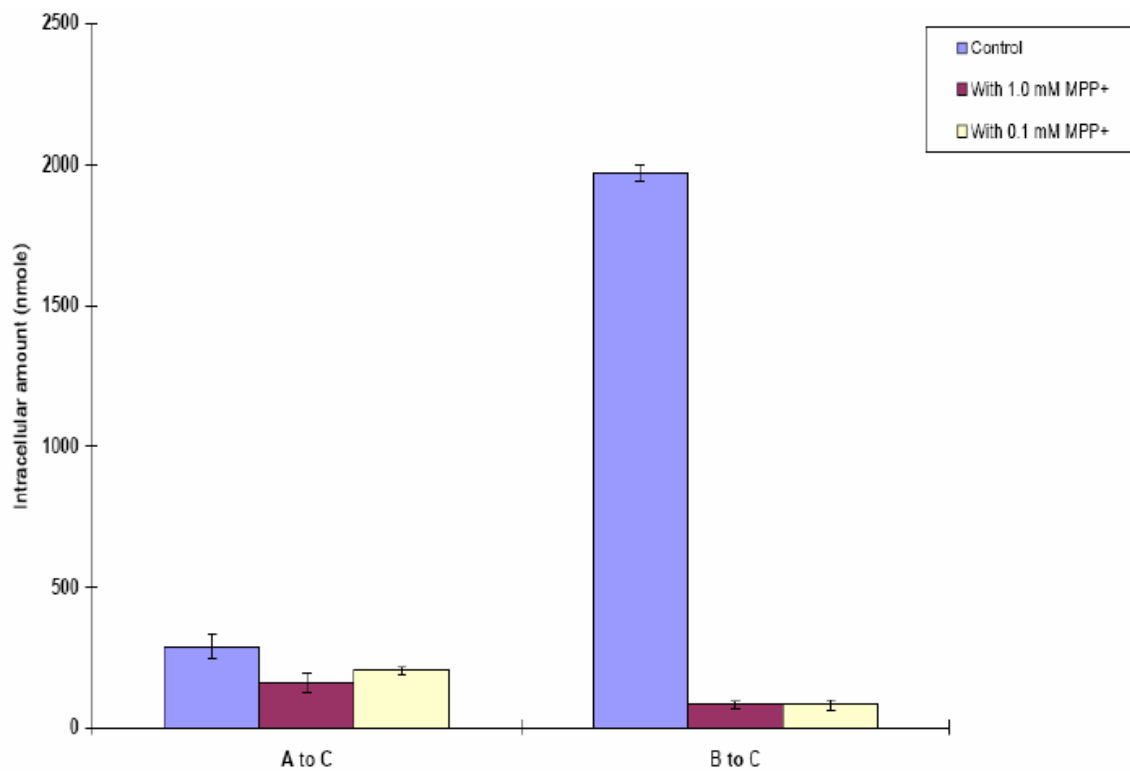


Figure 4.12b Intracellular accumulation of metformin ($10 \mu\text{M}$) in VECTOR-MDCK cells in the presence or absence of MPP^+ .

4.3.4 The multiple transporter effect of metformin in PMAT-MDCK and VECTOR-MDCK cells

In order to evaluate what we hypothesized to be a multiple carrier effect observed in the PMAT-MDCK cells, we ran additional bidirectional transport studies (Figures 4.13 and 4.14). Again we conducted experiments with 1.0 mM MPP⁺ (inhibitor of both PMAT and OCT1) but, in addition, we utilized 0.5 mM TEA because of its ability to inhibit OCT1 but not PMAT.^{28,31,42}

Figure 4.13a depicts the transport profile of metformin in PMAT-MDCK cells in control media, with 1.0 mM MPP⁺, or with 0.5 mM TEA. As expected and as seen previously in Figure 4.11a, both the A to B and B to A transport of metformin was significantly reduced with the addition of MPP⁺. However, the addition of TEA results in an inhibition of transport only in the B to A direction (Figure 4.13a). As a control, experiments performed in the parental VECTOR-MDCK cells did not result in any inhibition of transport flux in either direction (Figure 4.13b).

Intracellular accumulation resulting from an apical dose (A to C) decreased 81% in the presence of 1.0 mM MPP⁺ but was unchanged in the presence of 0.5 mM TEA (Figure 4.14a). Intracellular accumulation resulting from a basolateral dose (B to C) was

reduced by both MPP⁺ and TEA (0.5 mM), a 96% and 82% decrease, respectively (Figure 4.14a). In the VECTOR-MDCK cells, we observe a similar inhibition of B to C transporter flux with both MPP⁺ and TEA but the A to C flux is affected to a lesser degree (Figure 4.14b)

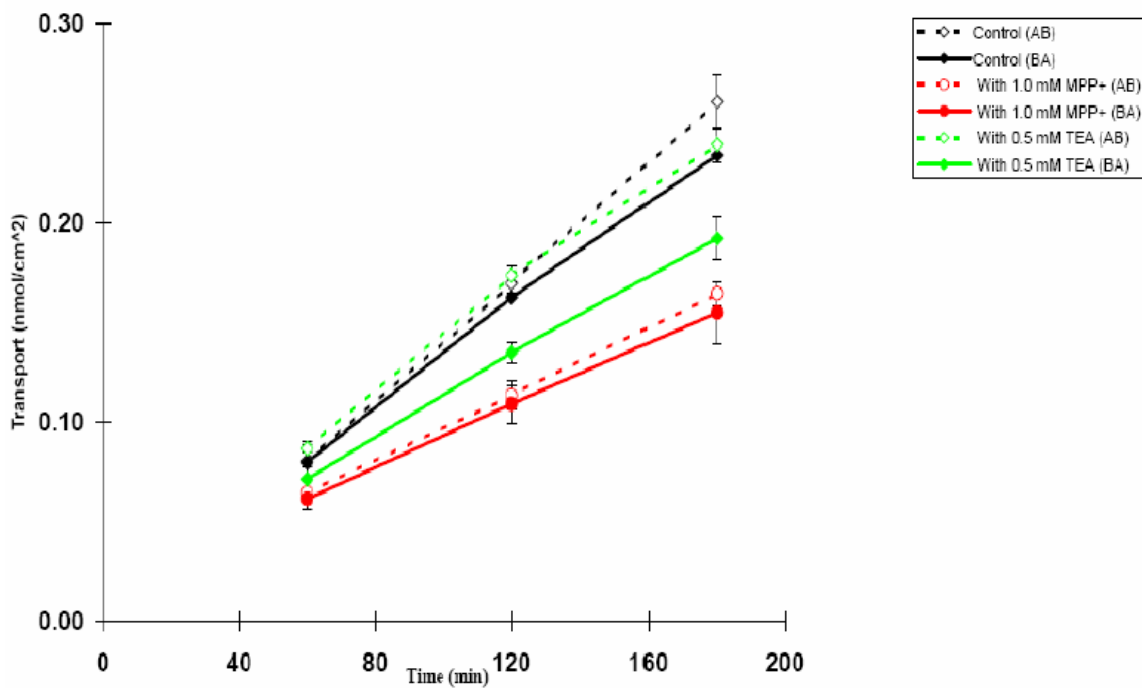


Figure 4.13a Bidirectional transport of metformin (10 μM) in PMAT-MDCK cells in control media (black lines); MPP⁺ (red lines); and TEA (green lines).

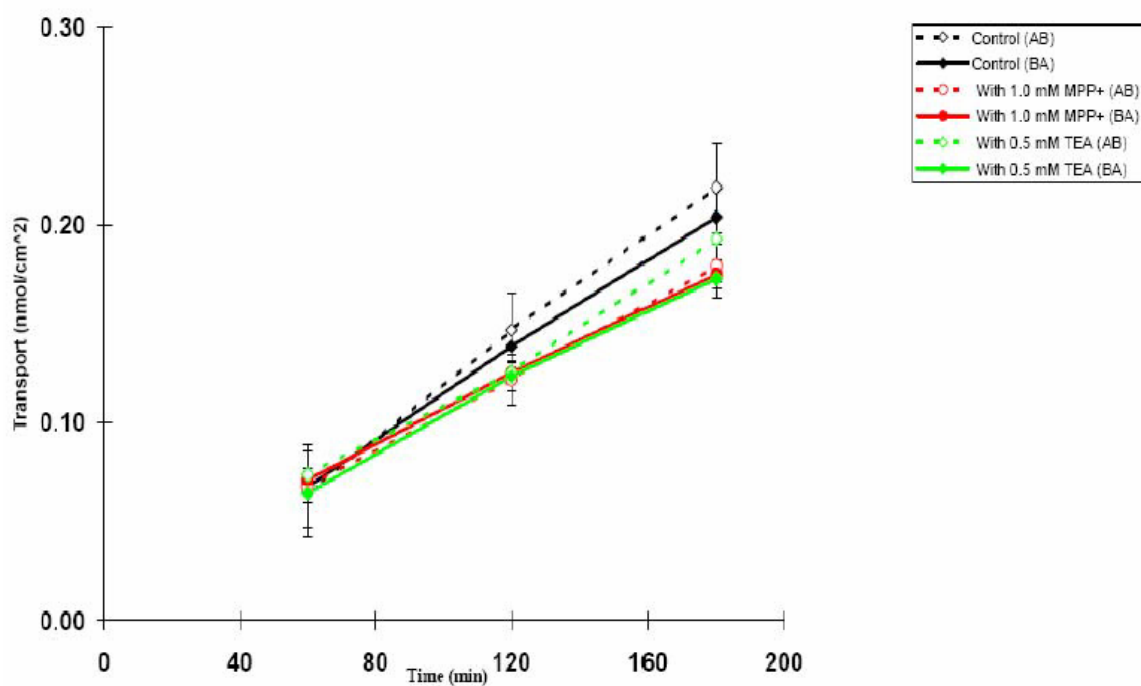


Figure 4.13b Bidirectional transport of metformin (10 μM) in VECTOR-MDCK cells in control media (black lines); MPP⁺ (red lines); and TEA (green lines).

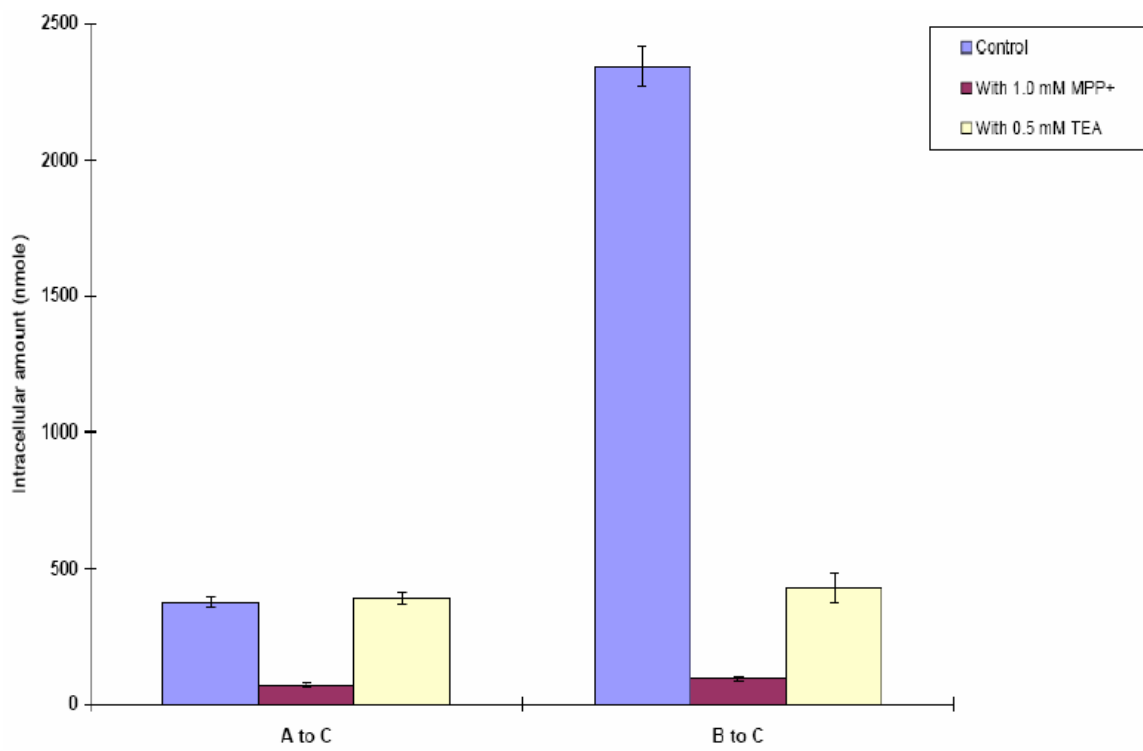


Figure 4.14a Intracellular accumulation of metformin (10 μM) in PMAT-MDCK cells in control media, MPP⁺, or TEA.

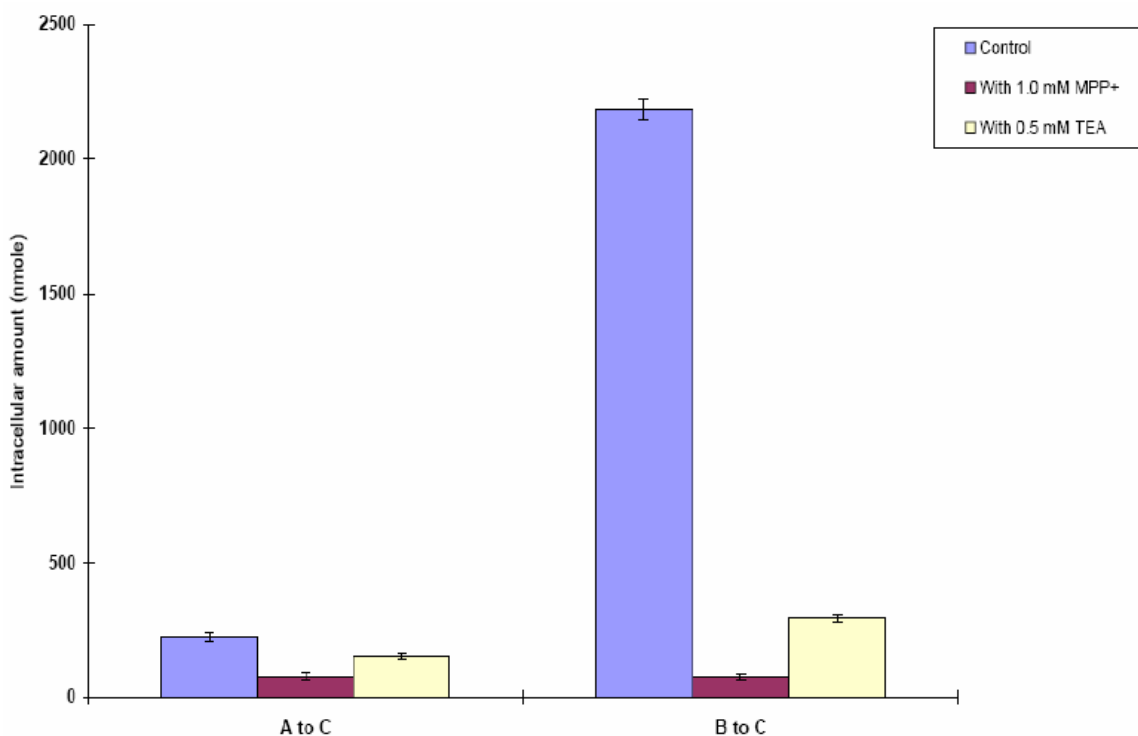


Figure 4.14b Intracellular accumulation of metformin (10 μM) in VECTOR-MDCK cells in control media, MPP⁺, or TEA.

4.3.5 Exploring the multiple transporter effect of metformin in Caco-2 cells

In order to explore the correlation between the flux of metformin across the PMAT-MDCK monolayers versus the flux measured across Caco-2 monolayers, we performed bidirectional transport assays with Caco-2 cells and observed no significant differences in transport in either direction with or without the inhibitors MPP⁺ (1.0 mM) or TEA (0.5 mM) (Figure 4.15).

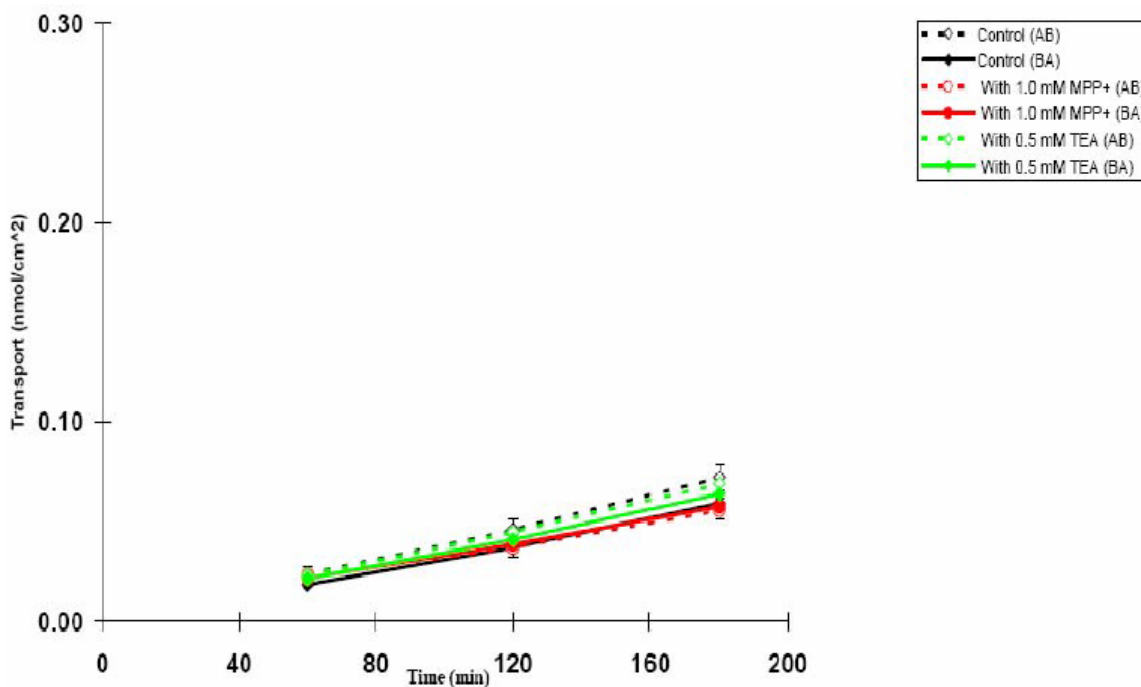


Figure 4.15 Bidirectional transport of metformin (10•M) in Caco-2 cells in control media (black lines); MPP⁺ (red lines); and TEA (green lines).

4.3.6 Single pass intestinal perfusion experiments in the rat model

To determine if the *in vitro* transporter effects we observed in our cellular systems are reflected *in vivo*, we utilized *in situ* jejunal segments from male albino Wistar rats. Figure 4.16 represents the single pass intestinal perfusion of metformin run in the rat model in control conditions of metformin alone, metformin perfused with MPP⁺ (0.5 mM), or metformin perfused with TEA (0.5 mM). The effective permeability (P_{eff}) of metformin is unchanged in the presence of MPP⁺ but is significantly reduced when

perfused with TEA (Figure 4.16). Metformin P_{eff} is unchanged when perfused in the presence of monoolein (0.5 mM) (data not shown).

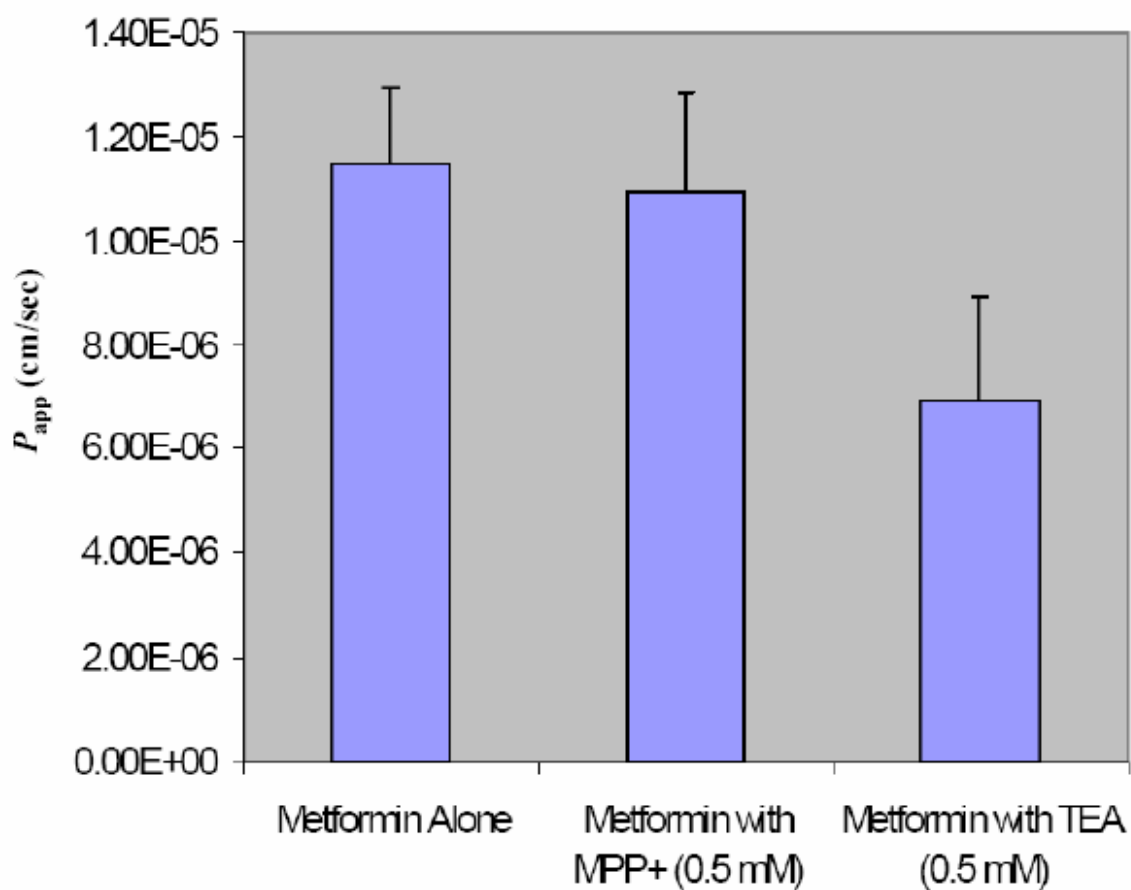


Figure 4.16 The effective permeability (P_{eff}) of metformin in the rat intestinal perfusion model when dosed alone, with MPP⁺, or with TEA.

4.4 Discussion

With advances in the pharmaceutical sciences, new molecular entities that violate the "Rule of 5" proposed by Lipinski⁴³ are not necessarily discarded. It is not uncommon for medicinal chemists to synthesize molecules that are either poorly soluble or poorly permeable, or both. In the previous chapters we discussed the high permeability, low solubility and extensively metabolized BCS and BDDCS Class 2 drugs. These are the compounds that are often dual substrates of metabolizing enzymes and efflux transporters in the gut.^{3,44} In this chapter, we concentrate on the absorption mechanisms of the nonmetabolized compounds. It is our hypothesis that the poorly permeable Class 3 compounds generally rely on uptake transporters to get into the cell. It is also our hypothesis that food-drug interaction trends observed in the literature for Class 3 drugs, that being a decrease in availability, may be attributed in part to an inhibition of intestinal uptake transporters following coadministration with a meal.

We began our investigation of Class 3 drugs with the angiotensin converting enzyme (ACE) inhibitor captopril. This compound was ideal not only because its bioavailability is reduced when given with food,²⁴ but also because it has been previously identified a

substrate of the intestinal, apical uptake peptide transporter 1 (PEPT1).²³

Our decision to perform the captopril experiments in the Caco-2 cell system was not necessarily for a lack of a better model at the time. There is evidence in the literature of the expression of uptake carriers in the Caco-2 cell line.¹⁷ However, Caco-2 cells have largely been a tool for permeability screening and efflux assessment. It was our aim to utilize the endogenous activity of PEPT1 in the Caco-2 cells and evaluate the absorption and inhibition profile of captopril *in vitro*. We developed an accurate method to detect captopril levels by LC/MS (Figure 4.8) but we were unable to achieve sufficient cellular uptake of captopril to measure levels over background or to observe changes in the presence of various compounds including monoolein, rifampicin, and the known PEPT1 inhibitor, glycyl-L-sarcosine.

Another roadblock occurred with our attempts to investigate the intestinal absorption of the histamine H₂-receptor antagonist Class 3 drug ranitidine. In this case, we were not focused on a particular uptake transporter because one had not yet been identified. Instead, we were interested in determining if we could successfully apply the Caco-2 cell model to better understand ranitidine absorption and its potential

transporter interactions such as that described by Chen and coworkers.²⁵ Unfortunately, we again were unable to achieve sufficient drug intracellular levels for analysis.

With ranitidine, this roadblock was a dead-end because no transporter has been shown to be responsible for its absorption. With captopril, however, PEPT1 was a known candidate and this has already resulted in the development of the stably transfected cell system, PEPT-MDCK.⁴⁵ Through communication with Dr. Faria at Bristol-Myers Squibb (BMS), we arranged to obtain this cell line in exchange for our cMOAT-MDCK cell line. Yet despite agreement from both parties, the transfer of cell lines never materialized.

Therefore, we moved forward with our investigation of the oral anti-diabetic agent, metformin, also a BCS and BDDCS Class 3 drug. This time the decision to conduct our studies in the Caco-2 cell systems was indeed for a lack of a better model. However, one relies on the tools at hand. That said, metformin was an especially good model compound because it has been on the market for over 20 years but its mechanism of intestinal absorption remains unclear. It is among the more commonly taken drugs and its absorption is significantly decreased when administered with a high fat meal.^{26,27}

In the Caco-2 cell model, we were able to demonstrate a saturable carrier-mediated uptake process involved in the absorption of metformin (Figure 4.9a). Our ability to achieve quantifiable intracellular levels of drug provided us the ability to examine the inhibitory effects on carrier mediated uptake by conducting the assay in the presence of various transporter substrate inhibitors. We demonstrated that metformin uptake could be significantly reduced by compounds such as 1-methyl-4-phenylpyridinium (MPP+), tetraethylammonium (TEA), and the zwitterion L-carnitine (Figure 4.8b). The known novel organic cation transporter (OCTN1 and OCTN2) substrate and inhibitor, L-carnitine inhibits the uptake of metformin in a concentration dependent manner (Figure 4.9c). In addition, we observed a 42% decrease in metformin uptake in Caco-2 cells in the presence of monoolein (0.5 mM) (Figure 4.9d). The pH of the buffer appeared to have no influence on transport. Also, GG918 had no effect confirming earlier reports that metformin is not a P-gp substrate. Although we were able to measure intracellular uptake, there was insignificant transport mediated flux when bidirectional assays were performed (Figure 4.15).

In the midst of our experimentation with metformin in Caco-2 cells, we added a new tool to our stock that has proven to be invaluable in our studies. Courtesy of

Dr. Joanne Wang, we obtained the MDCK cell line stably transfected with the recently cloned, plasma membrane monoamine transporter (PMAT-MDCK) (Figures 4.5 through 4.7).^{28,30,31} Dr. Wang has demonstrated that metformin is avidly transported by PMAT with comparable affinity to the organic cation transporters 1 and 2 (OCT1 and OCT2), both of which are documented transporters of metformin.^{28,46-48}

PMAT is an apical uptake transporter expressed on tips of the enterocytes in the human intestine. When expressed on the polarized MDCK cell monolayers, it serves as a model for evaluating absorption. In PMAT-MDCK cells, we observed significantly greater apical to basolateral (A to B) transport than in the basolateral to apical (B to A) direction; and both the A to B and B to A transport fluxes were significantly reduced with the addition of MPP⁺ (1.0 mM) (Figure 4.11a). These effects were not observed in control parental MDCK cells, consistent with an transporter effect (Figure 4.11b).

Although we expected to see this apical PMAT transporter result, we were also very interested in what we observed at the basolateral membrane (Figures 4.11 and 4.12). In addition to the reduced flux across the membrane, the intracellular accumulations resulting from both an apical dose (A to C) and a basolateral dose (B to C) were markedly decreased in the presence of MPP⁺ (1.0

mM). Moreover, this basolateral effect is observed in the parental control VECTOR-MDCK cells denoting that it is an effect unrelated to the transfection with the PMAT protein (Figure 4.12b). What we believe is occurring at the basolateral membrane is an OCT1 effect and the reduction in metformin flux and accumulation when basolaterally dosed in the presence of MPP⁺ is due to inhibition of OCT1 by MPP⁺.

To test our multiple transporter explanation of PMAT on the apical side and OCT1 on the basolateral side we again employed MPP⁺ as the inhibitor of PMAT and OCT1, but we also used TEA as an inhibitor of OCT1 only. This was necessary because PMAT, being a newly cloned protein, does not currently have a specific inhibitor. As expected, the apical PMAT transporter effect of reduced flux (A to B) and reduced intracellular accumulation (A to C) was observed with addition of MPP⁺, but not with the addition of TEA (Figures 4.13a and 4.14a) because MPP⁺ inhibits PMAT while TEA does not. The basolateral OCT1 effect ((B to A) and (B to C)) is observed with both MPP and TEA because both are inhibitors of OCT1. Moreover, the B to C effect is carried over to the parental VECTOR-MDCK cells indicating that it is due to the endogenous expression of OCT1 in MDCK cells (Figures 4.13b and 4.14b). The A to C effect is seen to a lesser degree in the VECTOR-MDCK cells suggesting an interaction with both

MPP⁺ and TEA but this may be attributed to inhibition of OCT1 on the basolateral membrane, which would block the reuptake of metformin into the cell from the basolateral compartment (Figures 4.13b and 4.14b). Combined, these data implicate the apical uptake transporter PMAT and the basolateral uptake transporter OCT1 in the absorption of metformin *in vitro*.

Revisiting our initial model, we replicated the experimental procedure employed to detect the multiple transport effect in the PMAT-MDCK cells, applying it to Caco-2 cell monolayers. Figure 4.15 clearly indicates that these dual transporter effects cannot be observed in the Caco-2 model. Furthermore, the results of our pH assays depicted in Figure 4.10 are in contrast to our results from Caco-2 cells, which remain constant with varying pH. In fact, Western blotting for the PMAT protein in Caco-2 cells results in a detectable band but immunohistochemistry on Caco-2 shows diffuse, nonspecific cytoplasmic staining (correspondence with Dr. Wang). This confirms that while the transporter protein may be present in Caco-2 cells, it is not functionally active or properly localized. This is supported by our calculated value of 0.51 mM for the apparent affinity (K_m) in Caco-2 cells, compared with a reported K_m of 1.32 mM in PMAT-MDCK cells.²⁸

The results reported herein indicate that Caco-2 cells are an inadequate model for evaluating carrier mediated absorption. The work in Caco-2 cells by Proctor *et al.*⁸ reporting that greater than 95% of metformin absorption is via a paracellular route is, therefore, not important in terms of *in vivo* relevance because the Caco-2 cell system lacks the apical transporter that may play a major role in the uptake of metformin.

To address the clinical relevance of a potential multiple transporter effect and to determine if we can recreate and observe a basolateral effect *in vivo*, we used the rat intestinal perfusion model. Figure 4.16 represents the data from metformin run alone, perfused with MPP⁺ (0.5 mM), or perfused with TEA (0.5 mM). It was our hypothesis that apical inhibition would be detectable but we were unsure if we would detect a basolateral inhibitory effect. In other words, we predicted, that similar to our PMAT-MDCK studies, we would see a decrease in permeability in the presence of MPP⁺ but not TEA due to an inhibition of PMAT-mediated uptake. However, our data reveal the opposite. The presence of MPP⁺ (0.5 mM) results in no change while the presence of TEA (0.5 mM) resulted in a significant decrease in the effective permeability (P_{eff}) of metformin (Figure 4.16).

While Barnes *et al.*²⁹ report that PMAT is present in the rat intestine, its contribution to metformin absorption in the rat model has, until now, not been considered. If PMAT does play a major role in the absorption of metformin, we should have been able to see a reduction in effective permeability when perfused with the known PMAT inhibitor MPP⁺. We did not see a change with MPP⁺. We did, however, observe a significant difference in the effective permeability of metformin when we perfused with TEA.

First of all, we can rule out a basolateral OCT1 effect because MPP⁺ did not show the same result as TEA. Secondly, the molecular weight of metformin is 129.2 g/mol and it follows that a component of its absorption will be paracellular. It has been postulated that a transport mechanism exists in the paracellular space.⁸ It is possible that the disparity in the influence on metformin's P_{eff} between MPP⁺ and TEA could be due to the two compounds' differential abilities to affect such a paracellular mechanism. TEA is a smaller molecule than MPP⁺ and could therefore have a greater effect on a mechanism within the paracellular space but this remains highly speculative.

It is also quite possible that we are detecting an apical transporter effect unrelated to PMAT.

Prior to obtaining the PMAT-MDCK cells, our Caco-2 data suggested the involvement of a carrier mediated uptake process and this is supported by the similar uptake data of Proctor and coworkers.⁸ Our Caco-2 data with L-carnitine suggests that the novel organic cation transporter (OCTN1 and/or OCTN2) may play a role in metformin absorption (Figure 4.9b,c). OCTN1/OCTN2 is an apical uptake transporter that is expressed in human intestine and it is also endogenously expressed in the Caco-2 cells as well as the rat intestine.¹⁷ TEA is inhibitor of OCTN1/OCTN2 while MPP⁺ is not.

Taken together, our data suggest that the reduction we observe in the effective permeability of metformin *in vivo* could be due in part to inhibition of OCTN1 and OCTN2.

4.5 References

1. Food and Drug Administration, Guidance for Industry: Waiver of in vivo bioavailability and bioequivalence studies for immediate release solid oral dosage forms based on a Biopharmaceutics Classification System, Food and Drug Administration, Rockville, MD, 2000. Retrieved from www.fda.gov/cder/guidance/index.htm.
2. G.L. Amidon, H. Lennernas, V.P. Shah, J.R. Crison, A theoretical basis for a biopharmaceutics drug classification: the correlation of in vitro drug product dissolution and in vivo bioavailability, *Pharm. Res.* 12 (1995) 413-420.
3. C.Y. Wu, L.Z. Benet, Predicting drug disposition via application of BCS: transport/absorption/elimination interplay and development of a Biopharmaceutics Drug Disposition Classification System, *Pharm. Res.* 22 (2005) 11-23.
4. N.C. Sambol, J. Chiang, E.T. Lin, A.M. Goodman, C.Y. Liu, L.Z. Benet, M.G. Cogan, Kidney function and age are both predictors of pharmacokinetics of metformin, *J. Clin. Pharmacol.* 35 (1995) 1094-1102.

5. N.C. Sambol, L.G. Brookes, J. Chiang, A.M. Goodman, E.T. Lin, C.Y. Liu, L.Z. Benet, Food intake and dosage level, but not tablet vs solution dosage form, affect the absorption of metformin HCl in man, *Br. J. Clin. Pharmacol.* 42 (1996) 510-512.
6. N.C. Sambol, J. Chiang, M. O'Conner, C.Y. Liu, E.T. Lin, A.M. Goodman, L.Z. Benet, J.H. Karam, Pharmacokinetics and pharmacodynamics of metformin in healthy subjects and patients with noninsulin-dependent diabetes mellitus, *J. Clin. Pharmacol.* 36 (1996) 1012-1021.
7. S. Davis, Insulin, oral hypoglycemic agents, and the pharmacology of the endocrine pancreas. In: L.L. Brunton, J.S. Lazo, K.L. Parker (Eds.), *Goodman and Gilman's The Pharmacologic Basis of Therapeutics*. 11th Edition. McGraw-Hill, New York, 2006, pp. 1634-1641.
8. W.R. Proctor, D.L. Bourdet, D.R. Thakker, Mechanisms underlying saturable intestinal absorption of metformin, *Drug Metab. Dispos.* 36 (2008) 1650-1658.
9. A. Balakrishnan, D.J. Sussman, J.E. Polli, Development of stably transfected monolayer overexpressing the human apical sodium-dependent

- bile acid transporter (hASBT), *Pharm. Res.* 22 (2005) 1269-1280.
10. A. Balakrishnan, J.E. Polli, Apical sodium dependent bile acid transporter (ASBT, SLC10A2): a potential prodrug target, *Mol. Pharmaceut.* 3 (2006) 223-230.
 11. P.V. Balimane, S. Chong, K. Patel, Y. Quan, J. Timoszyk, Y.H. Han, B. Wang, B. Vig, T.N. Faria, Peptide transporter substrate identification during permeability screening in drug discovery: comparison of transfected MDCK-hPepT1 cells to Caco-2 cells, *Arch. Pharm. Res.* 30 (2007) 507-518.
 12. H. Satoh, F. Yamashita, M. Tsujimoto, H. Murakami, N. Koyabu, H. Ohtani, Y. Sawada, Citrus juices inhibit the function of human organic anion-transporting polypeptide OATP-B, *Drug Metab. Dispos.* 33 (2005) 518-523.
 13. K. Watanabe, T. Sawano, K. Terada, T. Endo, M. Sakata, J. Sato, Studies on intestinal absorption of sulpiride (1): carrier-mediated uptake of sulpiride in the human intestinal cell line Caco-2, *Biol. Pharm. Bull.* 25 (2002) 885-890.
 14. K. Watanabe, T. Sawano, T. Endo, M. Sakata, J. Sato, Studies on intestinal absorption of sulpiride (2): transepithelial transport of

- sulpiride across the human intestinal cell line Caco-2, *Biol. Pharm. Bull.* 25 (2002) 1345-1350.
15. D. Sun, H. Lennernas, L.S. Welage, J.L. Barnett, C.P. Landowski, D. Foster, D. Fleisher, K.D. Lee, G.L. Amidon, Comparison of human duodenum and Caco-2 gene expression profiles for 12,000 gene sequences tags and correlation with permeability of 26 drugs, *Pharm. Res.* 19 (2002) 1400-1416.
16. D.L. Bourdet, G.M. Pollack, D.R. Thakker, Intestinal absorptive transport of the hydrophilic cation ranitidine: a kinetic modeling approach to elucidate the role of uptake and efflux transporters and paracellular vs. transcellular transport in Caco-2 cells, *Pharm. Res.* 23 (2006) 1178-1187.
17. C. Hilgendorf, G. Ahlin, A. Seithel, P. Artursson, A.L. Ungell, J. Karlsson, Expression of thirty-six drug transporter genes in human intestine, liver, kidney, and organotypic cell lines, *Drug Metab. Dispos.* 35 (2007) 1333-1340.
18. H. Han, R.L. de Vruh, J.K. Rhie, K.M. Covitz, P.L. Smith, C.P. Lee, D.M. Oh, W. Sadée, G.L. Amidon, 5'-Amino acid esters of antiviral nucleosides, acyclovir, and AZT are absorbed by the intestinal PEPT1 peptide transporter, *Pharm. Res.* 15 (1998) 1154-1159.

19. G.L. Amidon, D.R. Walgreen Jr., 5'-Amino acid esters of antiviral nucleosides, acyclovir, and AZT are absorbed by the intestinal PEPT1 peptide transporter, *Pharm. Res.* 16 (1999) 175.
20. P.V. Balimane, I. Tamai, A. Guo, T. Nakanishi, H. Kitada, F.H. Leibach, A. Tsuji, P.J. Sinko, Direct evidence for peptide transporter (PepT1)-mediated uptake of a nonpeptide prodrug, valacyclovir, *Biochem. Biophys. Res. Commun.* 250 (1998) 246-251.
21. H.K. Han, D.M. Oh, G.L. Amidon, Cellular uptake mechanism of amino acid ester prodrugs in Caco-2/hPEPT1 cells overexpressing a human peptide transporter, *Pharm. Res.* 15 (1998) 1382-1386.
22. A. Guo, P. Hu, P.V. Balimane, F.H. Leibach, P.J. Sinko, Interactions of a nonpeptidic drug, valacyclovir, with the human intestinal peptide transporter (hPEPT1) expressed in a mammalian cell line, *J. Pharmacol. Exp. Ther.* 289 (1999) 448-454.
23. D.A. Groneberg, F. Döring, P.R. Eynott, A. Fischer, H. Daniel, Intestinal peptide transport: ex vivo uptake studies and localization of peptide carrier PEPT1, *Am. J. Physiol. Gastrointest. Liver Physiol.* 281 (2001) 697-704.
24. Physicians' Desk Reference, 61st ed., Montvale, NJ, Thomson PDR, 2007, pp. 2149-2153.

25. M.L. Chen, A.B. Straughn, N. Sadrieh, M. Meyer, P.J. Faustino, A.B. Ciavarella, B. Meibohm, C.R. Yates, A.S. Hussain, A modern view of excipient effects on bioequivalence: case study of sorbitol, *Pharm. Res.* 24 (2007) 73-80.
26. *Drug Information Handbook*, 14th ed., Hudson, OH, Lexi-Comp Inc., 2006, pp. 1016-1018.
27. *Physicians' Desk Reference*, 61st ed., Montvale, NJ, Thomson PDR, 2007, pp. 1373-1378.
28. M. Zhou, L. Xia, J. Wang, Metformin transport by a newly cloned proton-stimulated organic cation transporter (plasma membrane monoamine transporter) expressed in human intestine, *Drug Metab. Dispos.* 35 (2007) 1956-1962.
29. K. Barnes, H. Dobrzynski, S. Foppolo, P.R. Beal, F. Ismat, E.R. Scullion, L. Sun, J. Tellez, M.W. Ritzel, W.C. Claycomb, C.E. Cass, J.D. Young, R. Billeter-Clark, M.R. Boyett, S.A. Baldwin, Distribution and functional characterization of equilibrative nucleoside transporter-4, a novel cardiac adenosine transporter activated at acidic pH, *Circ. Res.* 99 (2006) 510-519.
30. L. Xia, K. Engel, M. Zhou, J. Wang, Membrane localization and pH-dependent transport of a newly cloned organic cation transporter (PMAT) in kidney

- cells, *Am. J. Physiol. Renal Physiol.* 292 (2007) 682-690.
31. M. Zhou, L. Xia, K. Engel, J. Wang, Molecular determinants of substrate selectivity of a novel organic cation transporter (PMAT) in the SLC29 family, *J. Biol. Chem.* 282 (2007) 3188-3195.
 32. W.S. Putnam, L. Pan, K. Tsutsui, L. Takahashi, L.Z. Benet, Comparison of bidirectional cephalixin transport across MDCK and caco-2 cell monolayers: interactions with peptide transporters, *Pharm. Res.* 19 (2002) 27-33.
 33. S.D. Flanagan, C.L. Cummins, M. Susanto, X. Liu, L.H. Takahashi, L.Z. Benet, Comparison of furosemide and vinblastine secretion from cell lines overexpressing multidrug resistance protein (P-glycoprotein) and multidrug resistance-associated proteins (MRP1 and MRP2), *Pharmacology* 64 (2002) 126-134.
 34. C.L. Cummins, W. Jacobsen, U. Christians, L.Z. Benet, CYP3A4-transfected Caco-2 cells as a tool for understanding biochemical absorption barriers: studies with sirolimus and midazolam, *J. Pharmacol. Exp. Ther.* 308 (2004) 143-155.
 35. Y.Y. Lau, H. Okochi, Y. Huang, L.Z. Benet, Multiple transporters affect the disposition of atorvastatin and its two active hydroxy

- metabolites: application of in vitro and ex situ systems, *J. Pharmacol. Exp. Ther.* 316 (2006) 762-771.
36. C.L. Cummins, L. Salphati, M.J. Reid, L.Z. Benet, In vivo modulation of intestinal CYP3A metabolism by P-glycoprotein: studies using the rat single-pass intestinal perfusion model, *J. Pharmacol. Exp. Ther.* 305 (2003) 306-314.
37. G.L. Amidon, P.J. Sinko, D. Fleisher, Estimating human oral fraction dose absorbed: A correlation using rat intestinal membrane permeability for passive and carrier-mediated compounds, *Pharm. Res.* 5 (1988) 651-654.
38. J.S. Kim, S. Mitchell, P. Kijek, Y. Tsume, J. Hilfinger, G.L. Amidon, The suitability of an in situ perfusion model for permeability determinations: Utility for BCS class I biowaiver requests, *Mol. Pharmaceut.* 3 (2006) 686-694.
39. U. Fagerholm, M. Johansson, H. Lennernas, Comparison between permeability coefficients in rat and human jejunum, *Pharm. Res.* 13 (1996) 1336-1342.
40. Y.Y. Lau, C.Y. Wu, H. Okochi, L.Z. Benet, Ex situ inhibition of hepatic uptake and efflux significantly changes metabolism: hepatic enzyme-

- transporter interplay, *J. Pharmacol. Exp. Ther.* 308 (2004) 1040-1045.
41. U. Christians, W. Jacobsen, N. Serkova, L.Z. Benet, C. Vidal, K.F. Sewing, M.P. Manns, G.I. Kirchner, Automated, fast and sensitive quantification of drugs in blood by liquid chromatography-mass spectrometry with on-line extraction: immunosuppressants, *J. Chromatogr. B. Biomed. Sci. Appl.* 748 (2000) 41-53.
42. Y. Shu, C.L. Bello, L.M. Mangravite, B. Feng, K.M. Giacomini, Functional characteristics and steroid hormone-mediated regulation of an organic cation transporter in Madin-Darby canine kidney cells, *J. Pharmacol. Exp. Ther.* 299 (2001) 392-398.
43. C.A. Lipinski, Drug-like properties and the causes of poor solubility and poor permeability, *J. Pharmacol. Toxicol. Methods* 44 (2000) 235-249.
44. J.M. Custodio, C.Y. Wu, L.Z. Benet, Predicting drug disposition, absorption/elimination/ transporter interplay and the role of food on drug absorption, *Adv. Drug Deliv. Rev.* 60 (2008) 717-733.
45. T.N. Faria, J.K. Timoszyk, T.R. Stouch, B.S. Vig, C.P. Landowski, G.L. Amidon, C.D. Weaver, D.A. Wall, R.L. Smith, A novel high-throughput pepT1 transporter assay differentiates between

- substrates and antagonists, *Mol. Pharmaceut.* 1 (2004) 67-76.
46. N. Kimura, S. Masuda, Y. Tanihara, H. Ueo, M. Okuda, T. Katsura, K. Inui, Metformin is a superior substrate for renal organic cation transporter OCT2 rather than hepatic OCT1, *Drug Metab. Pharmacokinet.* 20 (2005) 379-386.
47. M.J. Dresser, G. Xiao, M.K. Leabman, A.T. Gray, K.M. Giacomini, Interactions of n-tetraalkylammonium compounds and biguanides with a human renal organic cation transporter (hOCT2), *Pharm. Res.* 19 (2002) 1244-1247.
48. N. Kimura, M. Okuda, K. Inui, Metformin transport by renal basolateral organic cation transporter hOCT2, *Pharm. Res.* 22 (2005) 255-259.

CHAPTER 5

- DIFFERENTIAL TRANSPORT OF CLASS 1 AND 2 COMPOUNDS IN TWO WELL-CHARACTERIZED CELL SYSTEMS: THE CACO-2 AND MDCK CELL LINES

5.1 Introduction

Research focused on elucidating the influence of transporters on drug disposition has been ongoing for many years.¹ Various *in vitro* technologies exist to investigate transporters, examples being the well characterized Madin Darby Canine Kidney (MDCK) cell line and the industry standard, human colonic adenocarcinoma (Caco-2) cell line. Cellular assays assessing the bidirectional transport of compounds across a cell monolayer is a widely accepted approach to evaluate the passive and active components of absorption. Another facet of this investigational approach includes introduction, via transfection, of the transporter of interest into an epithelial, adherent cell line such as the MDCK cells. Contrastingly, with the Caco-2 cell model, transporter effects may emerge from endogenously expressed proteins.^{2,3}

In this Chapter, we focus on the transfected MDR1-MDCK (MM) cell line incorporating the stable expression of the MDR1 gene encoding for the P-glycoprotein (P-gp) efflux transporter.⁴⁻⁷ We compare the MDR1-MDCK cell system to the Caco-2 endogenous cell system and evaluate the utility and adequacy of both systems in assessing the P-gp mediated efflux of Class 1 and Class 2 drugs.

Compared to Caco-2 cell monolayers, the MDR1-MDCK cell system possesses very tight junctions as reflected by their high transepithelial electrical resistance (TEER) values.^{8,9} TEER values are measured by the Millicell electrical resistance system utilizing "chopstick" electrodes (Millipore Corporation, Bedford, MA) and are expressed in units of resistance and surface area. Our laboratory, similar to other research groups, utilizes a transwell plate system employing semi-porous membrane cell culture inserts (Figure 5.1).

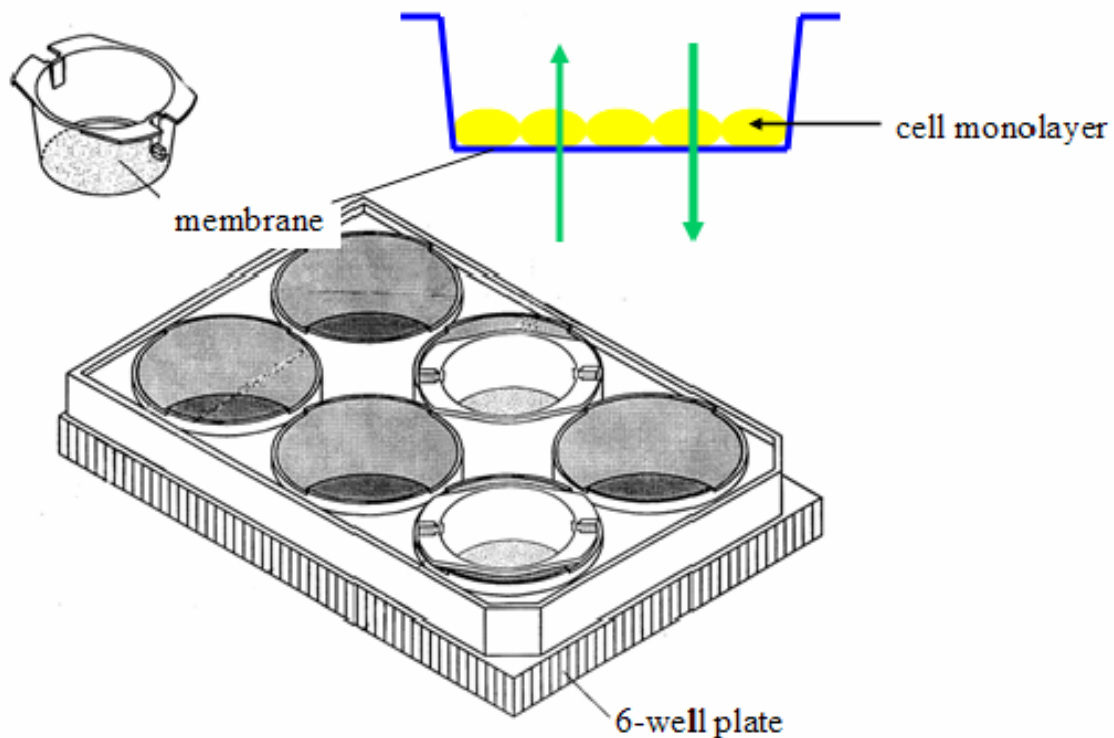


Figure 5.1 The transwell plate system utilized for bidirectional transport studies. The diagram includes the 6-well plate format that houses the semi-porous membrane cell culture insert (4.2 cm^2) upon which a cell monolayer is grown.

The membranes possess a pore size of $0.4 \text{ }\mu\text{m}$ and surface area of 4.2 cm^2 upon which a cell monolayer is grown and, therefore, the ohm (\bullet) resistance measured is then multiplied by 4.2 cm^2 . The MDR1-MDCK cells, mentioned above as having very high TEER, possess values of approximately $5000\text{-}6000 \text{ }\bullet\cdot\text{cm}^2$. The untransfected parental MDCK cell system possesses TEER values of approximately $200\text{-}300 \text{ }\bullet\cdot\text{cm}^2$. Caco-2

cells possess TEER values of approximately 800-1000 $\bullet \cdot \text{cm}^2$.

As discussed in Sections 1.4.2 and 1.4.3, we hypothesize that the effects of transporters on the highly soluble, highly permeable and extensively metabolized Class 1 drugs will be minimal and clinically irrelevant, while Class 2 drugs will be significantly affected by efflux transporters in the intestine like P-gp.¹⁰ As the Caco-2 cells are derived from the human gastrointestinal (GI) tract as opposed to the canine kidney derived MDCK cells, we believe the assays conducted in the Caco-2 cell system will more closely approximate *in vivo* drug behavior. That is, Class 1 drugs that are shown to be P-gp substrates in the MDR1-MDCK model will not appear as such in the Caco-2 model.⁸ In the case of Class 2 drugs, both cellular model systems will produce P-gp substrate properties.⁸ The study designed to investigate our hypothesis includes the Class 1 drug, verapamil and the Class 2 drug, saquinavir and the results are presented and discussed herein.

5.2 Materials and methods

5.2.1 Materials

MDR1-MDCK (MM) and MDCK cell lines were generously provided by Dr. Ira Pastan (National Cancer Institute,

National Institutes of Health, Bethesda, MD). The Caco-2 cell line (HTB-37) was purchased from the American Type Culture Collection (ATCC - Manassas, VA). All components necessary for proper cell culture growth conditions (described below) were purchased from the University of California, San Francisco Cell Culture Facility (San Francisco, CA). D-[1-³H(N)]-Mannitol was purchased from NEN (Boston, MA). [³H]-Saquinavir was purchased from Moravek Biochemicals and Radiochemicals (Brea, CA). [N-methyl-³H]-Verapamil hydrochloride was purchased from Perkin Elmer (Waltham, MA). GG918 (GF120918: N-{4-[2-(1,2,3,4-tetrahydro-6,7-dimethoxy-2-isoquinolinyl)-ethyl]-phenyl}-9,10-dihydro-5-methoxy-9-oxo-4-acridine carboxamine) was a kind gift from GlaxoSmithKline (Research Triangle Park, NC). All other chemicals were of reagent grade and purchased from Sigma-Aldrich (St. Louis, MO).

Six-well tissue culture treated polystyrene plates were obtained from Corning Life Science (Acton, MA). Falcon polyethylene terephthalate cell culture inserts (pore size 0.4 μ m, diameter 4.2 cm²) were obtained from BD Biosciences (Bedford, MA).

5.2.2 Cell culture

5.2.2.1 Caco-2 cell line

Caco-2 cells were grown in a humidified 5% CO₂ atmosphere at 37°C using minimum essential medium (MEM) Eagle's with Earle's balanced salt solution (BSS) containing 1.0 g/L glucose, 0.292 g/L l-glutamine, 2.2 g/L NaHCO₃, which was supplemented with 15% heat-inactivated FBS, 1.0 mM sodium pyruvate, 0.1 mM nonessential amino acids, 100 U/mL penicillin and 100 U/mL streptomycin. Cells were grown to 90-100% confluence and harvested using 0.05% trypsin EDTA. Monolayers were prepared by seeding harvested cells onto polyethylene terephthalate cell culture inserts at a density of approximately 60,000 cells/cm². Growth medium for the Caco-2 was refreshed 48 hours post-seeding and then twice weekly, including one day prior to the experiment. Caco-2 cell monolayers were used for bidirectional transport experiments 21-28 days

postseeding.

5.2.2.2 MDR1-MDCK (MM) and MDCK cell lines

MDCK cells were grown in a humidified 5% CO₂ atmosphere at 37°C using Dulbecco's modified Eagle's medium (DMEM) containing 4.5 g/L glucose, 3.7 g/L NaHCO₃, 0.584 g/L *l*-glutamine, which was supplemented with 10% heat-inactivated FBS, 100 U/mL penicillin and 100 U/mL streptomycin. MDR1-MDCK cell culture medium was as described above with the addition of 80 ng/mL colchicine as a selective supplement.² Cells were grown to 90-100% confluence and harvested using 0.05% trypsin EDTA. Monolayers were prepared by seeding harvested cells onto polyethylene terephthalate cell culture inserts at a density of approximately 1,000,000 cells/insert. Growth medium was refreshed once every two days and one day prior to the experiment, which was performed 5-7 days postseeding for both cell lines.

5.2.3 Bidirectional transport experiments

The transport assays were performed following a modified protocol previously described by our laboratory.¹¹⁻¹⁴ In brief, cell monolayers were preincubated in control transport buffer (Hank's buffered salt solution containing 25 mM HEPES and 1% FBS, pH 7.4) at 37°C for 20 minutes. Transepithelial electrical

resistance (TEER) values were then measured by the Millicell electrical resistance system utilizing "chopstick" electrodes (Millipore Corporation, Bedford, MA). On average, the MDR1-MDCK cells possessed values of approximately 4000-5000 $\bullet\cdot\text{cm}^2$, while the VECTOR-MDCK cells possessed TEER values of approximately 200-300 $\bullet\cdot\text{cm}^2$. On average, the Caco-2 cells system possessed TEER values of approximately 800-1000 $\bullet\cdot\text{cm}^2$. All experiments were performed in triplicate and conducted on at least three separate occasions to ensure reproducibility. In the case of the MDR1-MDCK and parental MDCK cells, both these transfected and control cell lines were run on the same day to account for potential between-day variability of radiolabeled counts and TEER values.

The experiment was started by the addition of test compound in control transport buffer to the donor compartment and control transport buffer only to the receiver compartment. The final volumes in each of the chambers were 1.5 mL on the apical side and 2.5 mL on the basolateral side. Experimental samples were isolated from the receiver compartment at three time points. At the first two time points, 200 $\bullet\text{L}$ samples were removed and then replaced with fresh media to restore initial starting volumes. At the final time point, following collecting of the last 200 $\bullet\text{L}$ sample, contents of both chambers were removed by suction, each cell culture

insert was dipped three times into ice-cold PBS and the cell culture insert membranes were collected. All experiments were run at 37°C with a shaking speed of 25 strokes/minute in the Boekel Shake 'N' Bake Incubator Shaker II (Boekel Scientific, Feasterville, PA).

5.2.4 Analysis of samples

5.2.4.1 Sample preparation

All samples were added to 5 mL Econo-Safe™ Counting Cocktail (Research Products International Corporation, Mount Prospect, IL) and vortex mixed. Cells monolayers were solubilized by sonication (in an ultrasonic bath) for 15 minutes.

5.2.4.2 Sample analysis

Samples were analyzed using a Beckman LS180 scintillation counter (Beckman Industries, Palo Alto, CA).

5.3 Results

5.3.1 Bidirectional transport studies with verapamil in MDR1-MDCK (MM) and MDCK cells

We investigated the effects of a known P-gp inhibitor, GG918 on the bidirectional transport of verapamil in MDR1-MDCK (MM) and MDCK cells (Figures 5.2 and 5.3).

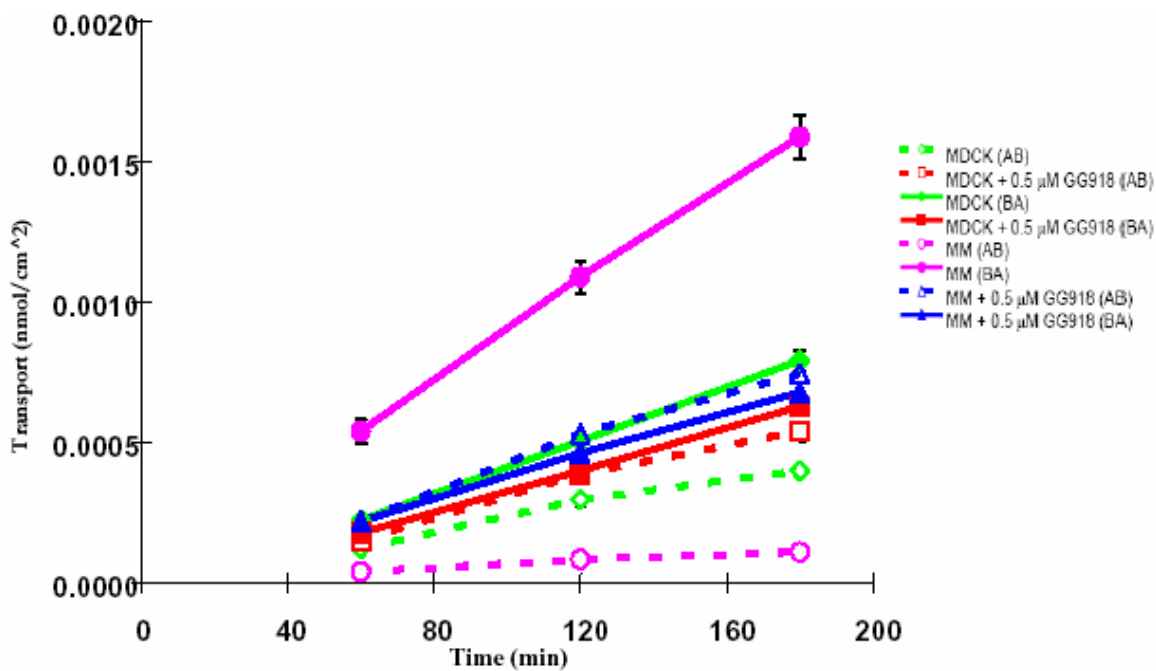


Figure 5.2 Bidirectional transport of verapamil (10 nM) in MDR1-MDCK cells (MM) and parental MDCK cells in the presence or absence of the known P-gp inhibitor, GG918 (0.5 μM).

Figures 5.2 And 5.3 depict the transport profiles in control and inhibitory conditions for 10 nM and 10 μ M verapamil and include the profiles of the parental control MDCK cells as well. The net flux ratio (B to A / A to B) for 10 nM verapamil in control transport buffer was 13.9 and was reduced to 0.86 in the presence of GG918 (0.5 μ M) (Figure 5.2). The net flux ratios for 10 μ M verapamil in control transport buffer and with the addition of GG918 were 4.14 and 0.90, respectively (Figure 5.3).

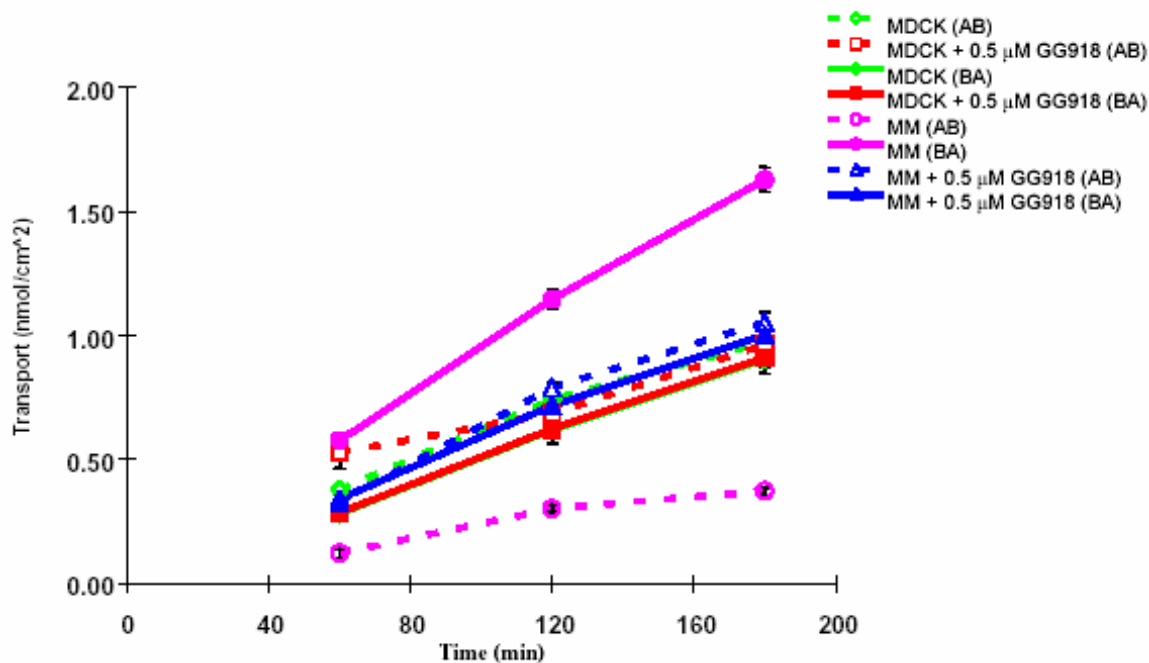


Figure 5.3 Bidirectional transport of verapamil (10 μ M) in MDR1-MDCK cells (MM) and parental MDCK cells in the presence or absence of the known P-gp inhibitor, GG918 (0.5 μ M).

5.3.2 Bidirectional transport studies with verapamil in Caco-2 cells

We investigated the effects of a known P-gp inhibitor, GG918 on the bidirectional transport of verapamil in Caco-2 cells (Figures 5.4 and 5.5). Figure 5.4 depicts the overlapping transport profiles in control and inhibitory condition for 10 nM verapamil. Figure 5.5 depicts results from the bidirectional transport assay with 10 μ M verapamil. The net flux ratio (B to A / A to B) in control transport buffer was nearly unity as observed by the insignificant difference in B to A and A to B transport. The presence of GG918 (0.5 μ M) resulted in no change in net flux ratios.

5.3.3 Bidirectional transport studies with saquinavir in MDR1-MDCK (MM) cells

We investigated the effects of a known P-gp inhibitor, GG918, on the bidirectional transport of saquinavir in MDR1-MDCK cells (Figure 5.6). Figure 5.6 depicts the observed decrease in the basolateral to apical (B to A) transport coupled with an increase in

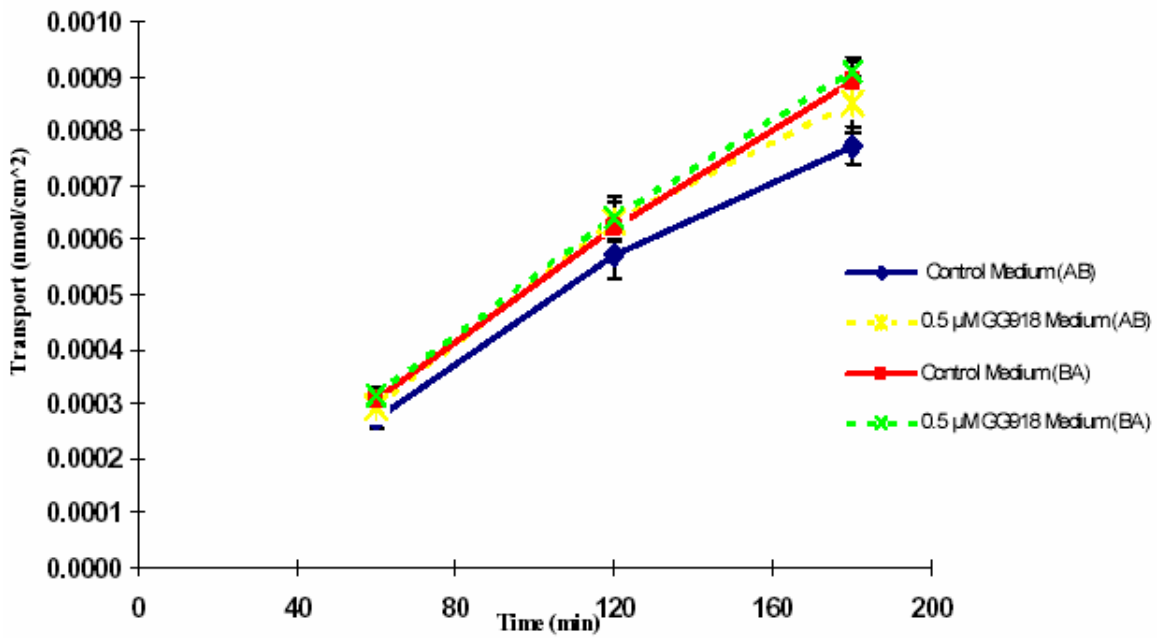


Figure 5.4 Bidirectional transport of verapamil (10 nM) in Caco-2 cells in the presence or absence of the known P-gp inhibitor, GG918 (0.5 μM).

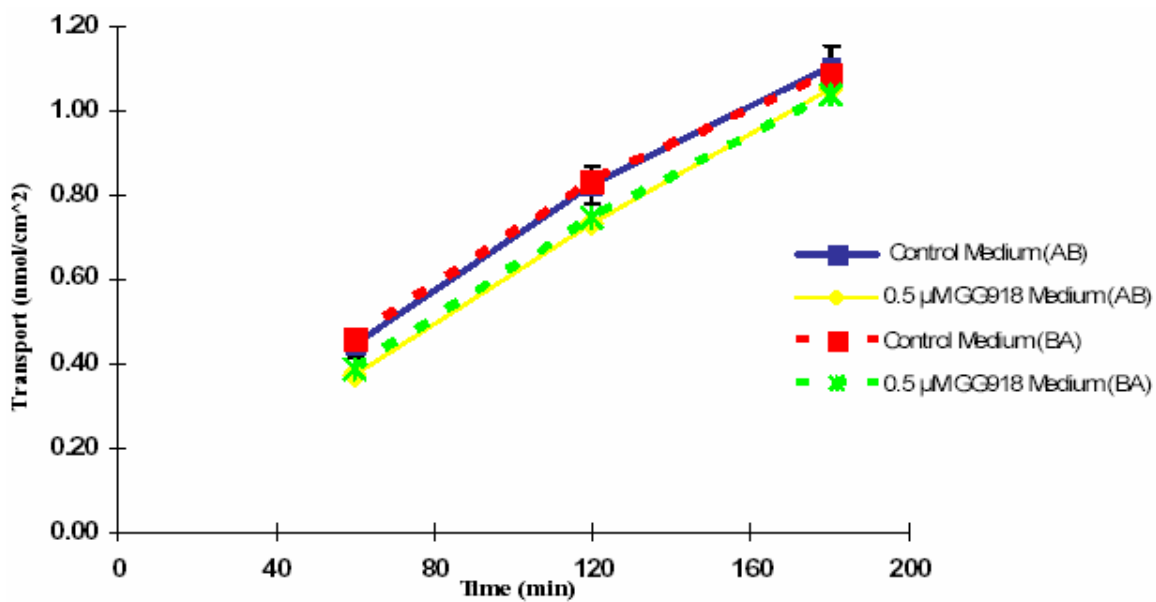


Figure 5.5 Bidirectional transport of verapamil (10 μ M) in Caco-2 cells in the presence or absence of the known P-gp inhibitor, GG918 (0.5 μ M).

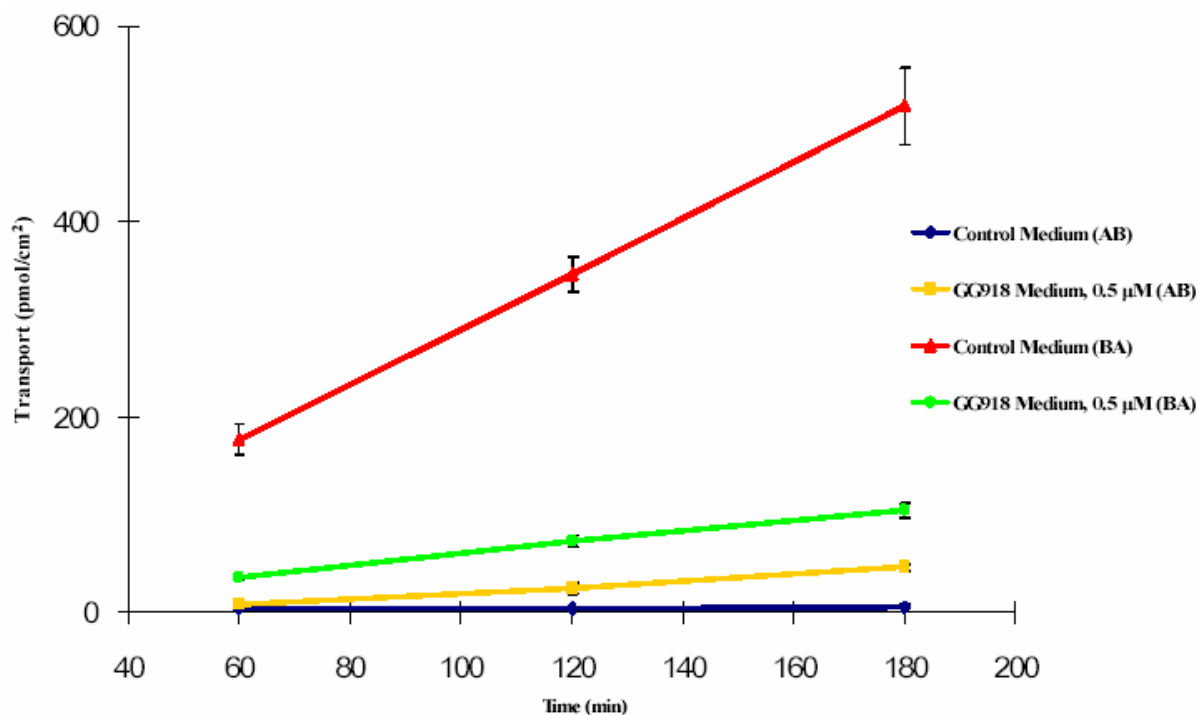


Figure 5.6 Bidirectional transport of saquinavir in MDR1-MDCK cells in the presence or absence of the known P-gp inhibitor, GG918 (0.5 μM).

apical to basolateral (A to B) transport. The presence of GG918 (0.5 μM) resulted in a reduction of the net flux ratio (B to A / A to B) by 98%, from 154 to 1.8.

5.3.4 Bidirectional transport studies with saquinavir in Caco-2 cells

We investigated the effects of GG918 on the bidirectional transport of saquinavir in Caco-2 cells (Figure 5.7). Figure 5.7 depicts the decrease in the basolateral to apical (B to A) transport and the increase

in apical to basolateral (A to B) transport. The net flux ratio (B to A / A to B) in control transport buffer was 2.3. The presence of GG918 (0.5 μ M) resulted in a reduction of the net flux ratio to 1.2, a decrease of 46%.

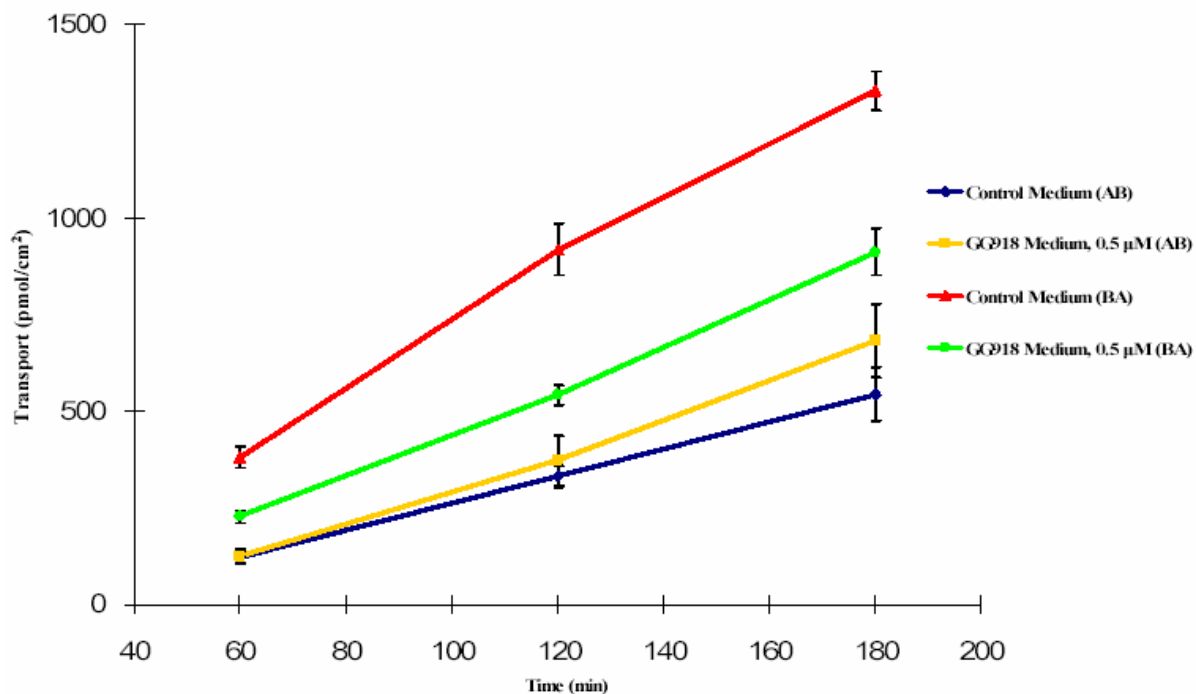


Figure 5.7 Bidirectional transport of saquinavir in Caco-2 cells in the presence or absence of the known P-gp inhibitor, GG918 (0.5 μ M).

5.3.5 Net flux and apparent permeability changes in Caco-2 and MDR1-MDCK cells

In addition to evaluating the transport profiles of verapamil and saquinavir in various cell lines in the presence or absence of the known efflux inhibitor GG918, we were also interested in determining the net change in

flux (Tables 5.1 and 5.2) as well as any influence on apparent permeability values (Tables 5.3 and 5.4). The net flux ratios (B to A / A to B) of verapamil resulting from control or inhibitory conditions are included in Table 5.1. The ratios for saquinavir are listed in Table 5.2. The resulting apparent permeability (P_{app}) values for verapamil in control or inhibitory conditions are included in Table 5.3. The P_{app} values for saquinavir are listed in Table 5.4.

Verapamil (10 •M)	Control Media	GG918 Media (0.5 •M)
Net Flux Ratio in Caco-2 Cells	0.90	0.91
Net Flux Ratio in MDR1-MDCK Cells	4.1	0.90

Table 5.1 Net flux ratios (B to A / A to B) for verapamil (10 •M) in Caco-2 and MDR1-MDCK cells in the presence or absence of the known P-gp inhibitor, GG918 (0.5 •M), each with n = 3 transwells.

Saquinavir (20 •M)	Control Media	GG918 Media (0.5 •M)
Net Flux Ratio in Caco-2 Cells	2.3	1.2
Net Flux Ratio in MDR1-MDCK Cells	154	1.8

Table 5.2 Net flux ratios (B to A / A to B) for saquinavir (20 •M) in Caco-2 and MDR1-MDCK cells in the presence or absence of the known P-gp inhibitor, GG918 (0.5 •M), each with n = 3 transwells.

Cell Line	Verapamil (10 •M)	Apparent Permeability (P_{app}) Values ($\text{nm}\cdot\text{sec}^{-1}$)	
		$P_{app(A\cdot B)}$	$P_{app(B\cdot A)}$
Caco-2	Control	93.3 ± 4.1	84.5 ± 2.9
	+ GG918 (0.5•M)	91.3 ± 1.2	82.9 ± 2.2
MDR1-MDCK	Control	31.5 ± 1.3	130.4 ± 3.8
	+ GG918 (0.5•M)	89.4 ± 3.5	80.3 ± 3.7

Table 5.3 Apparent permeability values (P_{app}) for verapamil (10 •M) in Caco-2 and MDR1-MDCK cells. $P_{app} = (dQ/dt)/(A\cdot C_0)$; where dQ/dt is the amount transported (Q) over time (t), A is the surface area of the insert, and C_0 is the initial concentration of the donor compartment. P_{app} values ± standard deviation are listed for the apical to basolateral (A•B) direction and the basolateral to apical (B•A) direction, each with n = 3 transwells.

Cell Line	Saquinavir (20 •M)	Apparent Permeability (P_{app}) Values ($\text{nm}\cdot\text{sec}^{-1}$)	
		$P_{app(A\cdot B)}$	$P_{app(B\cdot A)}$
Caco-2	Control	29.2 ± 2.7	65.8 ± 3.2
	+ GG918 (0.5•M)	38.8 ± 4.1	47.5 ± 2.3
MDR1-MDCK	Control	1.54 ± 0.3	237 ± 14.7
	+ GG918 (0.5•M)	26.4 ± 3.7	47.0 ± 4.2

Table 5.4 Apparent permeability values (P_{app}) for saquinavir (20 •M) in Caco-2 and MDR1-MDCK cells. $P_{app} = (dQ/dt)/(A\cdot C_0)$; where dQ/dt is the amount transported (Q) over time (t), A is the surface area of the insert, and C_0 is the initial concentration of the donor compartment. P_{app} values ± standard deviation are listed for the apical to basolateral (A•B) direction and the basolateral to apical (B•A) direction, each with $n = 3$ transwells.

5.4 Discussion

Comprehensive data resulting from years of *in vitro* cellular assays and *in vivo* animal studies in our laboratory has led to our presumption that almost all drugs are substrates for some transporter. However, this is not to say that transporter effects will always be clinically relevant. In other words, an *in vitro* net flux ratio (B to A / A to B) of 4 for a given drug, which according to the Food and Drug Administration (FDA) is indicative of a transporter substrate,¹⁵ may translate *in*

vivo to a negligible contribution of the transporter to that same drug's disposition.

For this component of the research project, we selected the antiarrhythmic drug, verapamil (Calan[®], Isoptin[®]) as our BCS and BDDCS Class 1 compound. We also selected the antiretroviral drug, saquinavir (Invirase[®], Fortovase[®]) as our BCS and BDDCS Class 2 compound. Both drugs are highly permeable and extensively metabolized by the CYP3A4 enzyme. Moreover, both are known substrates of the efflux transporter, P-gp. In fact, verapamil is considered by the FDA to be a model P-gp substrate and probe.¹⁶

We performed scores of bidirectional transport studies with each drug in the MDR1-MDCK, MDCK, and Caco-2 cell systems in the presence or absence of the known P-gp inhibitor, GG918. In general, a compound is considered a P-gp substrate if it exhibits a net flux ratio *in vitro* of 2-3 or greater.¹⁵ But the question remains, what cell line is the appropriate model system for determining these net flux ratios?

Following extensive experimentation with both verapamil and saquinavir we have reached the answer to that question and the answer is two-fold. First, the MDR1-MDCK cell system may be the appropriate model to utilize for determination of a P-gp substrate. Second, the Caco-2 cell system may be the appropriate model

system to utilize to determine whether a P-gp effect may play a significant role in human gut and liver absorption and disposition.

As stated earlier, both verapamil and saquinavir are known P-gp substrate. Our data in the MDR1-MDCK cells confirm this. Figures 5.2 and 5.3 depict the bidirectional transport profiles for verapamil. Figure 5.6 depicts the profile for saquinavir. In each case the basolateral to apical (B to A) flux is markedly greater than the apical to basolateral (A to B) flux. This results in significant net flux ratios representative of a P-gp substrate. For verapamil (10 μ M) the net flux ratio is 4.1 (Table 5.1) and for saquinavir (20 μ M) the ratio is 154 (Table 5.2). In each case, removing the P-gp mediated transport by addition of GG918 results in net flux ratios of nearly 1 (Tables 5.1 and 5.2).

Our data from Caco-2 cells, however, do not confirm that both drugs are P-gp substrates by definition. Only the Class 2 saquinavir results in data indicative of a P-gp substrate with transport in the B to A direction greater than A to B direction (Figure 5.7) and a net flux ratio of 2.2 (Table 5.2). The bidirectional transport of the Class 1 verapamil results in overlapping B to A and A to B profiles (Figures 5.4 and 5.5) and net flux ratios slightly less than 1 (Table 5.1), which indicate passive permeability as the driving force and no influence of P-

gp. It follows, that saquinavir transport, and not verapamil, is affected by addition of GG918, which results in returning the net flux ratio to unity (Table 5.2).

The apparent permeability (P_{app}) values for verapamil (10 μ M) in the MDR1-MDCK cells in control conditions demonstrate the strong influence of P-gp mediated transport with a permeability more than 4 times faster in the B to A direction than in the A to B direction, $130.4 \pm 3.8 \text{ nm}\cdot\text{sec}^{-1}$ versus $31.5 \pm 1.3 \text{ nm}\cdot\text{sec}^{-1}$ (Table 5.3). In the Caco-2 cells, however, the P_{app} values are nearly the same in both directions, $93.3 \pm 4.1 \text{ nm}\cdot\text{sec}^{-1}$ (A to B) compared to $84.5 \pm 2.9 \text{ nm}\cdot\text{sec}^{-1}$ (B to A). These P_{app} values are unaffected by addition of the P-gp inhibitor GG918 and the net flux ratio remains unchanged, suggesting that verapamil absorption is controlled by its passive diffusion and not P-gp (Table 5.3). Moreover, inhibiting the active P-gp mediated mechanism with GG918 in the MDR1-MDCK cells results in P_{app} values of $89.4 \pm 3.5 \text{ nm}\cdot\text{sec}^{-1}$ (A to B) and $80.3 \pm 3.7 \text{ nm}\cdot\text{sec}^{-1}$ (A to B) for verapamil. These P_{app} values are representative of the passive permeability observed in the values calculated for Caco-2 cells (Table 5.3).

The apparent permeability (P_{app}) values for saquinavir (20 μ M) in control conditions for both the Caco-2 and the MDR1-MDCK cell systems show the significant influence of

P-gp mediated transport resulting in B to A permeabilities greater than A to B permeabilities (Table 5.4). The P-gp effect is markedly greater in the MDR1-MDCK cells than in the Caco-2 cells. The MDR1-MDCK P_{app} values of $237 \pm 14.7 \text{ nm}\cdot\text{sec}^{-1}$ (B to A) and $1.54 \pm 0.3 \text{ nm}\cdot\text{sec}^{-1}$ (A to B) demonstrate the role of P-gp in the transport of saquinavir, which results in a BA/AB) ratio of 154 as seen above in Table 5.2 and confirms the ratio calculated by Polli and colleagues⁶ in their work describing saquinavir as an "unambiguous substrate." Furthermore, in both the MDR1-MDCK and the Caco-2 cell system, the P-gp inhibitor GG918 is capable of blocking the active transport mechanism, which results in faster A to B P_{app} values and slower B to A P_{app} values upon addition of GG918 (Table 5.4). Clearly, these data show that efflux is important for the Class 2 drug saquinavir.

One major criteria that leads researchers to employ the MDR1-MDCK cell line is its superior TEER values. This exceedingly tight cell system allows for increased sensitivity in identifying P-gp substrates. However, a transporter effect observed in the MDR1-MDCK cell system may not necessarily be observed in the Caco-2 cell system.¹⁷ The lower TEER values of the Caco-2 cells makes for a leakier system that we believe is far more representative of the human intestine. Verapamil, as well as drugs like midazolam and diazepam, are often used

as model substrates.^{15,16} However, each are Class 1 compounds thereby bringing that methodology into question because our data demonstrate that we can ignore the transporter effects for Class 1 compounds. Consequently, for certain drugs considered to be "model" P-gp substrates it may be difficult to predict their transporter interactions in the intestine.

5.5 References

1. K. Ito, H. Suzuki, T. Horie, Y. Sugiyama, Apical/basolateral surface expression of drug transporters and its role in vectorial drug transport, *Pharm. Res.* 22 (2005) 1559-1577.
2. D. Sun, H. Lennernas, L.S. Welage, J.L. Barnett, C.P. Landowski, D. Foster, D. Fleisher, K.D. Lee, G.L. Amidon, Comparison of human duodenum and Caco-2 gene expression profiles for 12,000 gene sequences tags and correlation with permeability of 26 drugs, *Pharm. Res.* 19 (2002) 1400-1416.
3. C. Hilgendorf, G. Ahlin, A. Seithel, P. Artursson, A.L. Ungell, J. Karlsson, Expression of thirty-six drug transporter genes in human intestine, liver, kidney, and organotypic cell lines, *Drug Metab. Dispos.* 35 (2007) 1333-1340.
4. I. Pastan, M.M. Gottesman, K. Ueda, E. Lovelace, A.V. Rutherford, M.C. Willingham, A retrovirus carrying an MDR1 cDNA confers multidrug resistance and polarized expression of P-glycoprotein in MDCK cells, *Proc. Natl. Acad. Sci. USA* 85 (1988) 4486-4490.
5. R.B. Kim, M.F. Fromm, C. Wandel, B. Leake, A.J. Wood, D.M. Roden, G.R. Wilkinson, The drug transporter P-glycoprotein limits oral absorption

- and brain entry of HIV-1 protease inhibitors, *J. Clin. Invest.* 101 (1998) 289-294.
6. J.W. Polli, S.A. Wring, J.E. Humphreys, L. Huang, J.B. Morgan, L.O. Webster, C.S. Serabjit-Singh, Rational use of in vitro P-glycoprotein assays in drug discovery, *J. Pharmacol. Exp. Ther.* 299 (2001) 620-628.
 7. M.E. Taub, L. Kristensen, S. Frokjaer, Optimized conditions for MDCK permeability and turbidimetric solubility studies using compounds representative of BCS classes I-IV, *Eur. J. Pharm. Sci.* 15 (2002) 331-340.
 8. J.M. Custodio, C.Y. Wu, L.Z. Benet, Predicting drug disposition, absorption/elimination/transporter interplay and the role of food on drug absorption, *Adv. Drug Deliv. Rev.* 60 (2008) 717-733.
 9. S. Lu, A.W. Gough, W.F. Bobrowski, B.H. Stewart, Transport properties are not altered across Caco-2 cells with heightened TEER despite underlying physiological and ultrastructural changes, *J. Pharm. Sci.* 85 (1996) 270-273.
 10. C.-Y. Wu, L.Z. Benet, Predicting drug disposition via application of BCS: transport/absorption/elimination interplay and development of a Biopharmaceutics Drug Disposition

- Classification System, Pharm. Res. 22 (2005) 11-23.
11. W.S. Putnam, L. Pan, K. Tsutsui, L. Takahashi, L.Z. Benet, Comparison of bidirectional cephalixin transport across MDCK and caco-2 cell monolayers: interactions with peptide transporters, Pharm. Res. 19 (2002) 27-33.
 12. S.D. Flanagan, C.L. Cummins, M. Susanto, X. Liu, L.H. Takahashi, L.Z. Benet, Comparison of furosemide and vinblastine secretion from cell lines overexpressing multidrug resistance protein (P-glycoprotein) and multidrug resistance-associated proteins (MRP1 and MRP2), Pharmacology 64 (2002) 126-134.
 13. C.L. Cummins, W. Jacobsen, U. Christians, L.Z. Benet, CYP3A4-transfected Caco-2 cells as a tool for understanding biochemical absorption barriers: studies with sirolimus and midazolam, J. Pharmacol. Exp. Ther. 308 (2004) 143-155.
 14. Y.Y. Lau, H. Okochi, Y. Huang, L.Z. Benet, Multiple transporters affect the disposition of atorvastatin and its two active hydroxy metabolites: application of in vitro and ex situ systems, J. Pharmacol. Exp. Ther. 316 (2006) 762-771.

15. Food and Drug Administration, Guidance for Industry (DRAFT GUIDANCE): Drug Interaction Studies – Study Design, Data Analysis, and Implications for Dosing and Labeling, Food and Drug Administration, Rockville, MD, 2006.
Retrieved from
www.fda.gov/cder/guidance/index.htm.
16. Food and Drug Administration, Guidance for Industry: Waiver of in vivo bioavailability and bioequivalence studies for immediate release solid oral dosage forms based on a Biopharmaceutics Classification System, Food and Drug Administration, Rockville, MD, 2000. Retrieved from www.fda.gov/cder/guidance/index.htm.
17. S. Sahin, J.M. Custodio, L.Z. Benet, Transepithelial transport of verapamil across Caco-2 cell monolayers, AAPS J. 9, S2 (2007) T3480.

CHAPTER 6

- CONCLUSIONS AND PERSPECTIVES

6.1 The intestinal interplay: the past, the present and the future

The investigation of food and drugs and how they interact is nothing new. It has long been a field of great interest and research within the pharmaceutical sciences community and will continue as such in the future. Considerable effort has been put into elucidating the effects of food on drug absorption and disposition. With very few exceptions, the mechanistic research representative of this effort has been retrospective in that first, an *in vivo* food effect is observed in a patient, followed by *in vitro* studies to determine the cause of that effect. Such is the scenario that led to the discovery of grapefruit juice's potent inhibition of metabolic function in the intestine.¹

The effects of food on absorption have been characterized as reduced, delayed, increased and accelerated, and those causing no change in absorption.² It is well documented in the literature, and recognized by the FDA,^{3,4} that food can influence the pharmacokinetics

of a drug by affecting factors such as bile flow, splanchnic blood flow, gastrointestinal (GI) pH, gastric emptying, metabolism and physical/chemical interactions with the drug product. Regarding intestinal metabolism, metabolic food-drug interactions have been widely reported with Cytochrome P450 3A4 (CYP3A4) receiving considerable attention. This is not surprising as numerous drugs marketed worldwide are metabolized by CYP3A4. Documented examples include, but are not limited to, modulations in metabolism of drugs such as cyclosporine, felodipine, and indinavir affected by interactions with garlic, grapefruit juice, St John's wort, and red wine.³ Except for the inducing effect of St. John's wort, these food constituents act as direct inhibitors or inactivators of CYP3A4.

The breadth of reports on food-enzyme interactions is in stark contrast to the more limited literature on food-transporter interactions but, as discussed throughout this thesis, new and improved tools are becoming more readily available for discovering and investigating transporters, their substrates, and factors (e.g., food) capable of influencing transporter-substrate interactions. For example, a number of diverse substances including curcumin,⁵ flavonoids,⁶ extracts from bitter melon,^{7,8} tea catechins,⁹ cnidiadin¹⁰ and alkyl gallates¹¹ have all recently been shown to be effective

inhibitors of P-glycoprotein. Moreover, in 2006, Fuchikami and coworkers¹² demonstrated that many herbal extracts can inhibit human OATP2B1 *in vitro*. Utilizing estrone-3-sulfate, a typical OATP2B1 substrate, the authors suggested that these inhibitory effects may be primarily attributable to flavonoids. Similarly, Satoh *et al.*¹³ documented the *in vitro* inhibition of OATP2B1-mediated uptake of the Class 2 drug, glyburide by grapefruit juice and orange juice. Fexofenadine, a Class 3 drug, has been shown to be a substrate for both OATP2B1 and P-gp. Dresser *et al.*¹⁴ described an inhibition of OATP2B1 leading to a decrease in fexofenadine's oral bioavailability when the drug was coadministered with fruit juices (i.e. orange, grapefruit, apple) to healthy volunteers. In addition, Dresser and colleagues^{15,16} investigated the intestinal interplay of efflux and uptake of fexofenadine demonstrating that, despite being a substrate of P-gp,¹⁷ the fruit juice effects on uptake were more pronounced than on efflux, therefore oral bioavailability is decreased. Less work has been carried out with other transporters, but Tseng *et al.*¹⁸ have shown that mustard oils can inhibit MRP1 mediated transport, while Wu and coworkers¹⁹ have shown that plant phenols can inhibit MRPs 1, 4 and 5.

Contrastingly, our work did not focus on one particular juice, herb or other food constituent.

Instead, we approached food-transporter interplay by considering the environment of the postprandial intestine. We began with simulated physiological media that mimic the fed state of the human intestine. We examined the effects of various intestinal media on cellular studies and *in vitro* transporter function and determined that the complexity of the media such as FeSSIF and Ensure Plus[®] leads to confounding results whereby the effects on transporters cannot clearly be discerned from other factors like solubility and viscosity.

Transitioning to less complex media, we built on previous work showing the ability of monoglycerides to inhibit efflux transport. This inhibitory effect is relevant to the intestinal interplay because of the high levels of monoglycerides in the gut following a meal and the fact that monoglycerides are found in lipidic excipients. Employing control transport media supplemented with monoolein, we demonstrated that a change in apparent permeability (P_{app}) values and a decrease in net flux ratios can be achieved similar to the result achieved by the known P-gp inhibitor GG918 and that these results are consistent with what we would expect if P-gp function were inhibited. However, we found that these inhibitory effects may be substrate specific in that drugs susceptible to both efflux and

uptake may exhibit counterposing effects *in vitro*. This led us to further explore intestinal uptake transporters and their role in the absorption of Class 3 compounds.

Following unsuccessful endeavors with captopril and ranitidine, we concentrated on metformin and our work became multifaceted in that, before we investigated its food effect, we first had to identify the mechanism controlling the absorption of metformin. Utilizing various cellular model systems and a rat intestinal model, our data suggest multiple transporter effects on the absorption of metformin, yet we did not observe an influence of monoolein. Overall, our data suggest that intestinal transporters belong on the list of variables that must be considered in food-drug interactions.

Our extensive investigation into predicting transporter effects with Class 1, Class 2 and Class 3 compounds underscores the importance of an adequate model system. The MDR1-MDCK cell system may be the appropriate model to utilize for determination of a P-gp substrate. The lower TEER values of the Caco-2 cells makes for a leakier system that we believe is far more representative of the human intestine and, therefore, may be the appropriate model system to utilize to determine whether a P-gp effect may play a significant role in absorption and disposition. However, for Class 3 drugs, the Caco-2 model is not the appropriate system for evaluating

transporter effects. These poorly permeable compounds often rely on uptake carriers to gain access to the cell and the reliability of uptake transporter expression and function in the Caco-2 cells is inadequate. Our work with the Class 3 drug metformin will be the first published report in the literature recommending caution in the application of the Caco-2 model to Class 3 studies. More relevant results and improved predictive utility will be achieved with a transfected cellular system containing the transport protein of interest as well as an animal model such as the rat intestinal perfusion system.

In the future, cell lines such as the PMAT-MDCK cells (Chapter 4) will continue to be engineered and will become more widely available. As a result, the protocols associated with their use will become standardized. We hope this will lead to increased access of such tools to all researchers, where the ease in obtaining Caco-2 cells from the American Type Culture Collection (ATCC) is extended to all stably-transfected cellular systems. With greater transporter recognition and guidance from the FDA²⁰ coupled with the emergence of more studies such as recent work on OATP1B1 and statin-induced myopathy by the SEARCH Collaborative group,²¹ the investigation of uptake and efflux transporters and their role in drug absorption, disposition and elimination will expand

tremendously. It is our hope that with research, such as that reported in this thesis, we will contribute to the pharmaceutical sciences community by fostering new ideas, approaches and tools that will extended beyond academia into industry where knowledge ultimately leads to more safe and efficacious medicines.

6.2 References

1. D.G. Bailey, J.D. Spence, B Edgar, C.D. Bayliff, J.M. Arnold, Ethanol enhances the hemodynamic effects of felodipine, *Clin. Invest. Med.* 12 (1989) 357-362.
2. P.G. Welling, Effects of food on drug absorption, *Annu. Rev. Nutr.* 16 (1996) 383-415.
3. R.Z. Harris, G.R. Jang, S. Tsunoda, Dietary effects on drug metabolism and transport, *Clin. Pharmacokinet.* 42 (2003) 1071-1088.
4. Food and Drug Administration. Guidance for Industry: Food-effect bioavailability and fed bioequivalence studies. Food and Drug Administration, Rockville, MD, 2002. Available at <http://www.fda.gov/cder/guidance/index.htm>.
5. S. Anuchapreeda, P. Leechanachai, M.M. Smith, S.V. Ambudkar, P. Limtrakul, Modulation of P-glycoprotein expression and function by curcumin in multidrug-resistant human KB cells, *Biochem. Pharmacol.* 64 (2002) 573-582.
6. S Zhang, M.E. Morris, Effects of the flavonoids biochanin A, morin, phloretin, and silymarin on P-glycoprotein-mediated transport, *J. Pharmacol. Exp. Ther.* 304 (2003) 1258-1267.

7. T. Konishi, H. Satsu, Y. Hatsugai, K. Aizawa, T. Inakuma, S. Nagata, S.H. Sakuda, H. Nagasawa, M. Shimizu, Inhibitory effect of a bitter melon extract on the P-glycoprotein activity in intestinal Caco-2 cells, *Br. J. Pharmacol.* 143 (2004) 379-387.
8. T. Konishi, H. Satsu, Y. Hatsugai, K. Aizawa, T. Inakuma, S. Nagata, S.H. Sakuda, H. Nagasawa, M. Shimizu, A bitter melon extract inhibits the P-glycoprotein activity in intestinal Caco-2 cells: monoglyceride as an active compound, *Biofactors* 22 (2004) 71-74.
9. S. Kitagawa, T. Nabekura, S. Kamiyama, Inhibition of P-glycoprotein function by tea catechins in KB-C2 cells, *J. Pharm. Pharmacol.* 56 (2004) 1001-1005.
10. C. Barthomeuf, J. Grassi, M. Demeule, C. Fournier, D. Boivin, R. Béliveau, Inhibition of P-glycoprotein transport function and reversion of MDR1 multidrug resistance by cnidiadin, *Cancer Chemother. Pharmacol.* 56 (2005) 173-181.
11. S. Kitagawa, T. Nabekura, S. Kamiyama, T. Takahashi, Y. Nakamura, Y. Kashiwada, Y. Ikeshiro, Effects of alkyl gallates on Pglycoprotein function, *Biochem. Pharmacol.* 70 (2005) 1262-1266.

12. H. Fuchikami, H. Satoh, M Tsujimoto, S. Ohdo, H. Ohtani, Y. Sawada, Effects of herbal extracts on the function of human organic anion-transporting polypeptide OATP-B, *Drug Metab. Dispos.* 34 (2006) 577-582.
13. H. Satoh, F. Yamashita, M. Tsujimoto, H. Murakami, N. Koyabu, H. Ohtani, Y. Sawada, Citrus juices inhibit the function of human organic anion-transporting polypeptide OATP-B, *Drug Metab. Dispos.* 33 (2005) 518-523.
14. G.K. Dresser, D.G. Bailey, B.F. Leake, U.I. Schwarz, P.A. Dawson, D.J. Freeman, R.B. Kim, Fruit juices inhibit organic anion transporting polypeptide-mediated drug uptake to decrease the oral availability of fexofenadine, *Clin. Pharmacol. Ther.* 71 (2002) 11-20.
15. G.K. Dresser, D.G. Bailey, The effects of fruit juices on drug disposition: a new model for drug interactions, *Eur. J. Clin. Invest.* 33 (2003) 10-16.
16. G.K. Dresser, R.B. Kim, D.G. Bailey, Effect of grapefruit juice volume on the reduction of fexofenadine bioavailability: possible role of organic anion transporting polypeptides, *Clin. Pharmacol. Ther.* 77 (2005) 170-177.

17. N. Petri, C. Tannergren, D. Rungstad, H. Lennernas, Transport characteristics of fexofenadine in the Caco-2 cell model, *Pharm. Res.* 21 (2004) 1398-1404.
18. E. Tseng, A. Kamath, M.E. Morris, Effect of organic isothiocyanates on the P-glycoprotein-and MRP1-mediated transport of daunomycin and vinblastine, *Pharm. Res.* (2002) 1509-1515.
19. C.-P. Wu, A.M. Calcagno, S.B. Hladky, S.V. Ambudkar, M.A. Barrand, Modulatory effects of plant phenols on human multidrugresistance proteins 1, 4, and 5 (ABCC1, 4 and 5), *FEBS J.* 272 (2005) 4725-4740.
20. S.M. Huang, J.M. Strong, L. Zhang, K.S. Reynolds, S. Nallani, R. Temple, S. Abraham, S.A. Habet, R.K. Baweja, G.J. Burckart, S. Chung, P. Colangelo, D. Frucht, M.D. Green, P. Hepp, E. Karnaukhova, H.S. Ko, J.I. Lee, P.J. Marroum, J.M. Norden, W. Qiu, A. Rahman, S. Sobel, T. Stifano, K. Thummel, X.X. Wei, S. Yasuda, J.H. Zheng, H. Zhao, L.J. Lesko, New era in drug interaction evaluation: US Food and Drug Administration update on CYP enzymes, transporters, and the guidance process, *J. Clin. Pharmacol.* 48 (2008) 662-670.

21. The SEARCH Collaborative Group, SLC01B1 Variants and Statin-Induced Myopathy - A Genomewide Study, N. Engl. J. Med. 359 (2008) 856-858.

further to fly

It is the policy of the University to encourage the distribution of all theses and dissertations. Copies of all UCSF theses and dissertations will be routed to the library via the Graduate Division. The library will make all theses and dissertations accessible to the public and will preserve these to the best of their abilities, in perpetuity.

I hereby grant permission to the Graduate Division of the University of California, San Francisco to release copies of my thesis or dissertation to the Campus Library to provide access and preservation, in whole or in part, in perpetuity.

A handwritten signature in black ink, consisting of a large, stylized initial 'R' followed by a horizontal line that curves upwards at the end.

Author Signature

09.04.08

Date